ENVIRONMENTAL FATE STUDIES ON CERTAIN MUNITIONS WASTEWATER CONSTITUENTS

Phase IV - Lagoon Model Studies

Final Report

By

Ronald J. Spanggord
William R. Mabey
Theodore Mill
Tsong-Wen Chou
James H. Smith
Shonh Lee
Darvl Roberts

September 1983

Supported by:

U.S. ARMY MEDICAL RESEARCH AND DEVELOPMENT COMMAND
Fort Detrick, Frederick, Maryland 21701

Contract No. DAMD17-78-C-8081

SRI Project LSU-7934

SRI International
333 Ravenswood Avenue
Menlo Park, California 94025

Katheryn F. Kenyon, Contracting Officer Technical Representative
U.S. Army Medical Bioengineering Research and Development Laboratory
Fort Detrick, Frederick, Maryland 21701

SECURITY CLASSIFICATION OF THIS PAGE (When Data Entered)

REPORT DOCUMENTATION PAGE

READ INSTRUCTIONS BEFORE COMPLETING FORM

1. REPORT NUMBER	2. GOVT ACCESSION NO. AD-A138550
3. RECIPIENT'S CATALOG NUMBER	
4. TITLE (and Subtitle) ENVIRONMENTAL FATE STUDIES ON CERTAIN MUNITIONS WASTEWATER CONSTITUENTS Phase IV - Lagoon Model Studies	5. TYPE OF REPORT & PERIOD COVERED Final Report, Phase IV
	6. PERFORMING ORG. REPORT NUMBER
7. AUTHOR(s) Ronald J. Spanggord, William R. Mabey, Theodore Mill, Tsong-Wen Chou, James H. Smith, Shonh Lee, Daryl Roberts	8. CONTRACT OR GRANT NUMBER(s) DAMD17-78-C-8081
9. PERFORMING ORGANIZATION NAME AND ADDRESS SRI International 333 Ravenswood Avenue Menlo Park, CA 94025	10. PROGRAM ELEMENT, PROJECT, TASK AREA & WORK UNIT NUMBERS 62720A.3E162720A835.AA.034
11. CONTROLLING OFFICE NAME AND ADDRESS US Army Medical Research and Development Command Fort Detrick Frederick, Maryland 21701	12. REPORT DATE September 1983 / 13. NO. OF PAGES 146
	15. SECURITY CLASS. (of this report) Unclassified
14. MONITORING AGENCY NAME & ADDRESS (if diff. from Controlling Office) US Army Medical Bioengineering Research and Development Laboratory Environmental Protection Research Division	15a. DECLASSIFICATION/DOWNGRADING SCHEDULE

16. DISTRIBUTION STATEMENT (of this report)

Approved for public release; distribution unlimited

17. DISTRIBUTION STATEMENT (of the abstract entered in Block 20, if different from report)

18. SUPPLEMENTARY NOTES

19. KEY WORDS (Continue on reverse side if necessary and identify by block number)

TNT, RDX, Photolysis, Biotransformation, Rate constant, Lagoon fate assessment, computer modeling.

.00010 cm/sec ... .00775 cm/sec

20. ABSTRACT (Continue on reverse side if necessary and identify by block number)

This study was conducted to investigate the persistence of 2,4,6-trinitrotoluene (TNT) and hexahydro-1,3,5-trinitro-1,3,7-triazine (RDX) in waste disposal lagoons at Louisiana Army Ammunition Plant. The waste disposal lagoons are complex environments due to a heterogeneous distribution of solid TNT and RDX munitions on the lagoon sediment surface. These solids serve as a constant input source of munitions to the lagoon waters through dissolution. Flux rates for the dissolution of munitions were measured at 1.08×10^{-4} cm sec^{-1} for TNT and 7.75×10^{-5} cm sec^{-1} for RDX at 25°C in the lagoon.

DD FORM 1 JAN 73 1473

EDITION OF 1 NOV 65 IS OBSOLETE

SECURITY CLASSIFICATION OF THIS PAGE (When Data Entered)

19. KEY WORDS (Continued)

20 ABSTRACT (Continued)

The major loss processes for the transformation of TNT were phototransformation and biotransformation. A first-order, depth-independent rate constant for the indirect photolysis of TNT in mid-March was measured at 4.3 cm d^{-1} which yield an estimated half-life of eight days in a body of water 50 cm deep. A major stable TNT phototransformation product was 2-amino-4,6-dinitrobenzoic acid. Biotransformation occurred in the lagoon with a pseudo-first-order rate constant of 0.010d^{-1} and a second-order rate constant of 8.95 x 10^{-9} ml $cell^{-1}$ d^{-1}. The half-life of TNT resulting from biotransformation was calculated to be 69 days. The major biotransformation products were 2-amino-4,6-dinitrotoluene and 4-amino-2,6-dinitrotoluene.

The major transformation process for RDX was found to be photolysis. RDX transformed with first-order rate constants ranging from 0.016 cm d^{-1} in winter to 0.076 cm d^{-1} in summer. The half-life of RDX was estimated to range from over 2000 days in winter to 456 days in summer in a lagoon 50 cm deep.

Although photolysis was found to be the major transformation process for TNT and RDX, the rate of transformation was slowed due to the high absorptivity of the lagoon waters, whose absorbances ranged from 3.0 in winter to 9.0 in summer. These high absorbances allow little light to penetrate for a significant distance below the lagoon surface. The light absorption, however, heats the lagoon water, thus accelerating the dissolution process of solid TNT and RDX on the lagoon sediment surface. Thus, TNT and RDX concentrations in the lagoon water were found to increase from the winter to the summer months.

A computer model was constructed to simulate the lagoon enviroment. Using the laboratory-developed transformation and dissolution rate constants, the persistence of TNT and RDX can be estimated as a function of time from initial inputs of lagoon depth and aqueous and sediment-surface munition concentrations.

A1

EXECUTIVE SUMMARY

This study was conducted to investigate the persistence of 2,4,6-trinitrotoluene (TNT) and hexahydro-1,3,5-trinitro-1,3,7-triazine (RDX) in waste disposal lagoons at Louisiana Army Ammunition Plant. The waste disposal lagoons are complex environments due to a heterogeneous distribution of solid TNT and RDX munitions on the lagoon sediment surface. These solids serve as a constant input source of munitions to the lagoon waters through dissolution. Flux rates for the dissolution of munitions were measured at 1.08×10^{-4} cm sec^{-1} for TNT and 7.75×10^{-5} cm sec^{-1} for RDX at 25°C in the lagoon.

The major loss processes for the transformation of TNT were phototransformation and biotransformation. A first-order, depth-independent rate constant for the indirect photolysis of TNT in mid-March was measured at 4.3 cm d^{-1} which yields an estimated half-life of eight days in a body of water 50 cm deep. A major stable TNT phototransformation product was 2-amino-4,6-dinitrobenzoic acid. Biotransformation occurred in the lagoon with a pseudo-first-order rate constant of $0.010 d^{-1}$ and a second-order rate constant of 8.95×10^{-9} ml $cell^{-1}$ d^{-1}. The half-life of TNT resulting from biotransformation was calculated to be 69 days. The major biotransformation products were 2-amino-4,6-dinitrotoluene and 4-amino-2,6-dinitrotoluene.

The major transformation process for RDX was found to be photolysis. RDX transformed with first-order rate constants ranging from 0.016 cm d^{-1} in winter to 0.076 cm d^{-1} in summer. The half-life of RDX was estimated to range from over 2000 days in winter to 456 days in summer in a lagoon 50 cm deep.

Although photolysis was found to be the major transformation process for TNT and RDX, the rate of transformation was slowed due to the high absorptivity of the lagoon waters, whose absorbances ranged from

3.0 in winter to 9.0 in summer. These high absorbances allow little light to penetrate for a significant distance below the lagoon surface. The light absorption, however, heats the lagoon water, thus accelerating the dissolution process of solid TNT and RDX on the lagoon sediment surface. Thus, TNT and RDX concentrations in the lagoon water were found to increase from the winter to the summer months.

A computer model was constructed to simulate the lagoon environment. Using the laboratory-developed transformation and dissolution rate constants, the persistence of TNT and RDX can be estimated as a function of time from initial inputs of lagoon depth and aqueous and sediment-surface munition concentrations.

CONTENTS

CONTENTS (Concluded)

ILLUSTRATIONS

ILLUSTRATIONS (Concluded)

TABLES

TABLES (Continued)

TABLES (Concluded)

ACKNOWLEDGMENTS

The studies reported herein could not have been performed without the assistance of an excellent support staff. We therefore gratefully acknowledge the help of Doris Tse (photochemistry), Daniel Haynes (physical transport), Philip Alferness (analytical chemistry), and Justine Whaley (microbiology). We also want to thank Dr. John Winterle for his contribution to the development of equations describing sensitized photochemical processes in LAAP water and the observed effect of depth on the photochemical rate constant.

I. INTRODUCTION

The U.S. Army is currently involved in assessing the overall hazard of munitions-related water pollutants to aquatic and mammalian systems. Part of this assessment involves the loss and movement (fate) of militarily unique chemicals when they are discharged into various aquatic environments. Munitions have been produced and handled for many years with minimal pollution-abatement controls, but it has now become important to estimate the environmental persistence of selected chemicals used in present and past military operations.

Environmental persistence can be estimated through the use of computer modeling, in which the loss and movement processes as well as critical environmental parameters can be described by mathematical equations and approximations. In most environmental situations or in cases of low chemical concentrations, simple first-order or pseudo-first-order rate expressions and equilibrium constants adequately describe the loss and movement processes. Once the rate and equilibrium constants are known for the dominant processes, environments can be simulated under any number of specified conditions. Thus, it becomes possible to estimate the concentration of a chemical as a function of time when the chemical is subjected to various environmental stresses. In a previous study (Spanggord et al., 1981), we applied the modeling concept to munitions-related chemicals in the Holston River and generated concentration- time-dependent profiles that allowed the prediction of chemical concentrations 20 km from the discharge point. Actual data on samples taken from the river verified the applicability of the modeling concept.

On the basis of that experience, this study was undertaken to estimate the persistence of 2,4,6-trinitrotoluene (TNT) and hexahydro-1,3,5-trinitro-1,3,5-triazine (RDX) in disposal lagoon environments. The lagoon disposal of munitions wastes has been practiced for many

years and the Army would like to dispose of these lagoons in a safe manner. The studies reported herein describe the major transport and transformation processes that affect the persistence of TNT and RDX in lagoons. We also developed a computerized simulation model to describe the loss and movement of these chemicals as a function of time, concentration, and location in the lagoon.

II. SITE DESCRIPTION

This investigation covered evaluation of the persistence of TNT and RDX in the waste disposal lagoons at Louisiana Army Ammunition Plant (LAAP) in Minden, Louisiana. LAAP is a load, assemble, and pack facility that generates munitions wastewaters during shell-washout operations in the loading/unloading process. The wastewaters are transported by truck to disposal lagoons, where natural evaporation concentrates the residues.

We conducted a field study at LAAP on December 7-11, 1981. At that time, no wastes had been transported to the lagoons since May and a new carbon-column waste-treatment facility was to be installed prior to further waste disposal.

The lagoon disposal area at LAAP is outlined in Figure 1. Lagoon No. 9 was selected for our investigations mainly because it is one of the larger lagoons and because previous reports had indicated that TNT and RDX were still being found in the lagoon waters and sediments (Wentzel, et al., 1981).

Lagoon No. 9 is a nearly square, flat-bottomed reservoir measuring 56.7 m × 52.1 m (186 ft × 171 ft). During the week of December 7-11, 1981, it was filled to a depth of 60 cm (2.0 ft) with a dark tea-colored water. Water input into the lagoon is from seasonal rains, and water output is due to seepage and evaporation. Trees and shrubbery line the lagoon enbankments, but no plant or aquatic life was evident in the lagoon water.

To begin our field study, a tow line was secured across the middle of the lagoon and the center position was tagged. We used an inflatable raft to transport monitoring and sampling equipment to the center of the lagoon for sample collection and monitoring measurements.

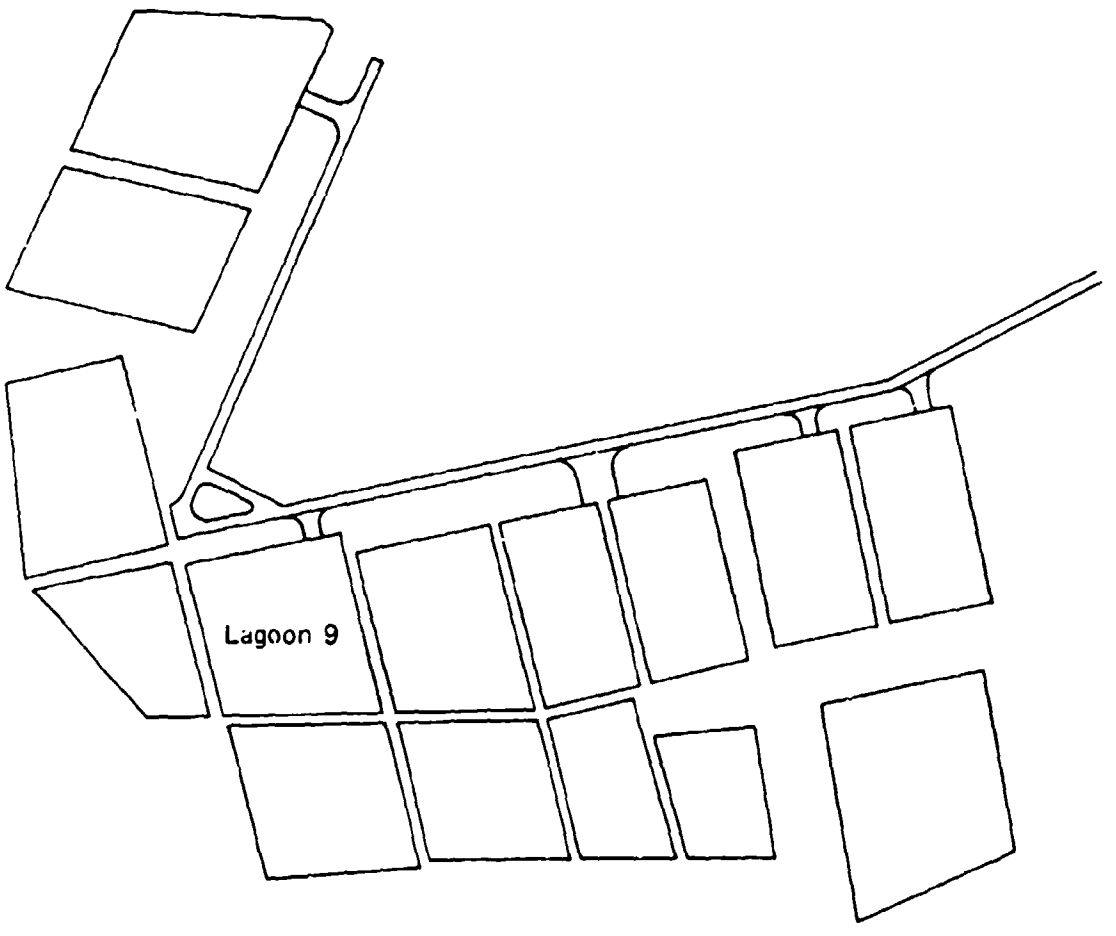

FIGURE 1 LAGOON AREA AT LOUISIANA ARMY AMMUNITION PLANT

Water samples were collected with a variable-water-depth sample collector in 50-ml amber glass jars with Teflon-lined caps. We analyzed these samples on site, using a high-pressure liquid chromatograph (HPLC). We collected other water samples in 4-liter amber glass bottles and transported them by air overnight to SRI for total microbial counts. Sediment samples, removed from the lagoon with a hand corer, were collected at various locations and transported to SRI for analysis. These samples indicated a heavy clay bottom that was difficult to penetrate. Except for sorption properties, we did not evaluate the morphological characteristics of the sediment.

To determine the ability of light to penetrate into the lagoon water, we placed photochemical "trees" at various depths in the lagoon. These trees consisted of aluminum rods, cross bars, and flotation supports and were equipped with sealed PNA/PYR* actinometer solutions attached to the ends of the crossbars. After selected time intervals, the PNA/PYR tubes were removed from the apparatus, wrapped in aluminum foil, and transported to SRI for analysis.

Meteorological conditions that were measured periodically at the site were temperature, pressure, wet and dry bulb temperatures (relative humidity), and wind velocity. In the lagoon water, we measured temperature, pH, and dissolved oxygen. LAAP personnel obtained a water sample in March 1982. During a second visit to the site on May 25, 1982, we collected water and sediment samples. In addition, sample bottles were left with plant personnel to collect samples at two-week intervals and to mail them to SRI. Depth at the center of the lagoon was measured during the December visit and again on July 24, 1982, to estimate water loss over an 8-month period. The lagoon was completely dry in late August.

---

*PNA/PYR, p-nitroacetophenone/pyridine, sunlight actinometer developed at SRI.

The yearly meteorological conditions for the lagoon site were estimated from daily data collected by the Red River experimental weather station at Restin, LA, approximately 30 miles east of LAAP. The data collected at this site include daily maximum and minimum air and soil temperatures, 24-hour pan-evaporation, and 24-hour precipitation. We averaged the data collected from this station for three years (1979 through 1981) to estimate water balances within the lagoon at LAAP.

A graphic sketch of Lagoon No. 9 is shown in Figure 2. A concrete ramp in the southeast corner of the lagoon serves as an access point for vehicles to dump liquid and solid wastes. Analysis of sediment samples (Appendix A) collected on May 25, 1982, from a 5 × 5 sectioned matrix of the lagoon showed very high concentrations of munitions that decreased as a function of distance from the dump ramp (Figure 2). When the lagoon dried up in late August 1982, pure munitions compounds were visible on the sediment surface near the ramp. These solids serve as the primary input source of munitions to the lagoon waters. The concentration of munitions also decreased as a function of depth in the sediment. The distribution of munitions in small sediment cores taken from various locations in the lagoon is described in Section V.A.4.

Because the lagoon is a highly colored body of water, it absorbs much of the sunlight energy and converts it to heat, thus establishing a thermocline in the lagoon water. Temperature fluctuations during the course of a day are shown in Table 1 for the bottom, middle, and surface of the lagoon. Over the nine-month course of this study, the lagoon temperatures ranged from 10°C in December to 35°C in May and 41.5°C in August. This temperature change affects rates of dissolution, diffusion, and microbial activity as well as solubility.

The lagoon waters appeared to be well mixed in a vertical direction, as evidenced by similar concentrations of TNT, RDX, and dissolved oxygen measured at the surface and at depths of 25 and 50

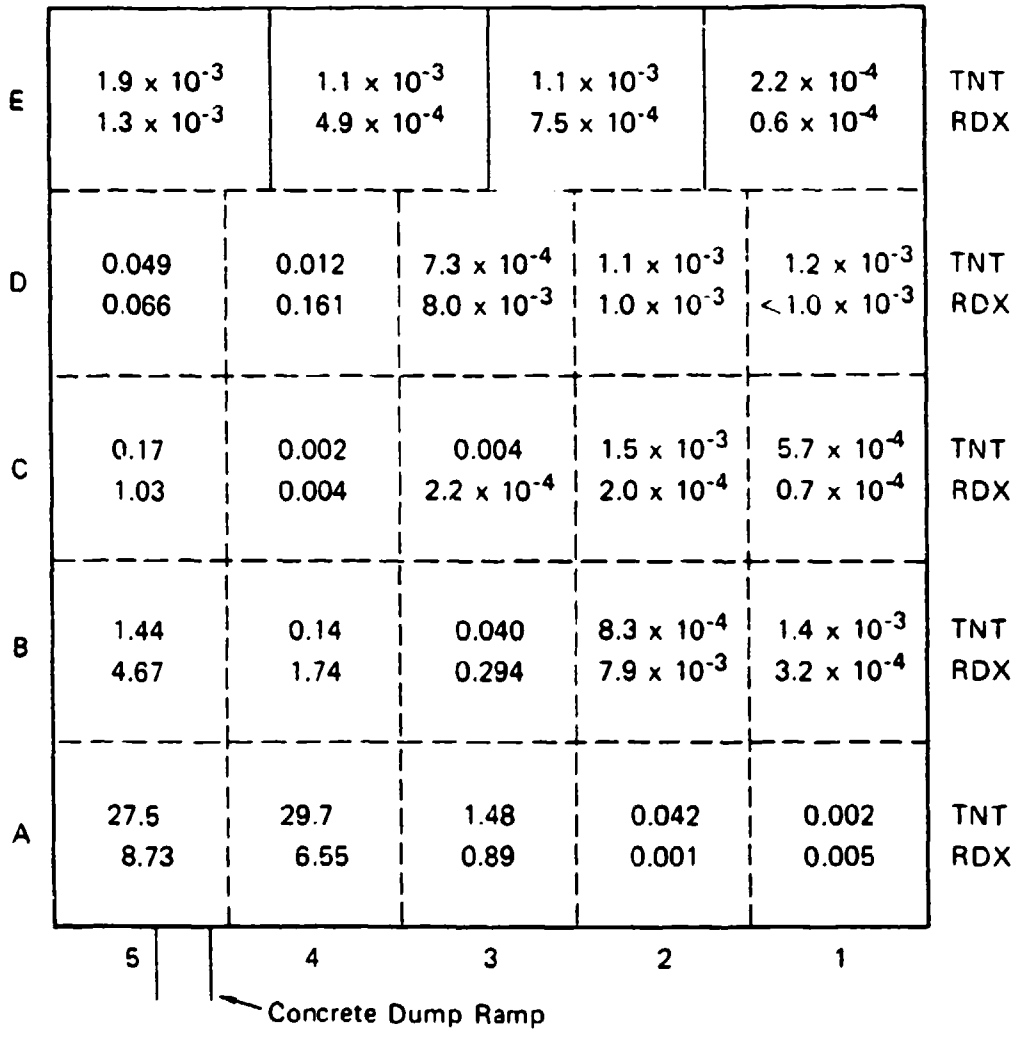

FIGURE 2 DIAGRAM OF LAGOON NO. 9 AND TNT-RDX DISTRIBUTIONS (%) IN THE SEDIMENT

cm. Horizontal mixing, however, was not complete; concentrations of TNT and RDX were higher in the south bank waters than those in the center of the lagoon (Table 2). The higher concentrations near the edge of the lagoon may be the result of the water there being warmer, which increases the rates of dissolution and diffusion of munitions from the near-shore sediments relative to bulk diffusion rates in the main lagoon.

Table 1

LAGOON WATER TEMPERATURES (°C) FOR THE BOTTOM, MIDDLE, AND SURFACE ON DECEMBER 9, 1981

Time	Bottom (50 cm)	Middle (25 cm)	Surface (0 cm)
0820	11.6	11.8	11.9
0925	11.6	11.9	12.1
1020	11.8	12.0	14.0
1120	11.7	12.0	13.5
1240	11.7	11.7	14.0
1350	12.0	12.0	16.5
1440	12.0	12.3	17.0
1550	12.0	13.8	16.0

Table 2

CONCENTRATIONS OF TNT AND RDX IN WATER AT LAGOON CENTER AND SOUTHEAST EDGE AS A FUNCTION OF TIME OF DAY

	TNT (ppm)		RDX (ppm)	
Time of Day	Edge	Center	Edge	Center
0800	8.34	4.81	12.7	12.9
0900	7.11	4.35	13.2	12.5
1000	7.00	4.95	13.6	12.9
1100	7.62	5.02	13.0	13.4
1200	6.80	4.88	12.7	12.6
1300	6.54	4.78	12.9	13.2
1400	7.27	4.99	12.8	12.9
1500	7.28	4.71	12.8	13.2

III. CHEMICALS IDENTIFIED IN LAGOON NO. 9

Water samples were collected from the lagoon during site visits in December 1981, May 1982, and July 1982. In addition, samples were sent to SRI by LAAP personnel at two-week intervals from June 1982 until the lagoon became dry in late August 1982.

The samples were analyzed by HPLC, using direct aqueous injection of the sample after the addition of an internal standard (3,5-dinitrotoluene).

The following conditions were employed:

Instrument:	Spectra-Physics Model 3500B Liquid Chromatograph
Column:	Waters Assoc C_{18} Radial-Pak A
Solvent:	30% B in A to 80% B in A. A = H_2O; B = methanol/acetonitrile (50/50)
Flow Rate:	2.0 ml min^{-1}
Detection:	UV @ 254 nm

A typical HPLC profile appears in Figure 3. The chemicals identified in this profile and confirmed by probe-mass spectrometry were octahydro-1,3,5,7-tetranitro-1,3,5,7-tetrazocine (HMX), RDX, 1,3,5-trinitrobenzene (TNB), 3,5-dinitroaniline (DNA), TNT, 2-amino-4,6-dinitrotoluene (2-A-4,6-DNT), and 4-amino-2,6-dinitrotoluene (4-A-2,6-DNT). Concentrations of each chemical in water samples at various dates are shown in Table 3.

Investigations were also conducted to identify stable munitions-related chemicals in the lagoon water. A 400-ml sample of lagoon water was extracted with benzene (2 × 400 ml) (benzene fraction) and ether (2 × 200 ml) (ether I fraction); then the water was acidified to pH 1 with HCl and re-extracted with ether (2 × 200 ml) (ether II fraction). Each fraction was dried over anhydrous sodium sulfate and rotary-evaporated to dryness. The residues were dissolved in a small amount of ether for chromatographic analysis.

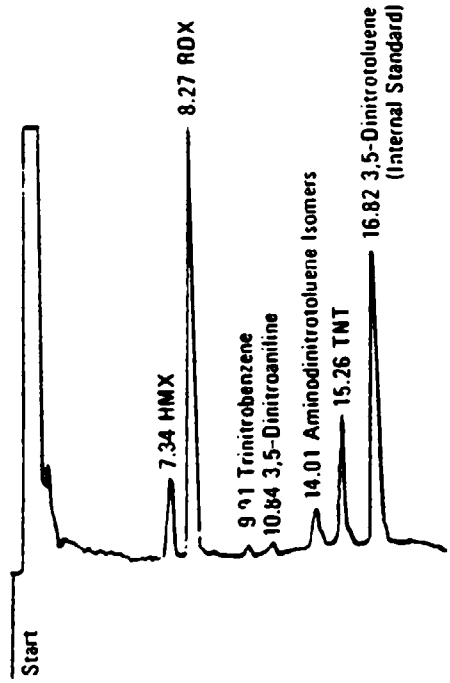

FIGURE 3 HPLC PROFILE OF LAGOON WATER
(SAMPLED 7/22/82)

Table 3

CONCENTRATIONS (ppm) OF MUNITIONS FOUND
IN WATER SAMPLES ON VARIOUS DATES

Date Sampled	Day	HMX	RDX	TNB	4-A-2,6-DNT	2-A-4,6-DNT	TNT	DNA
12/08/81	0	--	13.2	0.33	1.10	1.50	6.98	1.0
3/15/82	74	2.87	10.9	0.58	--	1.01	5.49	<0.10
5/25/82	145	3.15	18.3	0.65	0.91	1.33	19.8	0.54
6/09/82	160	4.31	22.4	0.91	2.35	1.33	11.5	0.54
6/23/82	174	4.40	20.9	0.75	2.31	1.39	5.65	0.68
7/07/82	188	5.71	28.9	0.84	0.83	1.48	6.31	0.99
7/22/82	203	4.03	17.1	0.20	0.42	0.77	2.81	0.73
8/04/82	216	6.36	42.1	4.17	0.58	1.37	12.3	0.87
8/20/82	232	6.03	12.6	2.06	0.65	0.83	0.50	0.34
9/03/82	246	5.07	5.6	<0.10	--	1.16	0.20	<0.10

We identified TNT, 2-amino-4,6-dinitrotoluene, 4-amino-2,6-dinitrotoluene, RDX, and trace amounts of 1,3,5-trinitrobenzene and 2,4,6-trinitrobenzyl alcohol by thin-layer chromatographic (TLC) analysis on silica gel, using benzene as a solvent and an ethylenediamine/DMSO spray reagent. In the ether I fraction, only one spot migrated, which coincided with RDX. In the ether II fraction, several spots were observed close to the origin but could not be identifed by cochromatography with standards or color development with the spray reagent.

The ether II fraction was treated with diazomethane and subjected to HPLC analysis under the following conditions:

Column: Water's C_{18} Radial Pak A
Solvent: 0-99% methanol in water with a 10 min delay and a 50 min linear gradient
Flow rate: 2.0 ml min^{-1}
Detection: UV @ 254 nm

A typical HPLC chromatogram appears in Figure 4. Components from the HPLC profile in Figure 4 were collected and evaluated by probe mass spectrometry. The fraction 57.34 component was identified as the methyl ether of 3,5-dinitrophenol. Fraction 54.31 was tentatively identified as methyl 2-hydroxy-4,6-dinitrobenzoic acid, methyl ether and methyl ester, but could not be confirmed due to the lack of a reference standard. Fraction 54.31 also contained a component that was identified as methyl 2-amino-4,6-dinitrobenzoic acid, methyl ester, and was confirmed by the synthesis of a reference standard in our laboratory. The other component could not be identified due to multicomponent spectra and elevated background signals. Fraction 43.50 was identified as methyl 2,4-dinitrobenzoic acid, methyl ester.

Thus, the majority of chemicals in the LAAP lagoon water are related to the photochemical transformation of TNT with the exception of 2-amino-4,6-dinitrotoluene and 4-amino-2,6-dinitrotoluene, which arise from microbial sources. Based on the work of Kaplan et al. (1975), who showed that many of the identified components are the result of photochemical processes, Scheme I indicates the probable route of formation of the identified products.

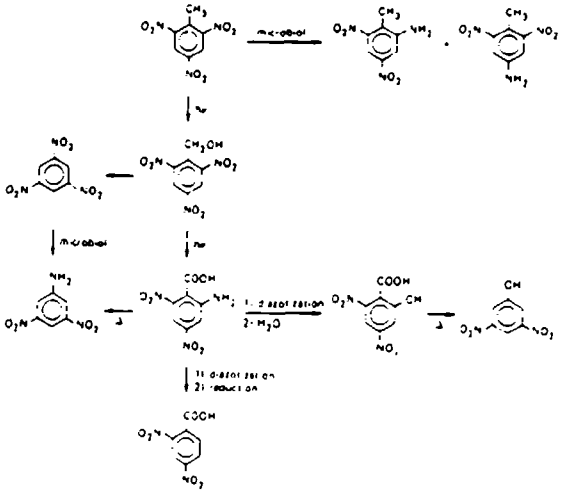

Scheme I

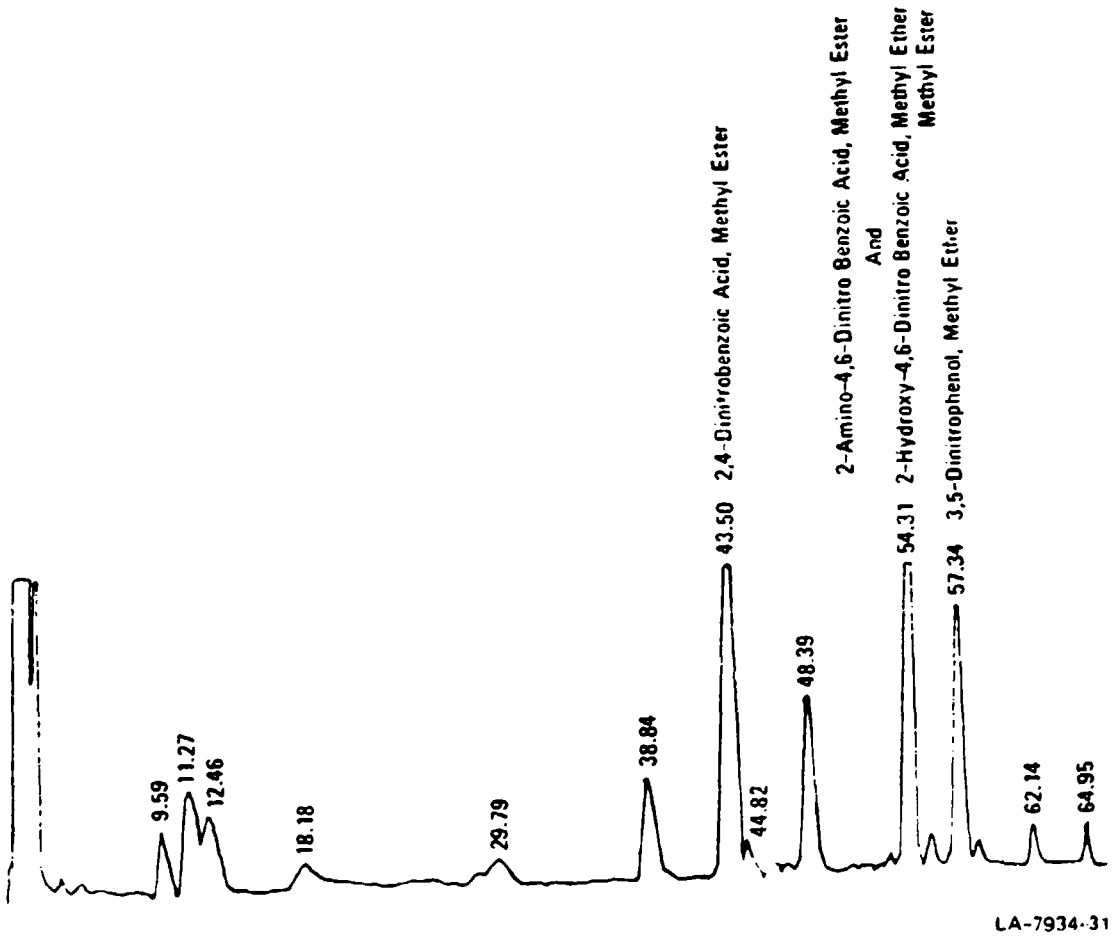

FIGURE 4 HPLC PROFILE OF THE METHYLATED ETHER II FRACTION OF LAGOON WATER

A key step in this scheme is the series of oxidative-reductive disproportionations leading to 2-amino-4,6-dinitrobenzoic acid, as shown in Scheme II.

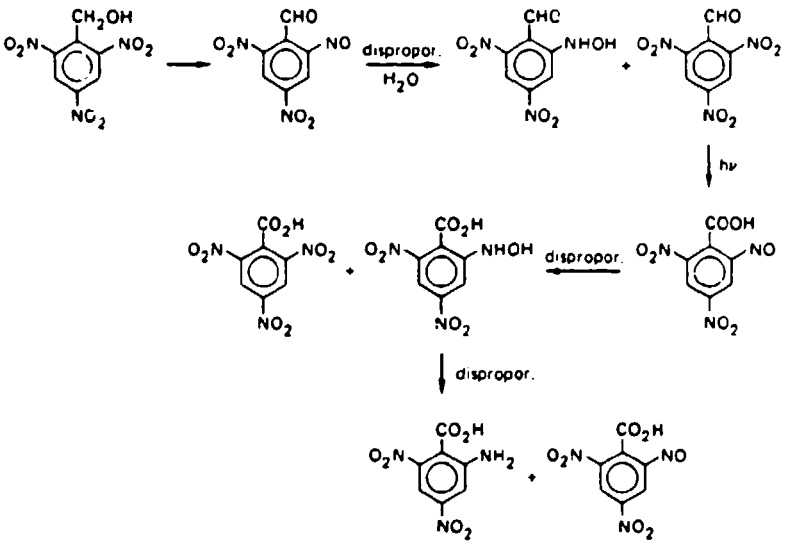

Scheme II

All the chemicals identified in the lagoon water were also found in the sediment. In addition, the explosive, tetryl, was found in the sediment.

Because 2-amino-4,6-dinitrobenzoic acid appeared to be a major transformation product in the lagoon water, we developed an HPLC procedure to monitor this compound. The following conditions were employed:

Column: 250 mm × 4.6 mm Alltech C_{18} 10 μm
Solvent: 40% B in A → 50% B in A in 10 min after a 5-min hold. A = 0.1M phosphate buffer (pH 7) with 0.05 M tributylammonium phosphate (TBAP); B = 0.005 M (TBAP) in methanol.
Flow rate: 1.8 ml min^{-1}
Detector: UV @ 254 nm
Retention time: 3.62 min

A typical chromatographic profile of lagoon water appears in Figure 5. Lagoon waters that were collected throughout this study were analyzed for 2-amino-4,6-dinitrobenzoic acid. The results (Table 4) suggest that 2-amino-4,6-dinitrobenzoic acid is a major transformation product in lagoon waters.

The lagoon waters were found to be nearly saturated with oxygen. Measurements taken with a dissolved oxygen probe during the December field trip indicated 9.0 ppm O_2 at the surface and 8.8 ppm near the bottom sediment (50 cm deep). In such a highly aerated environment, nitrite is readily oxidized. In fact, when the lagoon water collected in December 1981 was analyzed for nitrite and nitrate according to the method of Thayer (1979), only nitrate was found (16.7 ppm); the pH of the lagoon waters ranged from 7.3 to 7.8, and the total dissolved solids concentration was 540 ppm.

Absorbance measurements were obtained at 290 and 400 nm as indicators of the light-absorbing properties of the lagoon water as a function of time of year. These values, reported in Table 5 along with the measured water volume at the sampling date, indicate that the UV-absorbing materials are concentrated as the lagoon waters evaporate, as evidenced by a 3-fold increase in the absorbance between December and August with the concurrent decrease in volume by a factor of three over the same period. This has the effect of reducing the penetrability of light into the lagoon water in the summer months compared to winter.

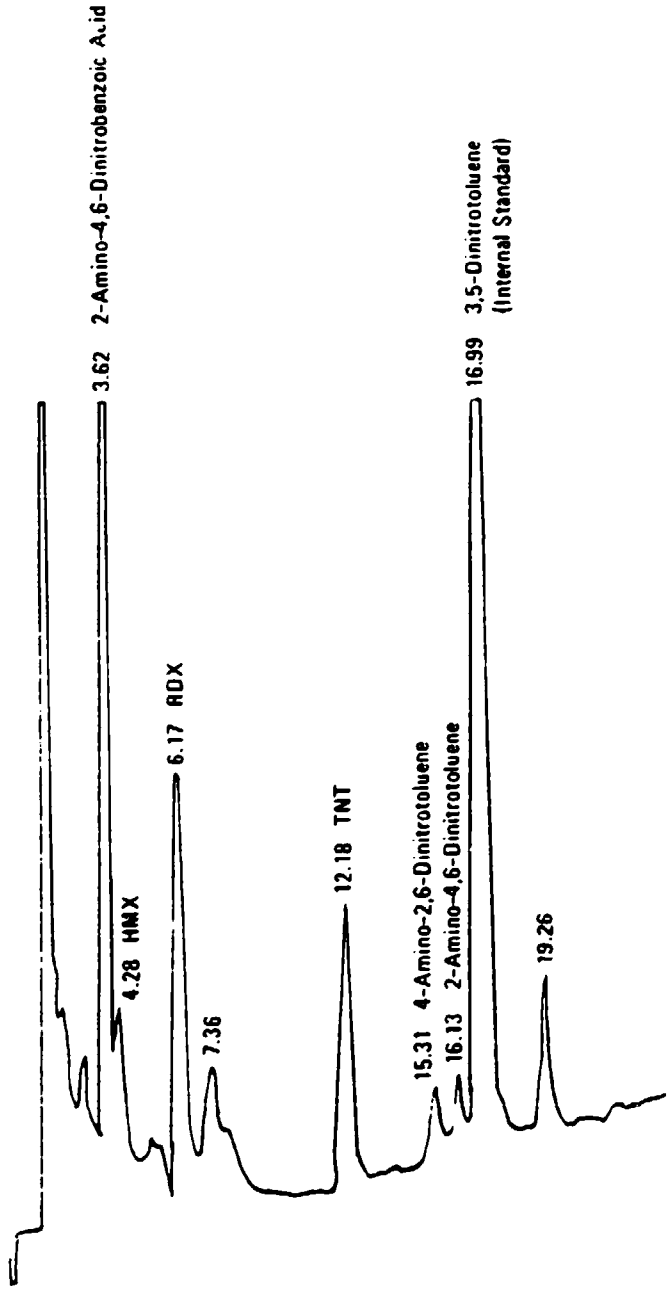

FIGURE 5 HPLC PROFILE OF LAGOON WATER RESOLVING 2-AMINO-4,6-DINITRO BENZOIC ACID AND OTHER COMPONENTS

Table 4

LEVELS OF 2-AMINO-4,6-DINITROBENZOIC ACID OBSERVED IN LAGOON NO. 9 ON VARIOUS SAMPLING DATES

Date of Sample	2-Amino-4,6-Dinitrobenzoic Acid ($mg\ \ell^{-1}$)
12/18/81	28.9
03/15/82	24.3
03/15/82	24.3
05/25/82	30.7
06/09/82	35.2
06/23/82	43.9
07/07/82	45.5
08/04/82	49.9
08/20/82	45.7

Table 5

ABSORBANCE VALUES OF LAGOON NO.9 WATER AT 290 AND 400 nm AT VARIOUS TIMES OF THE YEAR

Date of Sample	Absorbance (1-cm cell)		Lagoon Volume, m^3
	290 nm	400 nm	
12/08/81	3.19	1.41	1772
03/15/82	3.21	1.38	
06/09/82	4.68	2.01	1270
06/23/82	5.28	2.25	
07/07/82	6.09	2.56	
08/04/82	9.78	4.27	532
08/20/82	8.62	3.74	
09/03/82	9.44	4.21	

IV. SITE EVALUATION

On the basis of on-site observations and analysis of the lagoon waters, transformation products, and sediments, we conclude that the lagoon is a complex environment governed by chemical inputs that are dependent on lagoon water temperature and transformation rates, which in turn are dependent on time of year, natural sensitizers, and depth at which measurements are made.

Near the dump ramp we found levels of TNT and RDX in the sediment (15 and 8%, respectively) that were significantly greater than amounts that would result from sorption alone. This suggested that particulate munitions were present; in fact, when the lagoon surface became visible, chunks of pure TNT appeared on the surface sediment. The percent of munitions in the sediment decreased as a function of distance from the dump ramp. Therefore, chemical input to the lagoon is controlled by diffusion of chemical through the sediment and dissolution of pure chemicals from the sediment surface to the bulk-water phase. Because the bottom sediment is a heterogeneous system, we could only estimate chemical inputs based on limited laboratory investigations.

Transformation products found in the lagoon suggested that both biological and photochemical transformations were occurring in the lagoon (see above). Most of the light is absorbed in the first few millimeters of the lagoon; consequently, good vertical mixing is required to renew depleted chemicals as rapidly as they are transformed. If good mixing is achieved, then a photochemical rate constant can be estimated as a function of depth. Moreover, because absorption of the sunlight by the lagoon produces radiant heat, lagoon water temperature varies widely throughout the year; for example, it was 10°C in December, 41.5°C in July. This increase in temperature could have a large impact on microbial populations and hence on

biotransformation rates; in addition, it could accelerate diffusion and dissolution rates of chemicals from the bottom sediment.

Estimation of the concentration of a chemical at any particular time is further complicated by the water balance within the lagoon. Water enters the lagoon through precipitation and is lost through evaporation and seepage. Therefore, an understanding of water input and output rates is an integral part of this fate assessment.

On the basis of the above evaluations, we perceived a number of processes that were affecting the concentration of chemicals in the lagoon environment. Processes that would increase concentration of a chemical in the lagoon water include 1) water evaporation and seepage, 2) dissolution of a pure chemical from the sediment surface, and 3) diffusion of munitions from the sediment. Processes that would decrease the concentration in the water include 1) precipitation, 2) photochemical transformation, and 3) biological transformation. We therefore performed laboratory investigations of these processes to provide rate and equilibrium constants that are applicable to the lagoon environment. From these data, we constructed a computer model to simulate the processes in the lagoon and compared the simulation data with actual data obtained for the lagoon.

V. TRANSPORT AND TRANSFORMATION STUDIES

A. Physical Transport

1. Water Balance

The volume of water in the lagoon is controlled primarily by precipitation, evaporation, and vertical seepage. Surface runoff or horizontal seepage was considered to have little impact on the net volume changes due to the flat bottom and banking of the lagoon.

We created a water-volume balance expression using:

$$\frac{dV}{dt} = R_p - R_{ev} - R_\ell \quad , \qquad (1)$$

where $R_p = r_p A$

$R_{ev} = r_{ev} A$

$R_\ell = r_\ell A$

and r_p represents precipitation, r_{ev} represents evaporation, r_ℓ represents leaching (all in cm day^{-1}), and A represents the surface area of the lagoon. Average values of r_{ev} and r_p were obtained from three years of weather data (1979-1981) collected by the Red River weather station near LAAP; these are shown in Table 6. Similar data for 1982 through August are presented in Table 7.

Leaching is usually estimated by a difference determination of volumes when the volume loss from evaporation is known. During the December field study we calculated the leaching rate to be 0.17 cm day^{-1}. However, we used this parameter as a variable in the model to adjust the overall water balance to approximate that observed in the lagoon.

Table 6

AVERAGE MONTHLY PRECIPITATION AND EVAPORATION DATA FROM 1979 THROUGH 1981 AT RED RIVER WEATHER STATION, RESTIN, LA

Month	Precipitation (cm/day)	Evaporation (cm/day)
1	0.28	0.13
2	0.30	0.20
3	0.46	0.35
4	0.34	0.45
5	0.61	0.52
6	0.28	0.67
7	0.39	0.69
8	0.12	0.66
9	0.18	0.50
10	0.44	0.38
11	0.25	0.20
12	0.16	0.17

Table 7

MONTHLY PRECIPITATION AND EVAPORATION DATA FROM JANUARY 1982 THROUGH AUGUST 1982 AT RED RIVER WEATHER STATION, RESTIN, LA

Month	Precipitation (cm/day)	Evaporation (cm/day)
Jan	0.31	0.13
Feb	0.26	0.15
Mar	0.19	0.29
Apr	0.27	0.34
May	0.17	0.59
June	0.22	0.61
July	0.25	0.62
Aug	0.17	0.62

Using the data in Tables 6 and 7, we plotted the depth of the lagoon as a function of time of year for various seepage rates (Figure 6). From depth measurements taken at various time points in the lagoon we found that a seepage rate of 0.12 cm day^{-1} gave the best approximation to the actual depths. This seepage rate projected the lagoon to go dry on Day 234 (August 22); the lagoon actually went dry during the following week. We therefore used the depth profile defined by the 0.12 cm day^{-1} seepage rate curve to determine the water volume on any particular day and to define the depth that was critical in estimating the magnitude of the photochemical rate constant at any particular time.

2. TNT and RDX Solubility

The aqueous solubilities of TNT and RDX were determined separately at 10, 20, and 30°C and simultaneously at 20°C by the method of May et al. (1978). Briefly, glass beads were coated with TNT or RDX and packed into a column. Then water was percolated through the column. After an equilibration period, the concentration of TNT or RDX was measured in the column effluent. As a check on this method, the solubilities of TNT and RDX were measured at 20°C by the method of Campbell (1930), in which the solids are equilibrated with water in a thermostated bath and filtered. The solubilities using the two methods are shown in Table 8.

Table 8

SOLUBILITY OF TNT AND RDX IN WATER AT 10, 20, AND 30°C

	TNT (mg/liter)			RDX (mg/liter)		
Method	10°C	20°C	30°C	10°C	20°C	30°C
May et al.	67 ± 1	104 ± 2	165 ± 2	21.9 ± 0.3	38.4 ± 0.4	67.0 ± 0.8
Campbell		113 ± 8			39 ± 2	

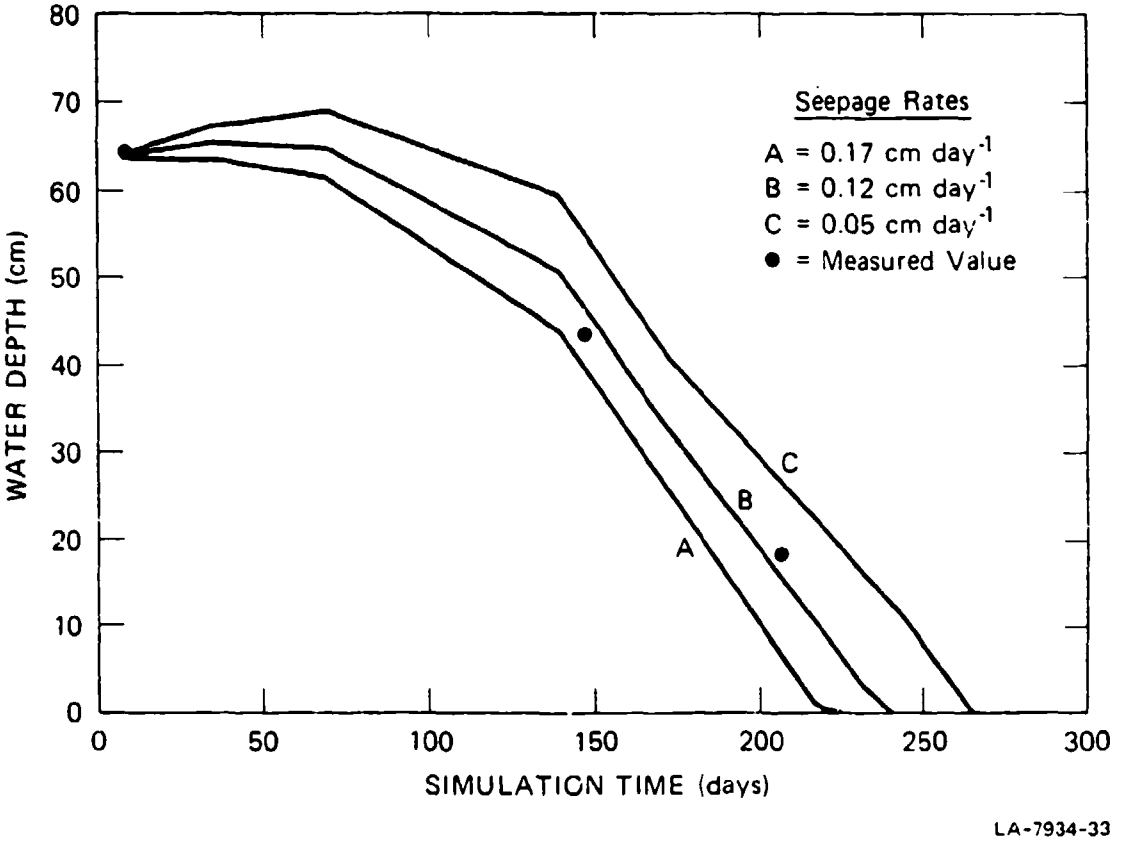

FIGURE 6 ESTIMATION OF LAGOON DEPTH PROFILE BASED ON VARIABLE SEEPAGE RATES

Solubilities were measured by the May method first at 10°, then 20°, then 30°C, and finally again at 10°C. No significant differences were noted between the two measurements at 10°C. The similarity of the measurements at 10°C demonstrates the repeatability of the method after equilibrating the column and showed that the column was not exhausted. Concentration versus flow-rate measurements were made to check that the saturation capacity of the column had not been exceeded. Finally, a column containing both RDX and TNT was used to measure the solubility of one compound in the presence of a saturated solution of the other compound. Solubilities obtained for RDX and TNT independently were in agreement within the standard error of the values for RDX and TNT in the presence of the other compound.

The results of the two methods are in agreement within the error of each measurement. The Campbell solubility values show a greater error than those using the May method, perhaps because the Campbell method requires more handling of the samples.

Because the temperature of the lagoon water ranged from 10° to 41°C, we developed mathematical expressions to use in the computer modeling to correlate solubility with temperature. These expressions are shown in Equations 2 and 3:

$$S_{TNT} = 5.567 \times 10^{7} \exp\left(\frac{-3860^{\circ}K}{T}\right) \mu g\ ml^{-1} \quad ; \quad (2)$$

$$S_{RDX} = 4.974 \times 10^{7} \exp\left(\frac{-4795^{\circ}K}{T}\right) \mu g\ ml^{-1} \quad . \quad (3)$$

The measured and calculated solubility values for TNT and RDX at 10°, 20°, and 30°C (283, 293, and 303°K) are shown in Table 9.

Table 9

MEASURED AND CALCULATED SOLUBILITIES (mg liter^{-1}) OF TNT AND RDX AT 283, 293, AND 303°K

Water Temperature (°K)	TNT		RDX	
	Measured	Calculated	Measured	Calculated
283	67	66.4	21.9	21.8
293	104	105.7	38.4	38.9
303	165	163.3	67	66.7

3. Sediment Sorption

It is generally accepted that adsorption of organics on soils and sediments usually fits the empirical Freundlich isotherm (Equation 4):

$$C_s = KC_w^n \quad , \qquad (4)$$

where C_s is the equilibrium concentration on the sediment ($\mu g\ g^{-1}$), C_w is the equilibrium concentration in the aqueous phase ($\mu g\ ml^{-1} = \mu g\ g^{-1}$), and K and n are constants. Thus, a plot of the logarithms of C_s versus C_w has a slope of n and an intercept of K. If n is equal to 1, the adsorption isotherm is linear and K is equal to K_s. If pure TNT and RDX are present, as in the LAAP lagoon, C_w is the saturated concentration regardless of C_s and the Freundlich isotherm may not hold.

We performed several isotherm measurements and fitted the data to both the linear ($C_s = K_p C_w$) and nonlinear ($\log C_s = \log K_p + n \log C_w$) cases. Very high values of K_p were obtained from the nonlinear equation and were rejected in favor of more reasonable values obtained from the linear equation. These K_p values, along with the calculated K_{oc} values (based on a measured organic carbon content of 1.5%), appear in Table 10.

Table 10

SORPTION PARTITION COEFFICIENTS FOR TNT AND RDX IN LAAP LAGOON NO. 9 SEDIMENT

Chemical	K_p	K_{oc}
TNT	7 ± 2	470 ± 130
RDX	4 ± 7	270 ± 470

4. Distribution of TNT and RDX in Sediment Cores

Several core samples were taken throughout the lagoon during the December 1982 visit to determine the horizontal and vertical distribution of RDX and TNT in the lagoon sediment. A 51-cm core sediment sample from the southeast corner of the lagoon was cut into 5-cm segments. Each segment was analyzed for percent TNT, RDX, and dry sediment. The results are presented in Table 11.

Table 11

SEDIMENT CORE SAMPLE DRY WEIGHT AND PERCENT TNT AND RDX WEIGHTS

Core Segment (cm from top)	% Dry Weight	% TNT[a]	% RDX[a]
5	71.5	9.34	12.6
5 - 10	76.8	2.74	1.28
10 - 15	79.4	2.38	0.83
15 - 20	80.3	1.25	0.39
20 - 25	83.2	0.14	0.004
25 - 31	82.8	0.010	0.005
31 - 36	82.3	0.0052	0.0065
36 - 41	82.3	0.0052	0.0065
41 - 46	83.2	0.023	0.029
46 - 51	74.2	0.04	0.04

[a]Based on dry weight of sediment.

Saturated sediment is represented by a concentration of >0.60% for TNT and >0.033% for RDX. Although the TNT and RDX concentrations in the sediment decrease with depth, the data suggest that the amounts exceed the absorption capacity for TNT and RDX at depths less than 25 cm and greater than 50 cm, respectively. The high amounts of TNT and RDX in the surface sediments suggest that the sediment is a source of these munitions in the lagoon water.

To determine the horizontal distribution of TNT and RDX, we took another set of core samples--three from the southeast (SE) corner and one each from the northwest (NW), southwest (SW), and northeast (NE) corners of the lagoon. The cores were about 12 cm in depth and were cut into 1-cm segments, which were extracted and analyzed by HPLC for their RDX and TNT content. The results are presented in Table 12.

Only the top and bottom three sections of each core were analyzed. Concentrations of TNT and RDX were highest in the SE cores, which are near the dump ramp, and they rapidly decrease with depth, as shown by comparing the top three sections with the bottom three. The TNT and RDX concentrations in the NW, NE, and SW cores are low and uniform throughout the core as compared with the SE cores.

5. Mass Transfer Rate From Sediment

The presence of sorbed and solid munitions chemicals in the LAAP sediment presents a complex problem in establishing the mass transfer rate of chemicals to the bulk-water phase. The processes that may be occurring in a sediment pore, described pictorially in Figure 7, include diffusion, seepage, sorption-desorption equilibria, transformation, and dissolution of solid munitions. These proceses can be described mathematically and their sum can be used to compute the overall mass transfer rate.

Diffusion is generally accepted as a second-order differential expression relating changes in the chemical concentration in the sediment (C_{sw}) with respect to depth (z) times a diffusion constant D_1. Seepage is a first-order differential expression relating

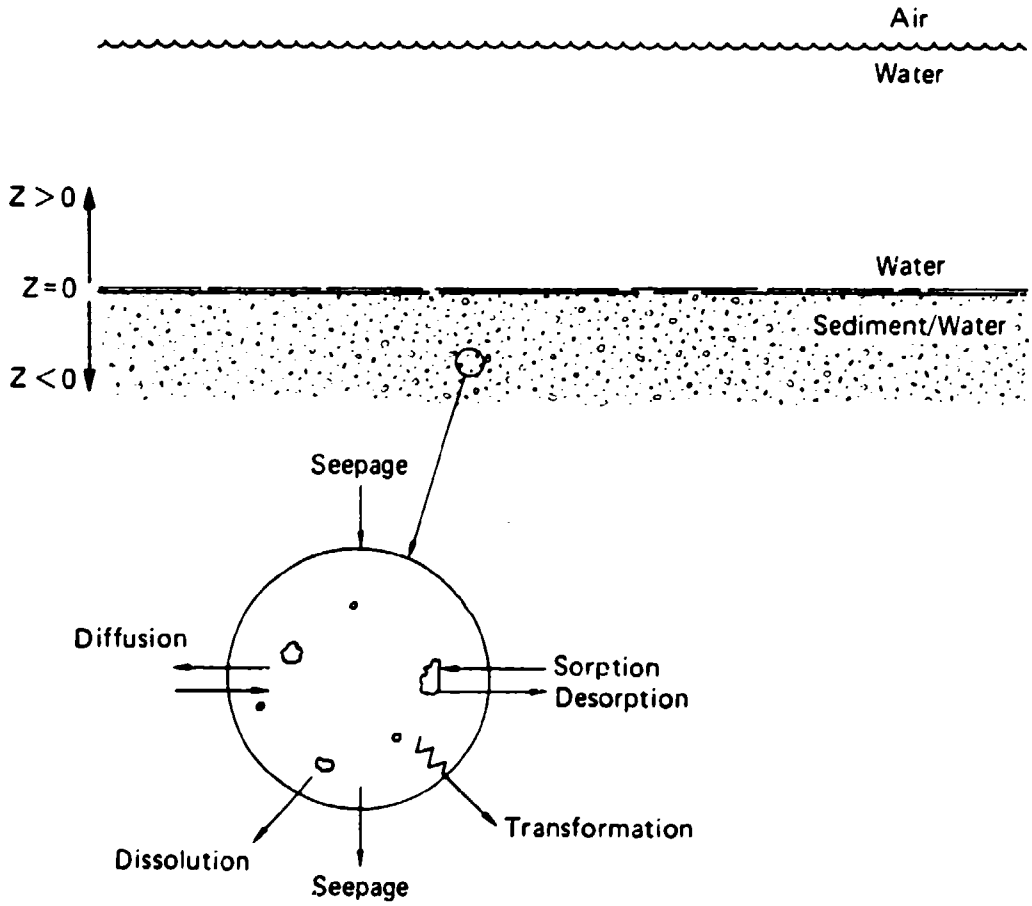

FIGURE 7 LAGOON WATER RESTS ON SEDIMENT

Pond and sediment are considered to be semi-infinite.

concentration to depth times a seepage velocity factor, v. The sorption-desorption equation was defined in Equation 4. The only transformation process believed to be occurring in the sediment is

Table 12

TNT AND RDX IN SECTIONED CORES FROM LAAP LAGOON NO. 9

Sample No.[a]	Section Identification					
	SE-A	SE-B	SE-C	NW	SW	NE
	TNT ($\mu g\ g^{-1}$)					
12					0.05	
11	501	6.4	367	0.04	0.55	0.03
10	525	71	38	0.05	0.23	0.1^
9	---	109	280	0.02	0.08	---
3	91	0.4	5.5	0.14	0.16	0.009
2	27	1.2	2.9	0.09	0.28	0.03
1	26	0.7	1.4	0.06	0.13	0.05
	RDX ($\mu g\ g^{-1}$)					
12					0.10	
11	89	3.0	88	0.01	0.01	0.02
10	48	22	226	0.02	0.02	0.01
9	--	51	88	0.01	0.01	---
3	4.7	0.2	2.1	0.05	0.05	0.001
2	1.3	0.3	0.8	0.05	0.05	0.02
1	1.3	0.3	0.9	0.01	0.01	0.04

[a]Sample 12 is at surface, sample 1 is lowest below surface.

biotransformation. Because of the high concentrations of munitions in the sediment, biotransformation is believed to be a zero-order process (k_o) for TNT (see Biotransformation, Section V.C).

To account for the dissolution, we envision solid TNT/RDX dispersed homogeneously throughout the sediment. The dissolution rate of any solid TNT or RDX, $\frac{dw}{dt}$, can be written as Equation 5:

$$\frac{dw}{dt} = k_r(C_{sat} - C_i) \quad , \tag{5}$$

where k_r is an experimentally determined dissolution coefficient, C_{sat} is the saturation concentration of the dissolving species in the liquid phase, and C_i is the actual concentration of the dissolving species at the solid/liquid interface.* If diffusion from the interface into the surrounding liquid is fast compared to dissolution, then C_i is approximately equal to the concentration of the dissolved species in the surrounding liquid. In this limit,

$$\frac{dw}{dt} = k_r(C_{sat} - C_{sw}) \quad . \tag{6}$$

Therefore, in the sediment, the change in chemical concentration with time ($\frac{\partial C_{sw}}{\partial t}$) is equal to the sum of the dissolution rate (Equation 6), diffusion rate ($D_l \frac{\partial^2 C_{sw}}{\partial z^2}$), and seepage rate ($\frac{\partial C_{sw}}{\partial z}$) minus the biotransformation rate (k_o, zero-order process in the sediment) and the amount of chemical that is sorbed to the sediment ($K_p n C_{sw}^{n-1} \frac{\partial C_{sw}}{\partial t}$) or

---

*This is a standard "concentration driving force" model that has been adopted by many workers (Wurster and Kildsig, 1965).

$$\frac{\partial C_{sw}}{\partial t} = k_{dis}[C_{sat} - C_{sw}] + D_1 \frac{\partial^2 C_{sw}}{\partial z^2} + v \frac{\partial C_{sw}}{\partial z} - k_o - K_p n C_{sw}^{n-1} \frac{\partial C_{sw}}{\partial t} . \quad (7)$$

Rearranging Equation 7 yields Equation 8:

$$(1 + K_p n C_{sw}^{n-1}) \frac{\partial C_{sw}}{\partial t} = k_{dis}[C_{sat} - C_{sw}] + D_1 \frac{\partial^2 C_{sw}}{\partial z^2} + v \frac{\partial C_{sw}}{\partial z} - k_o , \quad (8)$$

where C_{sw} = chemical concentration in the sediment/water phase

K_p = sediment partition coefficient ($C_s = K_p C_{sw}^n$)

t = time

D_1 = diffusion coefficient in the sediment/water phase

v = seepage velocity

z = distance from the sediment

k_o = zero-order rate constant for biotransformation in sediment.

Similarly, for the free-water phase, the change in concentration of a chemical with time can be described by

$$\frac{\partial C_w}{\partial t} = k_{dis}[C_{sat} - C_w] + D_2\frac{\partial^2 C_w}{\partial z^2} + v\frac{\partial C_w}{\partial z} - \Sigma k_1 C_w \quad , \tag{9}$$

where C_w = concentration of chemical in the free-water phase

t = time

D_2 = diffusion coefficient in the free-water phase

v = seepage velocity

$\Sigma k_1 C_w$ = first-order rate expression for the transformation process.

Solutions to these equations and the assumptions that are used to arrive at solutions appear in Appendix B. However, laboratory studies were necessary to determine k_{dis} so that a flux from the lagoon sediment could be computed.

6. Determination of TNT and RDX Flux Values for Sediment from LAAP Lagoon No. 9

From the sediment analyses and the visual observations of pure TNT and RDX on the sediment surface, we recognized that the bottom sediment was the predominant input source of TNT and RDX to the lagoon waters during the period of our study. Therefore, we designed experiments to determine the flux of these chemicals to the bulk-water phase.

To determine the fluxes, 460 g of LAAP Lagoon No. 9 sediment containing 12% TNT and 9% RDX was placed in a 1000-ml beaker (surface area, 780 cm) equipped with a water-inlet port directly above the sediment and a water-outlet port near the top of the beaker. The beaker was wrapped in aluminum foil. Water was pumped into the beaker from a Milton-Roy precision pump at various flow rates and stirred slowly with an overhead stirrer. The effluent was collected to verify total water volumes passing through the beaker. TNT and RDX in the

effluent were monitored until equilibrium values were obtained (usually in 3 to 4 days). We calculated the flux, N, from Equation 10:

$$N = \frac{CQ}{A} \quad , \tag{10}$$

where C = concentration of chemical at equilibrium

Q = flow rate through the beaker

A = surface area of the sediment.

Values for the fluxes of TNT and RDX at various flow rates are shown in Table 13. We would expect that as the flow rate increased, the concentration of chemical would decrease and the flux would increase. The changes in concentration between runs A and B for TNT and B and C for RDX do not follow the proper concentration trend. Also, the changes in flux between runs D and E for TNT and RDX do not follow the proper flux trend. These observations cannot be explained by any mass transfer model; however, we cannot be certain whether any of the data points are more or less valid than others and must

Table 13

TNT AND FLUX MEASUREMENTS
FROM LAAP LAGOON NO. 9 SEDIMENT

Run Code (Number)	Water Flow Rate (Q) ($ml\ min^{-1}$)	TNT (C) ($\mu g\ ml^{-1}$)	TNT Flux (N) ($10^{-9}\ g\ cm^{-2}\ sec^{-1}$)	RDX (C) ($\mu g\ ml^{-1}$)	RDX Flux (N) ($10^{-9}\ g\ cm^{-2}\ sec^{-1}$)
A (2)	1.9	16.9	6.8	5.6	2.3
B (5)	3.0	19.9	12.7	5.0	3.2
C (3)	3.3	18.5	12.9	5.5	3.8
D (4)	7.0	13.8	20.5	3.5	5.2
E (1)	8.1	5.7	9.8	2.0	3.4

allow for the imprecision of the data in our interpretations. A plot of TNT and RDX flux versus concentration appears in Figure 8.

From this plot and linear least-squares analysis (Appendix B) we calculated the TNT flux to be 1.08×10^{-4} cm sec^{-1} and the RDX flux to be 7.75×10^{-5} cm sec^{-1} in the lagoon. The first-order dissolution rate constants were calculated to be 1.18×10^{-5} cm sec^{-1} for TNT and 1.16×10^{-5} cm sec^{-1} for RDX (see Appendix B).

B. Photochemistry

Photochemical transformation of TNT in the lagoon environment was evident from the identification of photolytic transformation products and the deep orange-red color of the water that is reminiscent of the "pink water" at TNT production facilities. Because lagoon water absorbs all UV light near the surface, the photochemical rate constant has a depth dependence of the form $k_p' = k_p/D$. Moreover, the value of k_p/D also is subject to variations owing to changes in light intensity with changes in cloud cover and season.

1. TNT Photochemical Rate Constant--General Remarks

Usually, photochemical kinetic studies are performed using solutions that absorb less than 5% of the incident light. The amount of light absorbed at wavelength λ by a solution is given by the Beer-Lambert Law (Equations 11 and 12):

$$I_\lambda = I_o(1 - 10^{-A}) \quad , \tag{11}$$

$$A = \varepsilon_\lambda C\ell + \alpha_\lambda \ell \quad , \tag{12}$$

where I_o and I_λ are the incident and absorbed light intensities, respectively, A is the absorbance, ℓ is the path length of light in solution, C is the concentration of chemical, ε_λ is the molar absorption coefficient of a chemical at wavelength λ, and α_λ is the

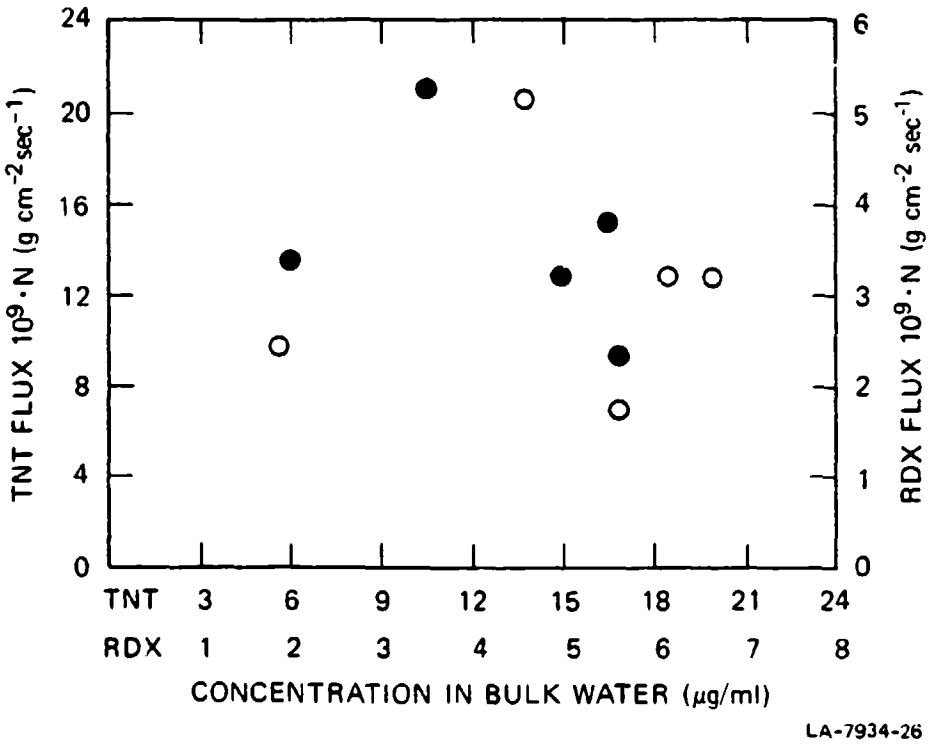

FIGURE 8 TNT (●) AND RDX (○) FLUX FOR LAAP LAGOON NO. 9 SEDIMENT

absorbance of solution without added chemical at wavelength λ in a 1-cm cell. The α_λ term is useful for characterizing a natural water because the molar concentration of humic acids and their ε_λ values in water are difficult to determine. Because I_λ is a function of pathlength ℓ, the value for I_λ can be calculated for any pathlength in solution.

If the solution absorbs less than 2% of the incident light ($A < 0.02$), Equation 11 takes the form of Equation 13:

$$I_\lambda = 2.3 I_o A \quad , \tag{13}$$

and the rate constant for photolysis, k_p, is given by Equation 14:

$$k_p = 2.3 \phi \varepsilon_\lambda I_o \ell \quad , \tag{14}$$

where ϕ is the photolysis reaction quantum yield (Mabey et al., 1982).

However, if the solution absorbs a significant amount of light due to some combination of long pathlength and/or large εC or α_λ values, then the photolysis rate constant will show a dependence on pathlength due to attenuation of I_o with increased absorbance, and the resulting equation for k_p is more complicated.

The solar photolysis rate constant k_{pE} for chemicals in aquatic systems in optically thin solutions (i.e., near the surface) can be calculated from Equation 15:

$$k_{pE} = b \phi \Sigma \varepsilon_\lambda I_\lambda \quad , \tag{15}$$

where b is a unit conversion factor and $\varepsilon_\lambda I_\lambda$ values for each wavelength interval are summed over the entire solar spectral region. If the water has a large $\alpha_\lambda \ell$ value, Equation 15 becomes more

complex because the α_λ values decrease as wavelengths become longer, and therefore longer wavelength light penetrates natural waters to greater depths than does shorter (more energetic) wavelength light.

Table 14 shows the $(\alpha_\lambda + \varepsilon_\lambda C)$ values at selected wavelengths for the LAAP water collected in December 1981 and the depths at which 99% of incident light at each wavelength is absorbed. These data clearly show that light of wavelengths below 500 nm will not penetrate below the top few centimeters of LAAP water. The absorbance of the water is almost entirely due to substances other than TNT ($\alpha_\lambda >> \varepsilon_\lambda C$); absorbance of 6 ppm TNT in a 1.0-cm cell is 0.02 AU at 320 nm (ε_λ = 840 M^{-1} cm^{-1}), which is negligible compared to the 2.60 AU measured for the water at 320 nm.

Table 14

DEPTH FOR 99% ABSORPTION OF LIGHT
OF SPECIFIC WAVELENGTHS FOR LAAP WATER

Wavelength, λ, (nm)	$(\alpha_\lambda + \varepsilon_\lambda C)^a$ (cm^{-1})	$D_{(cm)}^{99\%A}$
300	3.32	0.60
320	2.60	0.77
340	2.32	0.86
360	2.10	0.95
380	1.93	1.04
400	1.74	1.15
420	1.47	1.36
440	1.23	1.62
460	0.95	2.11
480	0.74	2.71
505	0.58	3.45
585	0.28	7.04
655	0.07	27.00

[a]Absorbance measured in 1.0-cm cell; light absorption is entirely due to substances other than TNT in the water (see text).

The TNT photolysis rate constant for use in modeling the fate of TNT in LAAP water must account for the loss of TNT in the entire volume of the lagoon. Although the mass of TNT undergoing photolytic transformation per unit time is dependent only on light intensity and spectral distribution entering the water, the rate of change of TNT concentration is dependent on volume. For photolysis of TNT in solution out of the photic zone, the rate constant must then be an inverse function of depth. The theory and validation of the procedure for estimating the photolysis rate constant in LAAP water where the photic zone is shallow compared to the total depth of the water are developed and discussed in the next section.

2. Effect of Depth on Photolysis Rate Constant of TNT in LAAP Water

To estimate a rate constant for TNT in LAAP water, we have developed an expression that relates the TNT photolysis rate constant to lagoon depth (D). This expression is valid only if vertical mixing in the lagoon is substantially faster than the photolysis rate of TNT near the surface so that the TNT concentration is the same throughout the lagoon. The expression also assumes that TNT decomposes by indirect photolysis; the data in Table 14 clearly show that substances other than TNT account for the major absorption of light, and our previous studies have demonstrated that indirect photolysis of TNT in natural waters is more rapid than direct photolysis (Spanggord et al., 1981). Light energy is absorbed by substances present in LAAP water (humic and fulvic acids, TNT reaction products, and other chemical contaminants in the lagoon water) and is then transferred to or induces reaction of TNT. TNT reacts even though it does not absorb light directly.

The proposed mechanism for TNT photolysis is described by Equations 16 to 19 below:

$$S + h_\upsilon \rightarrow S^* \quad , \tag{16}$$

$$S^* \xrightarrow{k_2} S \quad , \tag{17}$$

$$S^* + TNT \xrightarrow{k_3} S + TNT^* \quad , \tag{18}$$

$$TNT^* \xrightarrow{k_4} (f)\ (products) + (1 - f)\ (TNT) \quad , \tag{19}$$

where S is the sensitizer, S* and TNT* are excited states, and f is the fraction of TNT converted to products. The rate of photo-absorption, R (Equation 16), per unit volume is shown in Equation 20:

$$R = I_o A/V = I_o/D \quad , \tag{20}$$

where I_o is the incident light intensity (Einstein's per unit area per second), A is the exposed surface area, V is the volume of the container, and D is the average depth.

The quantum yield, ϕ, for TNT loss is defined in Equation 21:

$$\phi = \phi_{S*} k_3[TNT] f/(k_3[TNT] + k_2) \quad , \tag{21}$$

where ϕ_{S*} is the quantum yield for production of S^*. In dilute solutions of TNT, where $k_2 >> k_3[TNT]$,

$$\phi = \phi_{S*} k_3[TNT] f/k_2 \quad . \tag{22}$$

The loss rate of TNT can be defined as the TNT quantum yield times the rate of light absorption of the water body. Then,

$$d[TNT]/dt = \phi R = I_o \phi_{S*} k_3 [TNT] f / k_2 D \quad , \tag{23}$$

$$d[TNT]/[TNT] = f I_o \phi_S k_3 / k_2 D \quad . \tag{24}$$

On rearrangement and integration,

$$\ln([TNT]_0/[TNT]_t) = f I_o (k_3/k_2) \phi_S t/D = k_p t \tag{25}$$

and

$$k_p = f I_o (k_3/k_2) \phi_{S*}/D \quad . \tag{26}$$

I_o and D depend on sky conditions and lagoon geometry, respectively. D can be calculated for water in a container with vertical sides and a horizontal bottom.

By making the substitution $k_p' = I_o f (k_3/k_2) \phi_{S*}$ into Equation 26, we obtain Equation 27, which states that k_p will vary inversely with depth:

$$k_{pD} = k_p'/D \quad . \tag{27}$$

For containers of depth D_1 and D_2, respectively, relative photolysis rate constants can be calculated from Equation 28:

$$\frac{k_{pD_1}}{k_{pD_2}} = \frac{D_2}{D_1} \quad . \tag{28}$$

Using Equation 28, we can calculate the TNT photolysis rate constant in the lagoon from the sunlight photolysis rate constant measured for TNT in LAAP water in a shallow container. This is the only practical way to measure k_p because TNT in LAAP lagoon water photolyses too slowly in the lagoon or in containers of the same depth for convenient measurement.

3. Experimental Verification of Equation 27

To demonstrate the validity of Equation 27, we first photolyzed LAAP water with a constant intensity source in a merry-go-round apparatus (MGR) to determine the TNT concentration-time dependence of Equation 25. If Equation 25 holds, then a first-order plot (ln[TNT] versus time) will be linear. For these experiments, LAAP water containing 5 ppm TNT was irradiated in 13 × 100-mm borosilicate tubes with monochromatic light at 313 or 366 nm at room temperature.

The data for these experiments are summarized in Table 15 along with data for the same solution in tubes exposed to sunlight on January 22, 1982.

Table 15

PHOTOLYSIS OF 4.97 ppm TNT IN LAAP WATER IN AN MGR APPARATUS AND IN SUNLIGHT

Light Source	Duration of Experiment (min)	Final TNT Concentration (ppm)	10^3 k_p (min^{-1})
313 nm	110	3.29	4.30 ± 0.07
366 nm	240	2.34	3.17 ± 0.11
Sunlight (Jan. 22)	80	2.49	8.51 ± 0.23

First-order treatment of these data gave linear plots, as expected. Similar first-order behavior was observed in all other experiments.

We then verified Equations 27 and 28 by irradiating LAAP water in cylinders of different depths using a solar simulator light source--an intensity-regulated, 300-watt xenon lamp. Radiation from the lamp was filtered through water to remove infrared wavelengths and then through borosilicate glass to remove high-energy UV light. Cylinders were filled to depths of 2.0, 4.2, and 7.0 cm and irradiated from above. The sides and bottoms of the cylinders were blackened to reduce reflection and to prevent light from entering through the sides. Data from these experiments are shown in Table 16.

The observed photolysis rate constants are in the ratio 4.05:1.75:1.0; the expected values are 3.5:2.1:1.0. Stirring had no effect on the photolysis rate constant: when the stirrer was turned off after 240 min of irradiation of the dish containing 4.2 cm LAAP water, the rate constant did not change. We conclude that natural mixing of the LAAP water in our experiments was sufficiently fast to keep the mixture homogeneous and not allow depletion of TNT in the upper irradiated layers, which would slow down the reaction.

Table 16

PHOTOLYIS OF 4.97 ppm TNT IN LAAP WATER
AS A FUNCTION OF DEPTH USING A XENON LAMP[a]

Duration of Experiment (min)	Water Depth (cm)	Final TNT Concentration (ppm)	10^3 k_p (min^{-1})[b]
236	2.0	1.81	4.21 ± 0.09
542	4.2	1.81	1.82 ± 0.02
1075	7.0	1.33	1.04 ± 0.03

[a]300-W controlled-current lamp.
[b]r^2 = 0.99.

Finally, we exposed LAAP water to sunlight to measure TNT rate constants that could be adjusted for depth. Actinometer solutions of PNA/PYR were exposed to sunlight in parallel studies so that corrections for sky conditions could be made (discussed in the next section). These data permit calculation of the TNT photolysis rate constant in the LAAP lagoon for any water depth.

To measure the depth-independent photolysis rate constant k'_p for TNT exposed to sunlight, LAAP water filtered through a 0.45-micron filter was placed in opaque glass cylinders whose tops were exposed to sunlight on March 12 and 15, 1982. On the first day the container was filled to a 4.2 cm depth and on the other day the depth was 3.5 cm. The experimental conditions and results are given in Table 17, uncorrected for sky conditions.

If we assume that an insignificant amount of TNT photolysis occurred before the experiment began and after the experiment was ended on each day, the measured rate constant k_p (in m^{-1}) can be readily converted into a 24-hour day-averaged rate constant k_p (in

d^{-1}) by multiplying the observed rate constant by the fraction of a 24-hour day that the irradiation period represented. Multiplication of the latter by the depth value then gives a value of 3.0 cm d^{-1}, which is the depth-independent rate constant, k_p', used in Equation 26 for photolysis of TNT in LAAP water under weather conditions of mid-March. To obtain a rate constant for a specific depth, k_p' is divided by the lagoon depth. We must also correct k_p' for sky conditions during the experiments.

Table 17

SUNLIGHT PHOTOLYSIS OF 4.97 ppm TNT IN LAAP WATER[a,b] AND ACTINOMETERS

Date	3-12-82	3-15-82
Time	8:45-16:00	9:40-15:30
Sky Conditions	bright, sunny w/ low clouds	cloudy + hazy, windy
Depth, cm	4.2	3.5
Time, min	435	350
$k_p \times 10^3$, m^{-1}	1.67 ± 0.045	2.51 ± 0.041
$t_{1/2}$ h	6.9	4.6
k_p d^{-1} (day averaged)[c]	0.72	0.89
k_p' cm d^{-1}	3.02	3.12
k_p' cm d^{-1}, clear sky conditions	4.14	4.27

[a]Photolyses monitored using PNA/PYR actinometer [PYR] = 1.25×10^{-3} M; k_p (PNA) = 4.8×10^{-3} m^{-1}.

[b]All rate constants are uncorrected for sky conditions.

[c]k_p (day averaged) was calculated by multiplying the observed photolysis rate constant expressed in units of d^{-1} by the fraction of a 24-hour day that the irradiation represented.

4. Correction of Measured Rate Constants for Weather Conditions

Sunlight photolysis rate constants are dependent on weather conditions as well as the diurnal and seasonal light intensity and spectral variation. Diurnal and seasonal variations in light intensity (in terms of photon flux) and distribution are included in procedures to calculate direct photolysis rate constants of chemicals in optically thin solutions (Mill et al., 1982). These rate constants are estimated for clear-sky conditions and can be calculated as a 24-hour day-averaged rate constant. Corrections for weather conditions (overcast or cloudy cover) must be made using field data; they were performed as follows.

During the LAAP field study and in our outdoor studies at SRI, we exposed PNA/PYR actinometer solutions to sunlight simultaneously with our LAAP water/TNT experiments. The photolysis rate constants for this actinometer are available for clear-sky conditions as a function of season (Dulin and Mill, 1982). Rate constants calculated for PNA/PYR, with [PYR] = 1.25×10^{-3} M , were 4.3×10^{-3} m^{-1} for January and 9.6×10^{-3} m^{-1} for late April [winter and spring season dates, respectively, using the solar program of Zepp and Cline (1977)]. By interpolation, we estimate that an average rate constant of about 6.6×10^{-3} m^{-1} would then be expected for photolysis of PNA/PYR in mid-March. Because the actual rate constant measured for photolysis of PNA/PYR on both days was 4.8×10^{-3} m^{-1}, or 0.73 of that expected for clear-sky condition, we conclude that 73% of the clear-sky irradiance was available during our experiments with LAAP water.

The measured rate constant, k'_p, should therefore be divided by 0.73 to obtain the clear-sky rate constant. The depth-dependent rate constant for photolysis of TNT in LAAP water in mid-March under clear-sky conditions is $3.1/0.73 = 4.3$ cm d^{-1}. For LAAP water of 50-cm depth, the rate constant of 8.6×10^{-2} d^{-1} corresponds to a half-life of 8 days.

The above calculations assume that the 0.73 weather correction factor, f_w, obtained from the actinometer experiment, applies to light that induces photolysis of TNT in LAAP water. Although we know that this assumption is not strictly correct, it is sufficiently accurate for estimating environmental photolysis rate constants of chemicals that absorb in the same region of the spectrum. The assumption may not hold in the case of LAAP water where light absorption by products occurs into the visible region.

5. Effect of Time of Year on Photochemical Rate Constant of TNT in LAAP Water

Because concentrations of TNT were found to persist in the LAAP water at all times of year, in part due to dissolution of TNT out of the sediments (see Section V.A.5), modeling of the fate of TNT in the pond water required information on how the photolysis rate constant of TNT in the water will vary with the time of year (i.e., seasonal rate constants are needed). Equation 25 shows that the photolysis rate constant of TNT is seen to be a function of the incident light intensity and the reaction quantum yield, ϕ. Although we have no information on the rate of photolysis of TNT in LAAP water as a function of season, the relative rate constants for different times of the year can be calculated if we assume that L_λ values of Mabey et al. (1982) are useful approximations of I_λ. Then

$$k_{pE}(1)/k_{pE}(2) = \frac{\Sigma L_{\lambda 1}}{\Sigma L_{\lambda 2}} \quad , \tag{29}$$

where 1 and 2 denote different times of the year. This expression assumes that the quantum yield for photolysis of TNT in LAAP water is the same at all seasons. Use of L_λ values to estimate the I_λ values for this calculation is not strictly correct because L_λ values are day-averaged photon flux values for light passing through optically thin water, and therefore they are corrected for path length and the

refractive index of water. The actual flux values that should be used in the calculation are the flux values incident on the surface of the water with no path length correction because all light is absorbed by the water. This flux is referred to as W_λ by Zepp and Cline (1977), However, since the day-averaged analogs of W_λ are not known, we have used the L_λ values as approximations of the I_λ values needed for the calculation; comparison of W_λ and Z_λ values listed by Zepp and Cline for the season dates at 40° latitude indicates that the flux values corrected for path length are larger than the uncorrected values by 10-20% over a wide wavelength range.

The calculation of the relative photolysis rates of TNT in LAAP water also requires the knowledge or an assumption that the absorption of light above a certain wavelength will not photolyze TNT due to energy limitations. Therefore, we used several wavelength-cutoff regions to calculate the ratio in Equation 28 for the summer and winter solstices and the ratio for the September and March dates during which outdoor experiments were performed (Table 18). The data in the table show that photolysis of TNT in LAAP water will vary by a factor of about 3 between winter and summer seasons if only sunlight variations are considered; as discussed in other sections, the depth of the water, weather conditions, and possible changes in the nature of the lagoon water itself (absorbance and sensitizing abilities) will also affect the photolysis rates of TNT in the LAAP water throughout the year.

Table 18

VARIATION IN TNT PHOTOLYSIS RATES
IN LAAP WATER AS A FUNCTION OF TIME OF YEAR[a]

Wavelength[b] Cutoff	$\Sigma\alpha_\lambda L_{\lambda 1}/\Sigma\alpha_\lambda L_{\lambda 2}$ Summer season / Winter season	September[d] / March
400 nm	3.3	1.8
500 nm	2.9	1.8
600 nm	2.8	1.8

[a]Calculated using α_λ values for LAAP water collected in July.

[b]α_λ and L_λ values above this wavelength not used in calculation of rate constant ratio.

[c]L_λ value used for summer and winter solstices at 40° latitude.

[d]L_λ values used were interpolated between season dates.

5. UV-Visible Spectra of LAAP Water

As discussed above, the photic zone of the December LAAP water was thin (1-2 cm) compared to the total depth of the water (~60 cm) measured during the December site visit. In subsequent trips in May and July we found that the water depth was decreasing; therefore the absorption spectrum of the water was measured before use in our experiments. The UV spectrum of LAAP water in December is shown in Figure 9. The spectrum of the May LAAP water was nearly the same as that of the December water, whereas the absorption coefficients of July water were 1.7 to 1.5 times greater than those of the December water (Table 19). From the information and analyses obtained in our field and laboratory studies, it is impossible to determine how the constituents of the water affecting the UV spectra changed as a function of the time of year, although it is clear that the factor of 1.5-1.7 shown in Table 19 is less than a 3-fold increase expected from a simple concentration effect, considering that the water depth of ~60 cm in December decreased to approximately 18 cm in July.

Table 19

ABSORPTION COEFFICIENT[a] OF DECEMBER AND JULY LAAP WATERS AT SELECTED WAVELENGTHS

	α_λ, cm^{-1}		α_λ (July)
λ nm	Dec LAAP	July LAAP	α_λ (Dec)
300	3.38	5.82	1.72
400	1.76	3.02	1.72
500	0.66	1.06	1.62
600	0.22	0.34	1.53

[a]Absorbance of the natural water in a 1.0-cm cell.

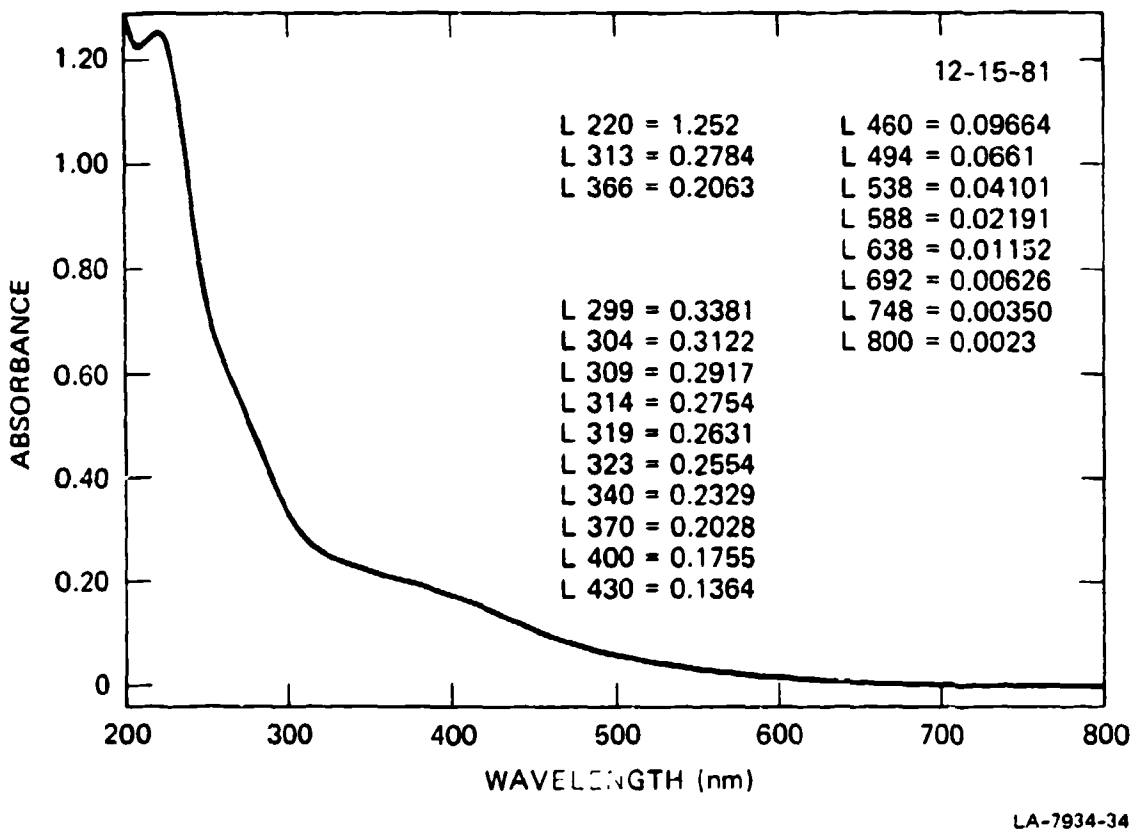

FIGURE 9 ABSORPTION SPECTRUM FOR LAGOON 9, SITE 1 WATER, FILTERED, 0.1-cm CELL

7. Experimental Studies of the Photolysis of TNT in LAAP Water

The photolysis of TNT was studied in different LAAP water samples collected during the field trips in December 1981, May 1982, and July 1982; no additional TNT was added to these samples for our experiments. The finding that the character of the lagoon itself and the LAAP water were different on each visit (see Section IV) required that photolysis of TNT be studied in each water so as to obtain the most relevant rate constant data that could be used in the lagoon-modeling efforts. The results from the several studies are summarized in Table 20. The studies are listed in the chronological order in which they were performed.

The rationale for the sequence is as follows. The studies in March (Expts. 2-4) using the December LAAP water were conducted after the effect of depth on the photolysis rate constant was found to be important (see Section V.B.3). In the late summer, Experiments 6 and 7 were conducted simultaneously using the December and July waters after it was found that the TNT rate constant measured in the July LAAP water in September (Expt. 5) was nearly the same as that measured in March (Expt. 3), which was unexpected because photolysis rates are more rapid in summer than in spring (see Section V.B.5). When these experiments showed that the photolysis rates of TNT were different in the two waters at the same time of year, Experiments 8-10 were conducted in which the absorbances of December, May, and July waters were made the same by dilution; the intent of these experiments was to determine whether the absorbances of waters were somehow responsible for the different rate constants observed, or whether the ability of the individual waters to promote TNT photolysis were indeed different among the water samples after allowing for the different absorbances. Unfortunately, the error in the measured rate constants is too large to clearly distinguish between the two effects.

From the data presented in Table 20, several conclusions can be offered that are important in estimating the photolysis rate constants of TNT in LAAP water. On the basis of the results of Experiments

8-10, the ability of the LAAP water to promote photolysis of TNT appears to be the same per unit absorbance of the water, although because of the error in the rate constant data, we cannot entirely rule out the possibility that the difference in the rate constants in Experiments 6 and 7 is not due to a slight effect of the concentration of natural substances, as would be observed by their absorbances.

Table 20

SUNLIGHT PHOTOLYSIS OF TNT IN LAAP WATER

Expt. No. (Date)	Water	[TNT] (ppm)	Time/Duration of Expt.	Temp (°C)	Water Depth, D (cm)	$10^3 k_p$ (min^{-1})	$10^3 k_p \times D$[c] ($cm\ min^{-1}$)	$10^3 k_p$[a,d] (min^{-1})
1. (1/26)	Dec. LAAP[a]	5.0	13:00–17:00, 240 min.	13–19	2.8	0.56 ± 0.13	1.56	16.3 ± 0.6[e]
2. (3/15)	Dec. LAAP[a]	5.0	13:00–17:00, 240 min.	13–19	2.8	0.56 ± 0.13	1.56	16.3 ± 0.6[e]
3. (3/15)	Dec. LAAP[a]	5.0	9:40–15:30, 350 min.	14–21	3.5	2.51 ± 0.04	8.78	11.3 ± 0.3[f]
4. (3/12)	Dec. LAAP[a]	5.0	9:00–16:00, 420 min.	15–26	4.2	1.67 ± 0.04	7.01	11.1 ± 0.4[f]
5. (9/18)	July LAAP	0.8	10:00–16:00, 360 min.	19–25	3.0	2.27 ± 0.05	6.81	---
6. (10/28)	Dec. LAAP[b]	1.8	10:00–17:00, 400 min.	16–24	3.0	1.09 ± 0.05	3.27	3.27 ± 0.11[g]
7. (10/28)	July LAAP	0.8	10:00–17:00, 400 min.	16–24	3.0	0.71 ± 0.08	2.13	3.27 ± 0.11[g]
8. (11/1)	Dec. LAAP[b]	1.9	12:15–17:00, 400 min.	19–25	3.5	0.74 ± 0.25[h]	2.59	3.13 ± 0.16[g,h]
9. (11/1)	July LAAP adjusted	0.5	12:15–17:00, 400 min.	19–25	3.5	0.70 ± 0.49[h]	2.45	3.13 ± 0.16[g,h]
10. (11/1)	May LAAP	11.4	12:15–17:00, 400 min.	19–25	3.5	0.62 ± 0.31[h]	2.17	3.13 ± 0.16[g,h]

[a]Water from Site 1.
[b]Water from Site 2.
[c]Depth-independent rate constant.
[d]PNA/PYR actinometer photolysis rate constant.
[e]PNA = 1.0×10^{-5} M; PYR = 5.0×10^{-3} M.
[f]PNA = 1.0×10^{-5} M; PYR = 1.25×10^{-3} M.
[g]PNA = 1.0×10^{-5} M; PYR = 1.24×10^{-4} M.
[h]Rate constant obtained with first three time points; later time point showed slower loss of TNT/actinometer in late afternoon (>15:00).

The data in Table 20 also show that the photolysis rate constant for TNT in the LAAP waters is independent of TNT concentration, as would be expected if the photolysis of TNT were a first-order process (Equation 26). However, we have insufficient data with which to evaluate the effect of changes in the properties of the lagoon water on the photolysis rate constant.

8. RDX Photolysis Rate Constant

Concurrent with the TNT studies, we performed calculations to estimate the RDX photolysis rate constant. The rate of RDX photolysis can be described by Equation 30 for wavelength λ:

$$-\frac{dC}{dt} = \frac{\phi I_{o\lambda}\left(1 - 10^{-(\alpha_\lambda + \varepsilon_\lambda C)\ell}\right)\varepsilon_\lambda C}{D(\alpha_\lambda + \varepsilon_\lambda C)} \quad , \qquad (30)$$

where D = depth (cm)

$I_o\lambda$ = incident light intensity

α_λ = absorptivity of the water

ε_λ = molar absorptivity coefficient for RDX at λ

ℓ = solution path length

In LAAP water, $\alpha_\lambda >> e_\lambda C$. Therefore, Equation 30 above reduces to Equation 31:

$$-\frac{dC}{dt} = \frac{\phi I_{o\lambda}(1 - 10^{-\alpha_\lambda \ell})\varepsilon_\lambda C}{D\alpha_\lambda} \quad . \qquad (31)$$

Since the exponential function $10^{-\alpha_\lambda \ell}$ is also very small compared to 1 in waters where α_λ is large, Equation 31 reduces to Equation 32:

$$-\frac{dC}{dt} = \frac{\phi I_{o\lambda}\varepsilon_\lambda C}{D\alpha_\lambda} \quad . \qquad (32)$$

Integration of Equation 32 gives a first-order rate expression where k_p is equal to the expression shown below at wavelength λ:

$$k_{p\lambda} = \frac{\phi I_{o\lambda} \epsilon_\lambda}{D\alpha_\lambda} \quad . \tag{33}$$

The environmental rate constant can now be summed over all wavelengths in the solar spectral region and the photochemical rate constant can be described as shown in Equation 34:

$$k_{pE} = \frac{\phi \Sigma \epsilon_\lambda I_{o\lambda}}{D\alpha_\lambda} \quad . \tag{34}$$

Using the molar absorptivity values measured for RDX from 299 nm (ϵ = 164) to 400 nm (ϵ = 0.02), the absorptivity of the LAAP water (α_λ) over the same spectral range, and the quantum yield (ϕ = 0.16), we calculated the photochemical rate constant (k_{pE}) at various depths of the LAAP water using a modified version (GC SOLAR) of the computer program developed by Zepp and Cline (1977) for calculating the intensity of ultra-violet radiation (297.5-380 nm) reaching the earth's surface as a function of time of day, longitude, latitude, and season. These data are shown in Table 21 for the four seasons. Also shown are the depth independent rate constants for RDX computed for LAAP waters collected in December and July. From the rate constants shown in parentheses, a comparison of the seasonal effects on photolysis can be made; however, these values are not environmentally revelant due to changes in the water's composition as a function of time of year.

Table 21

PHOTOCHEMICAL RATE CONSTANTS FOR RDX
IN LAAP WATERS AS A FUNCTION OF SEASON AND DEPTH

	Rate Constant ($\times 10^3$ d^{-1}) in July LAAP Water			
Depth (cm)	Fall	Winter	Spring	Summer
Surface[a]	390	200	710	930
15	2.0	1.0	3.8	5.0
30	1.0	0.52	1.9	2.5
60	0.51	0.26	0.95	1.3
90	0.34	0.17	0.63	0.83
Depth Independent Rate	(30)	(16)	(56)	76
Constant (cm d^{-1}) in July LAAP	---	---	---	---
Water[b]	---	---	---	---
Depth Independent Rate	(39)	19	(75)	(101)
Constant (cm d^{-1}) in December	---	---	---	---
LAAP water[b]	---	---	---	---

---

[a]Rate constant at surface not used

[b]Rate constants in ( ) are for comparison of seasonal effects on photolysis and are not environmentally relevant.

The above calculations showed that the light intensity for a particular LAAP water changed by a factor of five going from winter to summer months. The depth-independent rate constant, however, changed by only a factor of three due to the greater absorptivity of the LAAP water in the summer (α_λ = 9.0 at 300 nm) than in the winter (α_λ = 3.0 at 300 nm).

To determine how well the calculated depth-independent rate constant compared to a measured value, we performed an RDX sunlight photolysis experiment in a 19 × 3-cm wide crystallizing dish (darkened on sides and bottom) over a seven-day period (starting 9/18/82) using lagoon water collected on 24 July 1982 and filtered through a 0.25-μm filter. A plot of ln RDX versus time gave a straight line, from which a first-order rate constant (slope) was calculated to be 4.77×10^{-5} min^{-1}. In the same experiment, TNT photolyzed with a pseudo-first-order rate constant of $2.4 \pm 0.3 \times 10^{-3}$ min^{-1}, or approximately 50 times faster than RDX. The depth independent rate constant was calculated to be 0.20 cm day^{-1}.

This value is about three times larger than the calculated value for July LAAP water. Using the GC SOLAR program, we calculated the RDX photolysis rate constant in pure water to be 2.0 cm day^{-1} during the summer, which is in good agreement with an experimental value of 2.2 cm day^{-1} measured in the summer. Therefore, the differences in the measured and calculated photolysis rate constants for LAAP water could be due to sensitization reactions that are not understood at this time. For the modeling study, we used the measured rate constant in LAAP water corrected by the light intensity factors for the various seasons.

C. Biotransformation

1. Bacterial Count

The identification of aminodinitrotoluenes in the lagoon water suggested that biotransformation was occurring in the lagoon water and

sediment. To obtain an indication of aerobic and anerobic microbial populations in the lagoon and sediment, bacterial plate counts were performed on waters and sediment collected during the December field study. In the lagoon water (Table 22), the aerobic bacterial counts averaged 1.7×10^6 CFU ml^{-1} and the anaerobic bacteria averaged 1.7×10^3 CFU ml^{-1}. In the sediment (Table 23), the averages were 1.1×10^7 CFU ml^{-1} for the aerobic bacteria and 1.5×10^5 CFU ml^{-1} for the anaerobic bacteria.

Table 22

TOTAL AEROBIC AND ANEROBIC BACTERIA
IN LAGOON 9 WATER COLLECTED IN DECEMBER

Sample Site	Aerobic Bacteria (CFU ml^{-1})	Anaerobic Bacteria (CFU ml^{-1})
1	1.6×10^6	2.9×10^3
2	1.8×10^6	1.1×10^3
3	1.7×10^6	0.48×10^3
4	1.7×10^6	2.2×10^3

Table 23

TOTAL AEROBIC AND ANAEROBIC BACTERIA
IN LAGOON 9 SEDIMENT COLLECTED IN DECEMBER

Sample Site	Aerobic Bacteria (CFU ml^{-1})	Anaerobic Bacteria (CFU ml^{-1})
1	0.51×10^7	1.4×10^5
2	1.4×10^7	1.9×10^5
3	0.76×10^7	0.71×10^5
4	1.9×10^7	2.0×10^5

The tea-colored water and sediment contained unexpectedly high numbers of aerobic bacteria. The numbers of anaerobic bacteria were substantially smaller, reflecting the high dissolved-oxygen content (7

to 8 ppm) of the water in the winter. Total aerobic bacteria in a water sample collected on 25 May 1982 averaged 1.9×10^6 CFU ml^{-1}.

A lagoon water sample collected on 24 July 1982 was also evaluated for viable cells by bacterial plate counting. Because the lagoon water temperature had risen above 35°C, plates were incubated at 37°C and 25°C. The number of bacterial colonies formed at each temperature is shown in Table 24. These results indicate that more bacteria will grow at 25°C than at 37°C. However, the bacteria that do not grow at 37°C are still viable.

Table 24

BACTERIAL PLATE COUNT OF LAAP LAGOON WATER COLLECTED IN JULY

Incubation Temperature	Average Colonies Formed (CFU ml^{-1})
25°C	2.60×10^6
37°C	1.19×10^6

These counts do not differ significantly from those found in December 1981 and May 1982, thus suggesting that the microbial population within the lagoon remains fairly constant although populations of specific organisms may change.

2. Biotransformation Screening Tests

Because of the presence of substantial microbial populations in the water, we initiated screening tests for the biotransformation of TNT and RDX in lagoon water under aerobic and anaerobic conditions.

Lagoon waters from the four sites (north, south, east and west quadrants) were mixed in equal parts and three preparations of 2-liter samples were each placed in 4-liter bottles. The three preparations

were 1) water alone, 2) water plus 50 ppm sterile yeast extract, and 3) water plus 1% dry weight of bottom sediment. For the anaerobic incubation, 1 liter of each of the above solutions was placed in a 1-liter Erlenmeyer flask, which was flushed with N_2 gas and sealed with a rubber stopper. Flushing with N_2 gas was repeated after each sampling. The samples were analyzed periodically for total organic carbon (TOC), TNT, and RDX. The initial concentrations were 75 ppm TOC, 5.0 ppm TNT, and 13.0 ppm RDX. No additional TNT or RDX was added to the water.

a. Aerobic TNT Biotransformation

After 1 day of incubation, the bacterial population in the lagoon water under aerobic conditions increased slightly to 3×10^6 CFU ml^{-1}, then gradually decreased to 1.2×10^6 CFU ml^{-1} after 16 days of incubation, and remained constant at 1.1×1^6 CFU ml^{-1} from 34 days to 70 days. The TOC remained constant (75 ppm) over this period.

In the lagoon water alone, the TNT concentration slowly decreased from 5 ppm to 2 ppm over 90 days of incubation (Figure 10). The transformation followed first-order kinetics. The pseudo-first-order rate constant was calculated to be 4.1×10^{-4} hr^{-1}, and the second-order rate constant was calculated to be 3.7×10^{-10} ml $cell^{-1}$ hr^{-1}, based on microbial counts of 1.1×10^6 CFU ml^{-1}.

The addition of yeast extract to the lagoon water accelerated the transformation rate by increasing the microbial population. The microbial count increased from 0.3 to 1.6×10^7 CFU ml^{-1} after one day of incubation. However, it decreased rapidly to 1.6×10^6 CFU ml^{-1} after 16 days, and the transformation rate also decreased. The rate accelerated again when yeast extract was added at Day 41 (Figure 10).

In the lagoon water with added sediment, the total concentration of TNT increased to 74 ppm because the bottom sediment contained large amounts of solid TNT. Total TNT in this water decreased from 74 ppm to 59 ppm during the 90 days of incubation in a similar fashion to

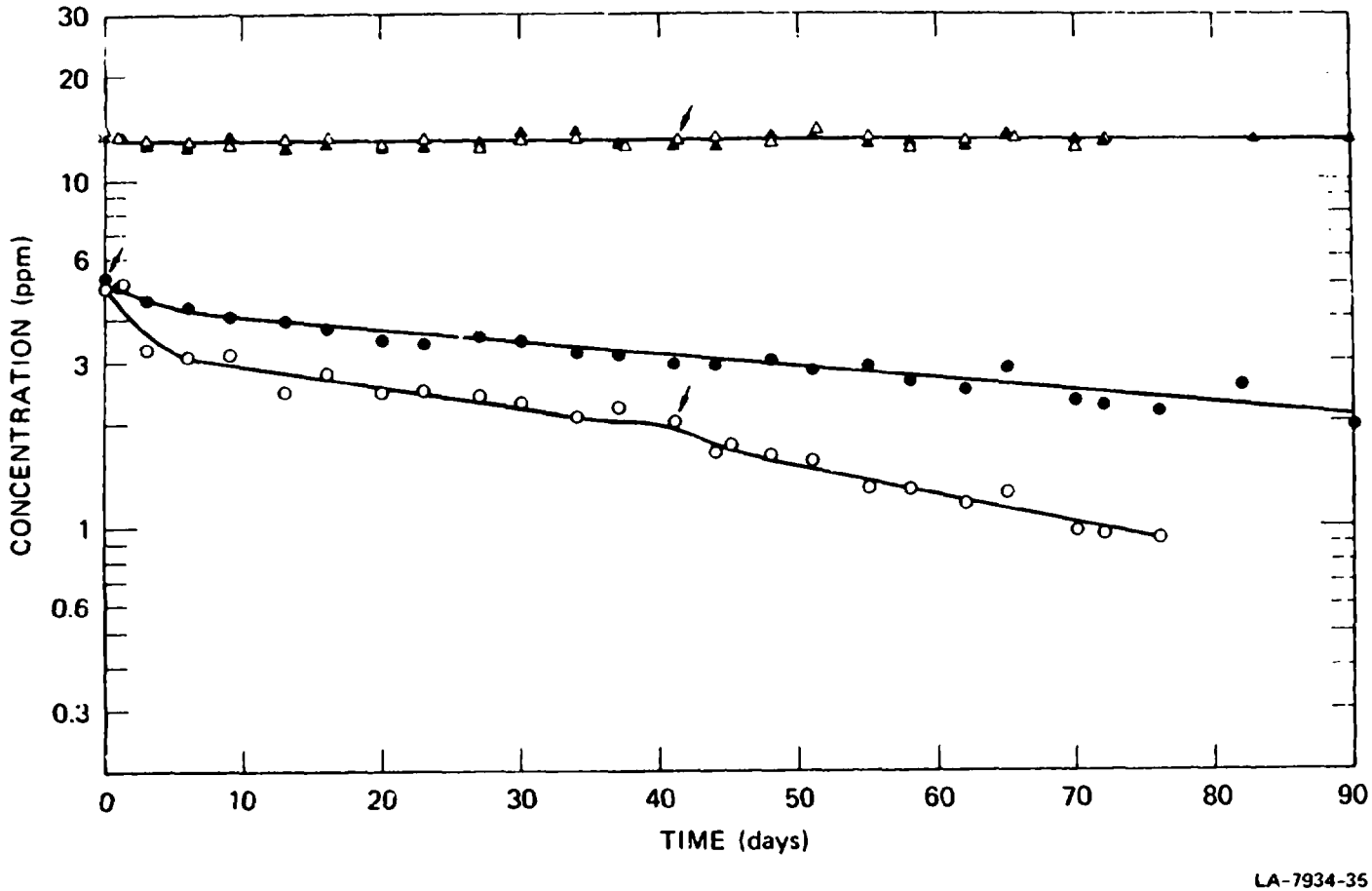

FIGURE 10 AEROBIC BIOTRANSFORMATION OF TNT AND RDX IN LAGOON WATER

● TNT in water alone; ▲ RDX in water alone; ○ TNT in water plus yeast extract; △ RDX in water plus yeast extract; ↓ 50 ppm yeast extract added.

that observed in lagoon water alone. Bacterial counts averaged 3×10^6 CFU ml^{-1} in the water-sediment mixture.

b. Anaerobic TNT Biotransformation

Under anaerobic conditions in the lagoon water alone, TNT was transformed at a slower rate than under aerobic conditions (Figure 11). This may be a result of a lower population of anaerobic microorganisms. The pseudo-first-order rate constant was calculated to be 1.6×10^{-4} hr^{-1}.

The addition of yeast extract to the water also accelerated the disappearance of TNT. Yeast extract was added at Day 0, Day 41, and Day 76; there was a significant drop in TNT concentration after each addition.

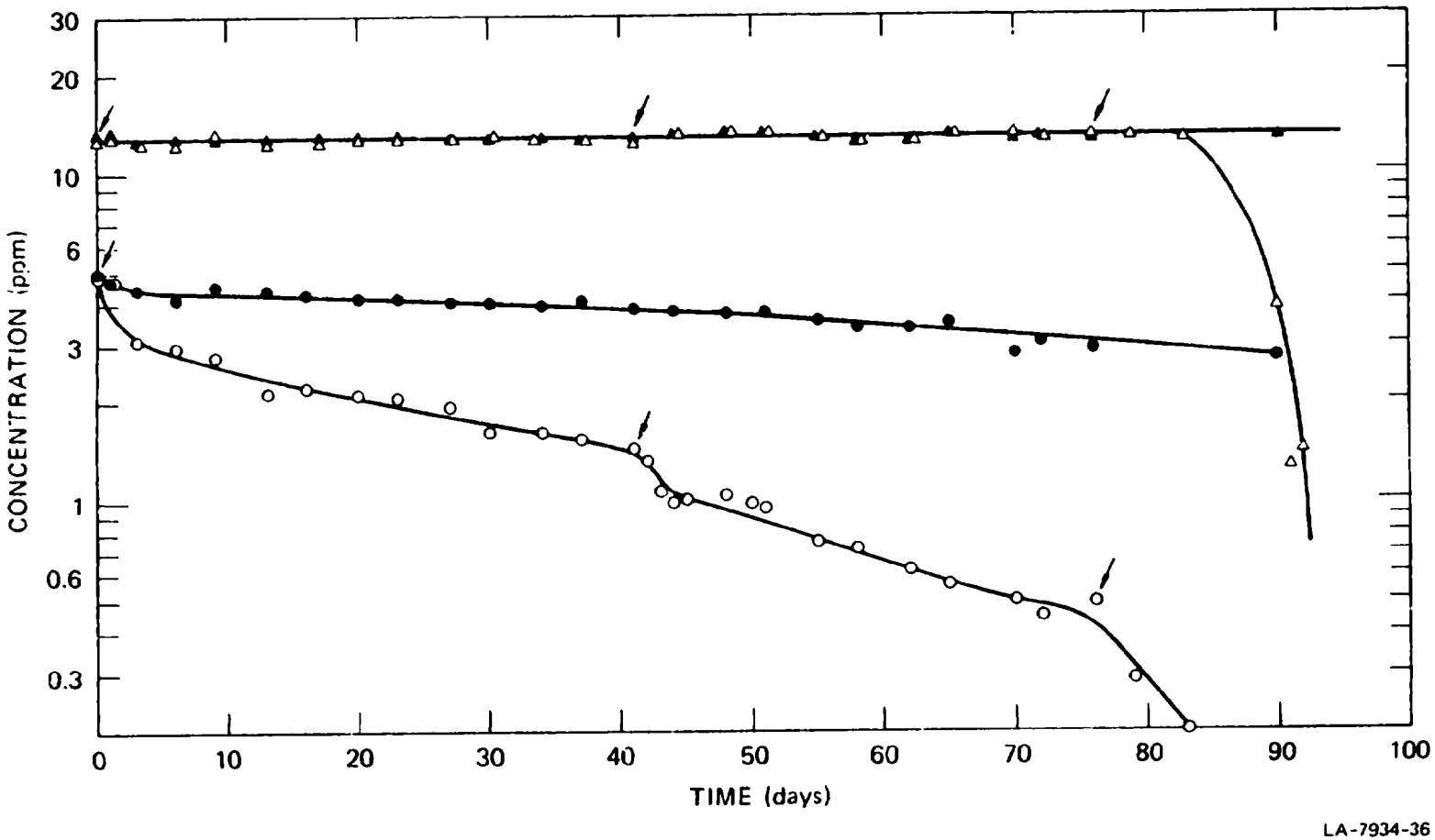

FIGURE 11 ANAEROBIC BIOTRANSFORMATION OF TNT AND RDX IN LAGOON WATER

● TNT in water alone; ▲ RDX in water alone; ○ TNT in water plus yeast extract; △ RDX in water plus yeast extract; | yeast extract added.

In the sediment-added lagoon water, TNT decreased from 74 ppm to 57 ppm during 76 days of incubation. Therefore, it appears that anaerobic biotransformations in anaerobic waters are similar to the aerobic biotransformation of TNT.

c. Aerobic TNT Biotransformation at High and Low Concentrations of TNT

The biotransformation of TNT was investigated at high and low concentrations of TNT and in the presence of a high microbial population. The lagoon water (stored at < 10°C) was exposed to room temperature for one week, centrifuged, and resuspended in one-tenth of the volume of lagoon water in two bottles. Pure TNT was added to one bottle to bring the aqueous concentration to ~50 ppm without changing the other chemical components of the lagoon water. The other bottle contained the original TNT concentration of lagoon water (4.2 ppm). The average bacterial counts in these waters were originally 7.8×10^6 CFU ml^{-1}, but they decreased to 4.0×10^6 CFU ml^{-1} after 25 days of incubation.

The TNT in the water with a low concentration of TNT transformed with a pseudo-first-order rate constant of 1.9×10^{-3} hr^{-1} (4.6×10^{-2} day^{-1}; correlation coefficient, $r^2 = 0.98$). The second-order rate constant was calculated to be 3.2×10^{-10} ml $cell^{-1}$ hr^{-1} (7.7×10^{-9} ml $cell^{-1}$ day^{-1}), based on a median bacterial count of 6.0×10^6 CFU ml^{-1}. This rate constant is close to that observed in the original water (3.7×10^{-10} ml $cell^{-1}$ hr^{-1}).

The TNT in the water with a high concentration of TNT decreased from 48 ppm to 33 ppm in 25 days. If the data are treated as pseudo-first-order, the rate constant, calculated by a least-squares method, is 6.3×10^{-4} hr^{-1} (1.5×10^{-2} day^{-1}; $r^2 = 0.95$). This rate constant is only one-third of that observed in the water with a low TNT concentration. If the data are treated as following zero-order kinetics, which is expected for high chemical substrate biotransformation, the zero-order rate constant is 2.5×10^{-2} ppm hr^{-1} (6.0×10^{-1} ppm day^{-1};

$r^2 = 0.96$). Because the correlation coefficients are nearly equal, more data points are required to prove the zero-order kinetic behavior. However, since the calculated pseudo-first-order rate constant is much lower than that observed in the low-TNT-concentration experiment, a zero-order kinetic process may better describe the transformation rate at high TNT concentrations (such as water in the sediment). The calculated rate constant for 6×10^6 cell ml^{-1} is 4.1×10^{-9} ppm $cell^{-1}$ hr^{-1} (9.8×10^{-8} ppm $cell^{-1}$ day^{-1}).

d. TNT Metabolities

During the laboratory biotransformation study of TNT in lagoon water, we observed that the concentrations of 2-amino-4,6-dinitrotoluene (2-A-4,6-DNT) and 4-amino-2,6-dinitrotoluene (4-A-2,6-DNT) remained nearly constant throughout the study. To investigate whether 2-A-4,6-DNT and 4-A-2,6-DNT are products of lagoon water biotransformation, we centrifuged lagoon water and resuspended the precipitate-containing microorganisms in 1/20th the volume of lagoon water. Ring-labeled ^{14}C-TNT (1.0 μCi in 50 ml) and unlabeled TNT (final concentration 40 ppm) were added to the water and the water was incubated in the dark.

After 3 days and 19 days of incubation, the water was extracted with ethyl acetate, then acidified to pH 2, and re-extracted with ethyl acetate. In the 3-day sample, more than 90% of the radioactivity was found in the neutral fraction. The extracts were dried, concentrated, and chromatographed by TLC using silicia gel plates and chloroform as the developing solvent. The plates were analyzed by radioautography. Most of the activity was associated with TNT; however, radioactive 2-A-4,6-DNT and 4-A-2,6-DNT were produced and identified by their yellow color and by co-chromatography against authentic standards.

In the 19-day sample, the distribution of the radioactivity among the neutral, the acid extract, and the remaining aqueous phase was

80%, 16%, and 4%, respectively. The radioautograph-TLC plate developed in chloroform, in benzene:ethyl acetate:acetic acid (6:3:1), and in chloroform:methanol (6:1) solvent systems showed the major activity at spots with R_f values corresponding to TNT, 4-amino-2,6-dinitrotoluene, and 2-amino-4,6-dinitrotoluene (Figure 12). The activity at spots corresponding to 2,4-diamino-6-nitrotoluene and 2,6-diamino-4-nitrotoluene were insignificant. Several minor spots with weak activity had R_f values similar to those for trinitrobenzyl alcohol and trinitrobenzaldehyde. However, further identification is needed. The acid extract showed several radioactive components with low R_f values.

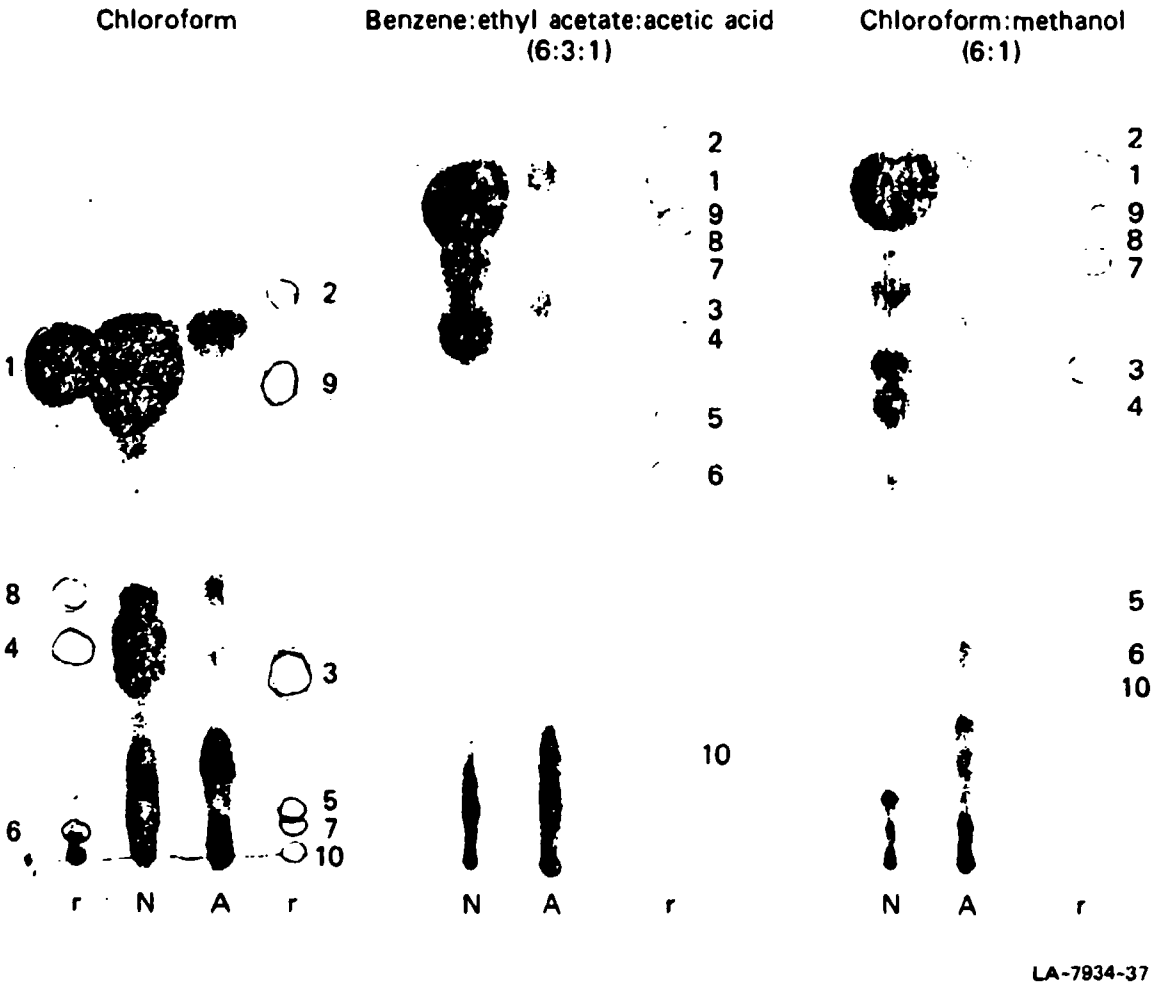

FIGURE 12 RADIOAUTOGRAPH OF THIN-LAYER CHROMATOGRAM OF TNT METABOLITES IN LAGOON WATER AFTER 19 DAYS OF INCUBATION

Samples: N = neutral extract; A = acidic extract; r = reference chemicals.

Compounds: 1 = TNT; 2 = 2,2',6,6'-tetranitro-4-azoxytoluene; 3 = 4-amino-2,6-dinitrotoluene; 4 = 2-amino-4,6-dinitrotoluene; 5 = 2,6-dinitroaniline; 6 = 2,4-dinitroaniline; 7 = trinitrobenzyl alcohol; 8 = trinitrobenzaldehyde; 9 = 1,3,5-trinitrobenzene; 10 = picric acid.

The extracts were streaked on preparative TLC plates. Several unknown compound spots were scraped from the plate and subjected to probe mass spectrometric analysis; however, they could not be identified because of large amounts of interfering phthalates and binders from the TLC plates.

On the basis of this study, we conclude that the formation of aminodinitrotoluenes in lagoon water is the result of microbial processes.

e. Biological Oxygen Demand of the Lagoon Water

The biological oxygen demand of the LAAP lagoon water was measured as an indicator of the oxygen-utilization rate of the microbes. The refrigerated lagoon water was left at room temperature overnight, then shaken to saturate the water with air, and poured into four biological oxygen demand (BOD) test bottles, which were then incubated at 20°C in the dark. The dissolved oxygen (DO) concentration was monitored with a DO meter after 0, 3, 5, 7, and 10 days of incubation. The DO decreased at each sampling point, yielding a first-order rate constant of 9.6×10^{-2} day^{-1}. We therefore expect that in the LAAP lagoon (DO = 8 ppm) the microbes will use oxygen at a rate of 0.77 ppm day^{-1}.

f. RDX Aerobic Biotransformation

The original concentration of RDX in the lagoon water was 13 ppm. No loss of RDX was observed during the aerobic experiment--whether RDX was in the lagoon water alone, with added yeast extract, or with 1% of bottom sediment (Figure 10). Therefore, it appears that RDX is biologically persistent in the lagoon water under aerobic conditions.

g. RDX Anaerobic Biotransformation

Under anaerobic conditions, no change in RDX concentration was observed in the lagoon water alone or in water plus sediment. RDX (13 ppm) in lagoon water with 50 ppm of added yeast extract did not show any loss of RDX after 46 days. An additional 50 ppm of yeast extract was added on Day 46 and 100 ppm on Day 76. After 83 days of incubation, the RDX concentration remained at 13 ppm and then dropped to 2.9 ppm at Day 90 and 1.4 ppm at Day 92. Perhaps the repeated addition of yeast extract acclimated RDX-utilizing organisms.

On Day 92, the microorganisms in the lagoon water were inoculated into basal salts medium (BSM) plus 500 ppm of yeast extract and 9.1 ppm of RDX. The RDX concentration decreased to 0.6 ppm after 5 days of anaerobic incubation. The organisms were transferred to a second flask containing BSM, 50 ppm yeast extract, and 9.4 ppm of RDX; the RDX was transformed to 3.4 ppm after 4 days of incubation.

The RDX-acclimated organisms were then inoculated into two flasks: one contained BSM plus 50 ppm yeast extract and 8.0 ppm RDX, the other contained lagoon water (12.9 ppm RDX) and 50 ppm of yeast extract. The results of the anaerobic incubation are shown in Table 25.

Table 25

RDX CONCENTRATION ON DIFFERENT DAYS AFTER ANAEROBIC INCUBATION IN LAAP LAGOON WATER

Day	RDX (ppm)
0	12.4
5	9.8
10	5.8
17	2.5
20	<0.1

When the above organisms were inoculated into BSM with 8.0 ppm RDX and 50 ppm of yeast extract, the RDX was transformed to nondetectable levels (<0.01 ppm) within 5 days.

In a second experiment, the above organisms were inoculated into samples of lagoon water with 50 ppm or 300 ppm yeast extract. A third flask was inoculated with RDX-transforming organisms [obtained from the HMX waste-line sediment at Holston Army Ammunition Plant (HAAP)], lagoon water, and 50 ppm of yeast extract. The RDX concentration was monitored over a 20-day period. The results (Table 26) indicate that the anaerobic biotransformation of RDX can be accelerated by extra organic nutrients (300 ppm yeast extract) or by a different source of RDX-transforming organisms.

Table 26

ANAEROBIC TRANSFORMATION OF RDX WITH SELECTED ORGANISMS AND YEAST EXTRACT CONCENTRATIONS

Source of Organisms	Yeast Extract (ppm)	RDX Concentration (ppm) at Day 0	7	13	17	20
LAAP Lagoon Water	50	13.0	11.3	7.0	5.3	3.6
LAAP Lagoon Water	300	12.7	11.1	8.4	7.8	<0.1
HAAP Sediment	50	12.6	11.2	4.8	1.0	<0.1

For comparison, RDX-tranforming organisms from the LAAP water and the HAAP sediment were each inoculated into flasks containing BSM with 9.0 ppm RDX and 50 ppm yeast extract; the RDX disappeared within three days. This result and the data in Table 26 show that the anaerobic biotransformation of RDX is much slower in lagoon water than in BSM even in the presence of large yeast extract concentrations (300 ppm) or with an alternate source of RDX-transforming organisms. These data suggest that lagoon water components have an inhibitory effect on RDX biotransformation.

To test the possibility that the slow RDX anaerobic biotransformation in lagoon water was due to the lack of mineral nutrients rather than to inhibition by some chemical present in the lagoon water, we investigated the biotransformation of RDX in lagoon water with yeast extract and BSM components. The results showed that the addition of mineral salts to lagoon water collected either in December or May did not significantly accelerate the RDX biotransformation, suggesting that the lack of salts is not responsible for the inhibitory effect of RDX anaerobic biotransformation in lagoon water.

3. Detailed Biotransformation Rate Study

The biotransformation of TNT depends on enzymes resulting from microorganisms utilizing organic nutrients other than TNT for growth. Under these conditions, the biotransformation rate will follow Michaelis-Menton kinetics at different concentrations of TNT. The transformation rate, $\frac{dc}{dt}$, can be represented as shown in Equation 35.

$$\frac{dC}{dt} = \upsilon = V_m C/(K_m + C) \quad , \qquad (35)$$

where C is the TNT concentration, V_m is the maximum transformation rate at a given enzyme concentration or microbial population, and K_m is the Michaelis constant, which is the TNT concentration that yields half the maximum transformation rate.

When the TNT concentration is very low, K_m is much greater than C and the transformation rate expression reduces to Equation 36:

$$\frac{dC}{dt} = \frac{V_m C}{K_m} = k_b' C \quad , \qquad (36)$$

which is the pseudo-first-order transformation rate expression.

In environments where the TNT concentration is high, such as near the sediment in the LAAP lagoon, C is much greater than K_m and Equation 35 reduces to Equation 37:

$$\frac{dC}{dt} = V_m \quad , \tag{37}$$

which is a zero-order rate expression with respect to TNT. When V_m is divided by the bacterial concentration, the maximum rate per organism can be obtained.

Equation 35 can be rewritten as shown in Equation 38, which is the Lineweaver-Burke equation. A plot of $1/\upsilon$ versus $1/C$ yields a straight line, from which the values K_m/V_m (slope) and $1/V_m$ (y-intercept) can be determined.

$$\frac{1}{\upsilon} = \frac{K_m}{V_m C} + \frac{1}{V_m} \quad . \tag{38}$$

To determine K_m and V_m, we incubated LAAP lagoon water with 100 ppm of yeast extract for two days to generate a high cell population. The water was dispensed into five flasks and TNT was added to give concentrations ranging from 2.39 to 37.7 ppm. TNT was monitored for 24 hr and the transformation rates were determined. These data are shown in Table 27.

Table 27

TRANSFORMATION RATES DETERMINED FOR VARIOUS TNT CONCENTRATIONS

Initial TNT Concentration (ppm)	Transformation Rate, (ppm day^{-1})
2.3	0.37
5.5	0.75
10.0	1.19
18.7	1.55

Using the Lineweaver-Burke method, we plotted the above data (Figure 13) and calculated K_m and V_m. Linear regression of the plot gave values of K_m = 19.3 ppm and V_m = 3.5 ppm day^{-1}. The initial microbial population was 1.0×10^8 CFU ml^{-1} and, therefore, the maximum rate per organism will be 3.5×10^{-8} ppm $cell^{-1}$ day^{-1} (1.5×10^{-9} ppm $cell^{-1}$ hr^{-1}). The value is slightly lower than the 9.8×10^{-8} ppm $cell^{-1}$ day^{-1} obtained with centrifuged lagoon water mico-organisms and 50 ppm TNT determined in a previous experiment. This may be the result of a modification of the mixed culture population when grown on yeast extract.

The above results indicate that the biotransformation of TNT will follow pseudo-first-order kinetics at TNT concentrations less than 19 ppm and zero-order kinetics at TNT concentrations greater than 19 ppm.

A second experiment was conducted with lagoon water microorganisms incubated without the addition of yeast extract. From the lagoon water collected in May, we prepared high cell populations by incubating the water at 20° to 25°C in the dark over a three-week period, centrifuging the microorganisms, and resuspending the cells in 1/35th of the volume of lagoon water. This water, containing 2.1×10^7 CFU ml^{-1}, was dispensed into flasks and TNT was added to give concentrations ranging from 8 to 47 ppm.

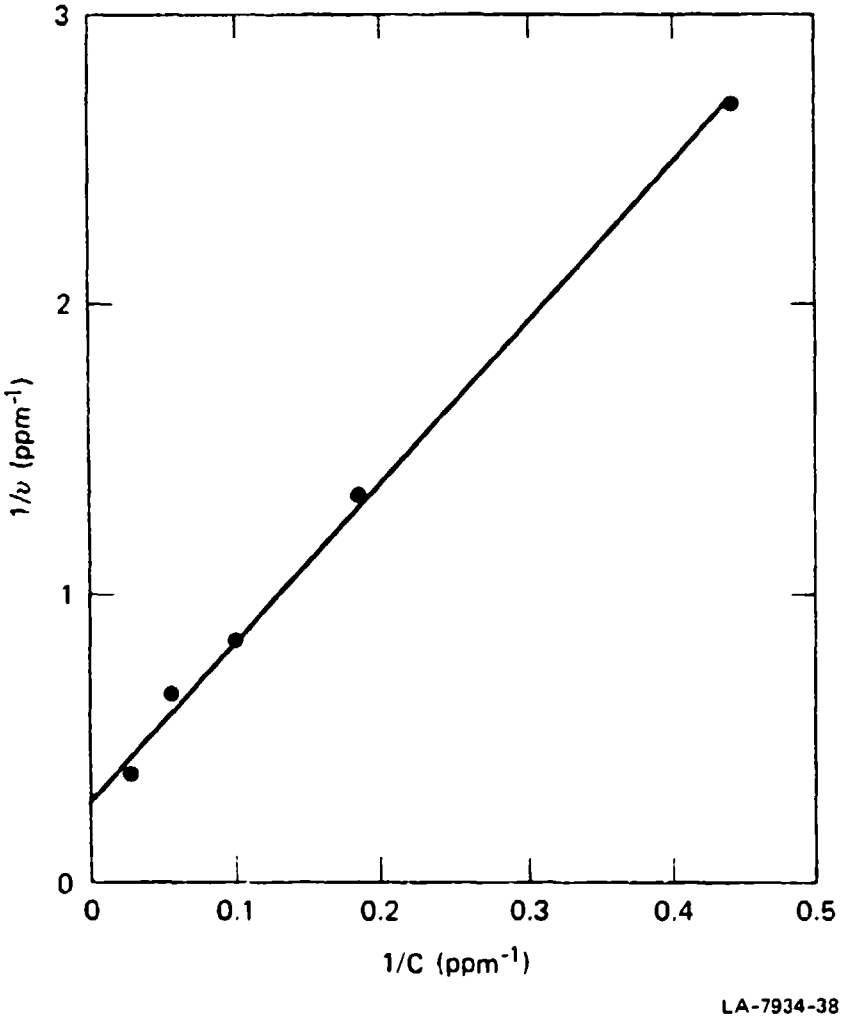

FIGURE 13 LINEWEAVER-BURKE PLOT OF TNT BIOTRANSFORMATION RATE 'N LAGOON WATER

The biotransformation of TNT was followed over five days. The initial TNT concentrations and biotransformation rates are shown in Table 28.

Table 28

INITIAL TNT CONCENTRATIONS AND BIOTRANSFORMATION RATES OVER 5 DAYS

Initial TNT Concentration (ppm)	Biotransformation Rate (ppm day^{-1})
8.04	0.33
10.7	0.40
16.3	0.51
21.3	0.55
34.7	0.61
47.3	1.02

Using the Lineweaver-Burke plotting method, we calculated K_m (the Michaelis Constant) to be 19.1 ppm and V_m (the maximum transformation rate at a given enzyme concentration or microbial population) to be 1.1 ppm day^{-1}. The maximum rate per organism is 5.3×10^{-8} ppm $cell^{-1}$ day^{-1} (2.2×10^{-9} ppm $cell^{-1}$ hr^{-1}), which is close to the value obtained for the yeast extract-generated lagoon water organisms.

VI. DEVELOPMENT OF THE SIMULATION MODEL

A. General Equations

A simulation model was developed based on a mathematical description of material balance. The basic equation for material balance is shown in Equation 39:

$$\frac{dM}{dt} = \sum_i I_i - \sum_i O_j \quad , \tag{39}$$

where M = total amount of chemical in the system

I_i = total input of chemical to the lagoon

O_j = total removal of chemical from the lagoon.

The change in total mass, dM/dt, can also be related to the chemical concentration, C, and volume, V, of the lagoon as shown in Equation 40:

$$\frac{dM}{dt} = C\frac{dV}{dt} + V\frac{dc}{dt} \quad . \tag{40}$$

Thus, from Equations 39 and 40, Equation 41 can be formulated:

$$V\frac{dc}{dt} = \sum_i I_i - \sum_j O_j - C\frac{dV}{dt} \quad . \tag{41}$$

Because no munitions wastes have been dumped since early in 1981, the only input source of munitions arises from the diffusion of accumulated chemicals in the sediment layer (D_{dif}) and the dissolution of solid chemicals lying on the bottom sediment surface (D_{dis}). Therefore, the chemical input can be described as shown in Equation 42:

$$\sum_i I_i = \sum_{i=1}^{25} (D_{dif_i} + D_{dis_i}) \quad . \tag{42}$$

Because the bottom sediment and surface are heterogeneous with respect to the amounts of TNT and RDX present, the bottom sediment was divided into 25 compartments (30' × 30') from which the diffusion flux and dissolution rate were calculated individually (i = 1 to 25).

Chemicals are removed from the lagoon through transformation processes (photolysis and biotransformation) and seepage. The seepage transport process has been accounted for in the calculation of net diffusion flux (D_{dif}); therefore the total removal of chemical can be expressed as Equation 43:

$$\sum_j O_j = \sum_\ell k_\ell CV \quad , \tag{43}$$

where k_ℓ represents the transformation rate constants.

Equation 41 can now be written as Equation 44:

$$V\frac{dC}{dt} = \sum_{i=1}^{25} (D_{dif} + D_{dis_i}) - \sum_\ell k_\ell CV - C\frac{dV}{dt} \quad . \tag{44}$$

A numerical integration scheme, using Euller's prediction and correction method, was used to integrate Equation 44 over selected time intervals to provide simulation results.

B. Program Structure

A flow chart of the computer program is shown in Figure 14. System parameters, transformation rate constants, weather data, lagoon descriptions, and initial conditions are read in when the program is

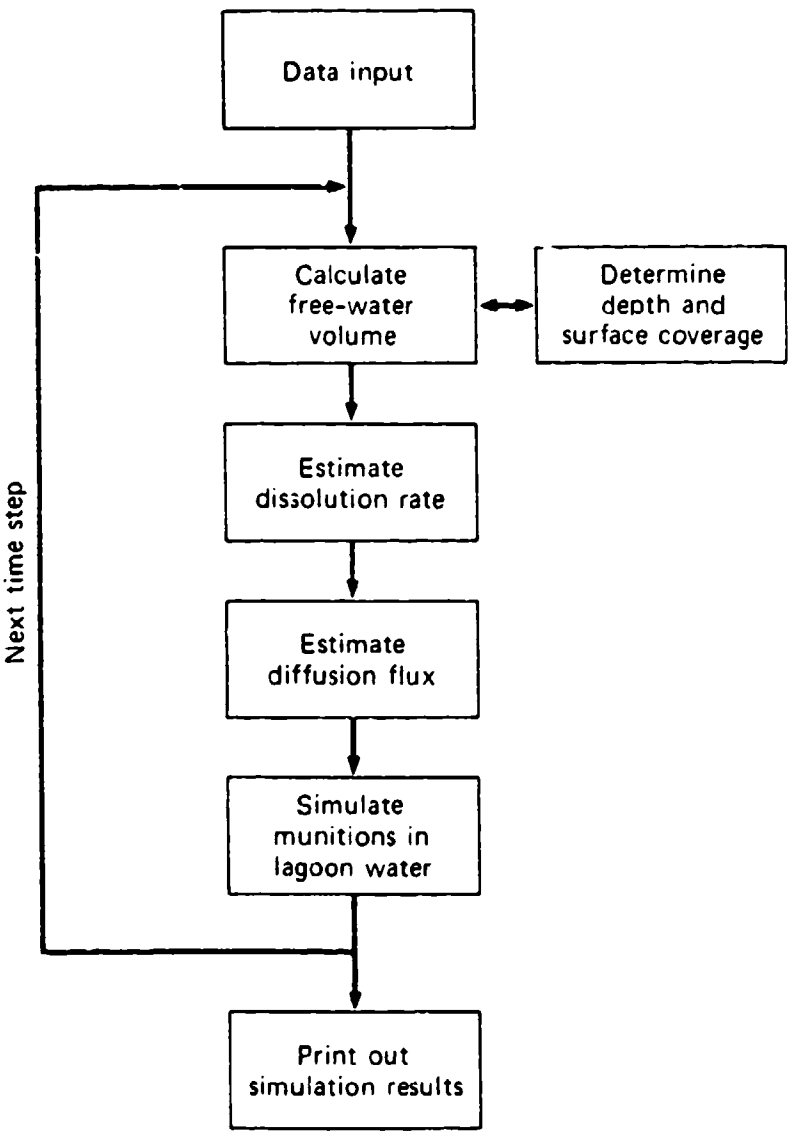

FIGURE 14 SIMULATION FLOW CHART OF THE LAGOON MODEL

initiated. The main program is linked to a number of subroutines such as VOLUME and SURFACE, which calculate the depth above each sediment compartment and the number of compartments covered by water. This number and the corresponding locations of sediment covered by water are then used separately in FLUX and FLUX 1 subroutines to calculate the diffusion flux and dissolution rate of chemicals from the bottom sediment, respectively. Material balance is performed in the subroutine COMPS when Euller's prediction and correction method is employed to predict the chemical concentration in the lagoon. The above procedures are repeated at every time step until the simulation period is complete or the lagoon goes dry. The status of the lagoon is obtained at specified print-out time intervals, and a plotting subroutine GRAPH 4 is used to plot the simulation results. The program interactions are shown in Figure 15, and a complete listing of the program appears in Appendix C.

C. Simulation Results

1. Simulation of the Water Surface

The effect of seepage rate on the lagoon depth was discussed in Section V.A.1; an estimated rate of 0.12 cm day^{-1} gave good agreement with measured values. Changes in the water surface were also simulated, as shown in Figure 16. As the lagoon dries, the southeast corner is the first to dry out and the lagoon recedes to the northwest corner. Observations of the water remaining in the lagoon in July and August were in good agreement with the model simulation.

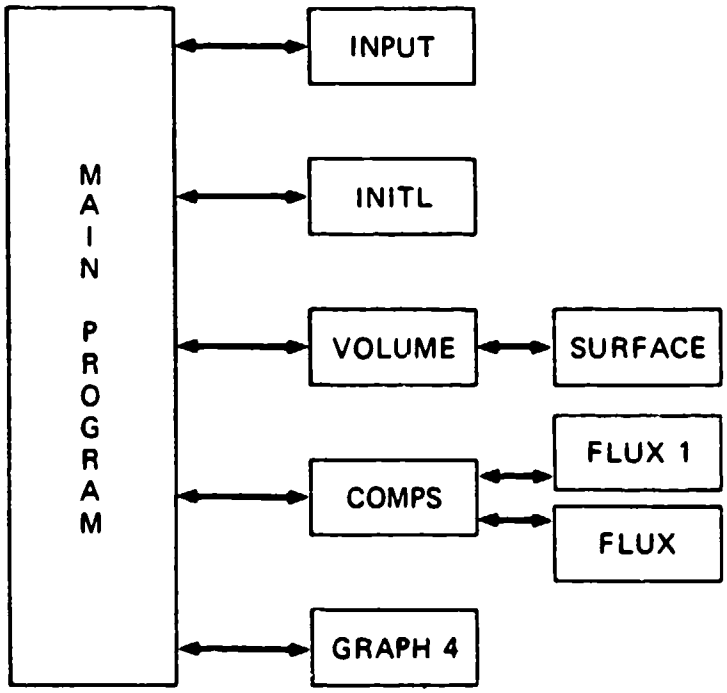

FIGURE 15 PROGRAM INTERACTIONS

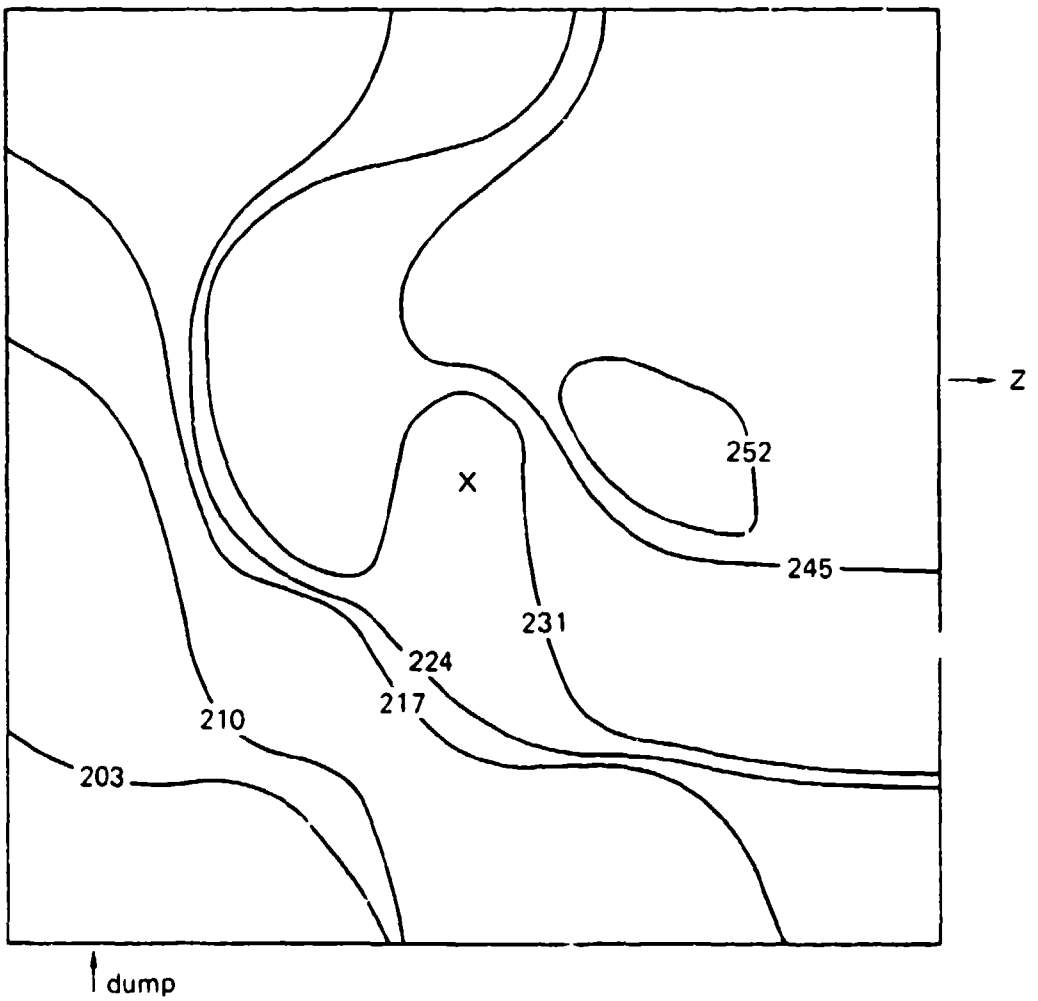

FIGURE 16 APPROXIMATE WATER CONTOUR LINES DURING THE SIMULATION

2. TNT Simulation

a. Case 1: Complete Mixing

Five scenarios were investigated in which the assumption was made that the lagoon is a completely mixed reactor. Figure 17A shows the TNT concentration as a function of time using inputs from diffusion flux and dissolution, a photolysis rate constant of 0.78 cm day^{-1}, and a biotransformation rate constant of 0.012 day^{-1}. The results indicate that the TNT concentration will increase until Day 200, with the peak concentration being 17.5 ppm. After Day 200, TNT concentration decreases due to decreases in the lagoon depth, which increases the magnitude of the photolysis rate constant.

To test the impact of the photolysis rate constant, a simulation was run under conditions identical to those above except that the photolysis rate constant was reduced by half--to 0.39 cm day^{-1}. Figure 17B shows the simulation result. In this case, the TNT concentration builds up faster than in the previous case and reaches a maximum of 23 ppm on Day 200. After Day 200, the TNT concentration decreases at a slower rate than before.

The photolysis rate constant is also seasonally dependent due to high light intensity in the summer months relative to that in the winter months. The magnitude of the intensity change is usually between a factor of 2 to 3. In Figure 17C, we adjusted the photochemical rate constant by a factor of 2, starting in June, and observed an accelerated decrease in TNT concentration in the late summer months. The overall effect appears to be a lowering of the maximum TNT concentration buildup followed by a rapid loss of TNT.

We performed a simulation in which the biotransformation rate constant was doubled for every 10°C rise in lagoon temperature, based on a number of assumptions involving the enzymatic reduction of a TNT nitro group. The result is plotted in Figure 18. In the early part of the simulation, the TNT concentration rises above that observed in Figure 17A due to the low biotransformation rate constant. However,

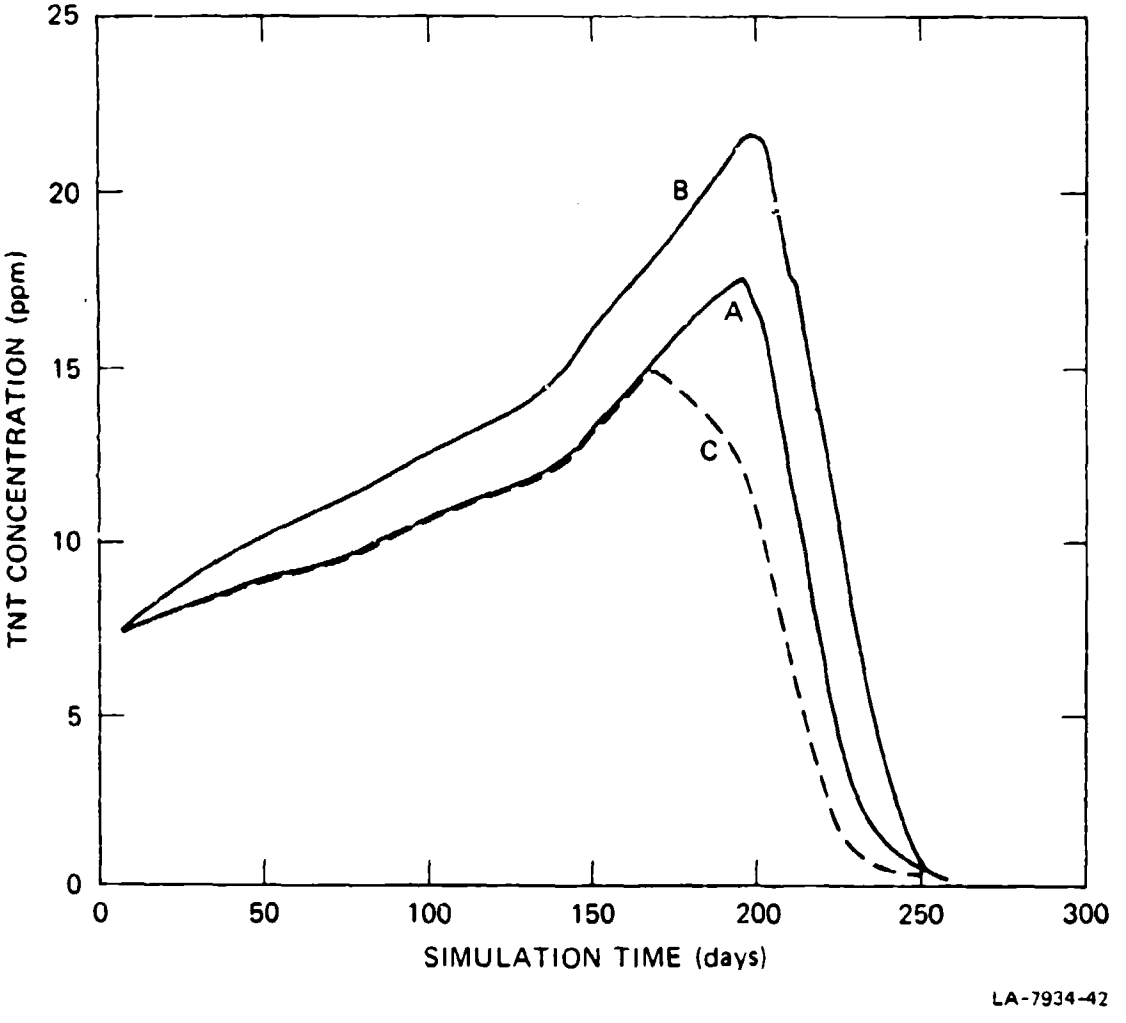

FIGURE 17 SIMULATED TNT CONCENTRATION WITH RESPECT TO TIME OF YEAR

Curve A: k_p = 0.78 cm day^{-1}, k_b^1 = 0.012 day^{-1}; input from diffusion and dissolution.
Curve B: k_p = 0.39 cm day^{-1}, k_b^1 = 0.012 day^{-1}; input from diffusion and dissolution.
Curve C: k_p = 0.78 cm day^{-1} plus radiant correction; k_b^1 = 0.12 day^{-1}; input from diffusion and dissolution.

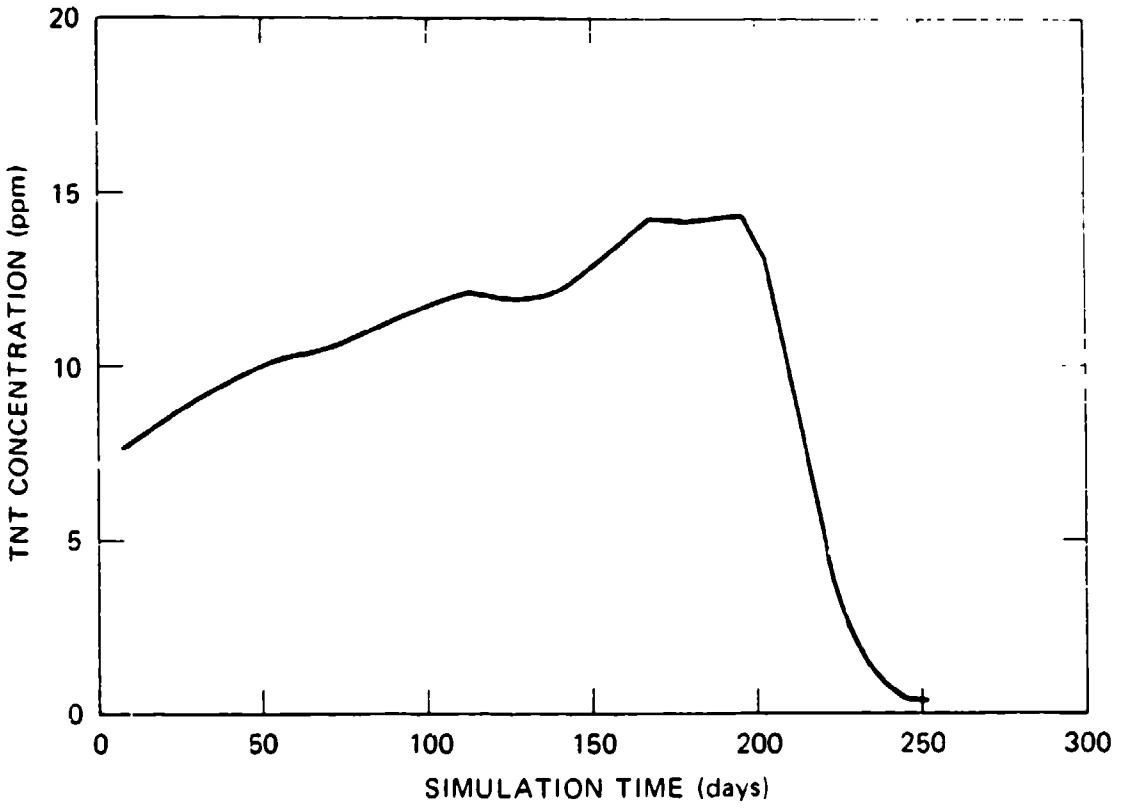

FIGURE 18 SIMULATED TNT CONCENTRATION AS A FUNCTION OF TIME OF YEAR

k_ρ = 0.78 cm day^{-1}; k_b^1 = 0.006 day^{-1} and doubled for every 10°C rise in temperature; input from diffusion and dissolution.

the effect of biotransformation becomes evident between Days 150 and 200. In the latter phase of the simulation, photolysis becomes the dominant transformation process.

Finally, we considered a case in which dissolution was the only input source of TNT (Figure 19). The simulation results show TNT concentration decreasing in the early stage of simulation and then increasing in May, reaching a maximum at Day 200 and then decreasing as the lagoon dries out.

The concentration-time-dependent profile measured in the lagoon for TNT appears in Figure 20. None of the above scenarios exactly match the measured data. The low concentration observed in March (Day 74) does not appear in any simulation except in the case of the sole input arising from dissolution (Figure 19). The maximum TNT concentration was observed in May (Day 145), whereas the simulation results predicted that the maximum would occur in July. To reach a maximum in May, a large input from the bottom sediment would be expected. The present model probably overestimates the diffusion and dissolution processes in the latter months. Also, the lagoon begins to dry out at the end of June; this process should concentrate chemicals due to volume reduction and concentrate the TNT in July unless the transformation processes are greatly accelerated. Both the photolysis and biotransformation of TNT in lagoon water collected in July give no suggestion of dramatic rate increases compared to other experimental data.

The discrepancy between the observed data and the simulations may be explained by the sampling technique and the lagoon location from which the samples were taken. Because the plant personnel did not have access to the center of the lagoon to collect samples, all sampling done by them was performed at the southeast edge near the dump ramp, where high levels of TNT were found in the sediment. As the lagoon dried, samples were taken progressively closer to the center of the lagoon approaching the northwest corner. Poor mixing of the lagoon water may therefore obscure the simulation results.

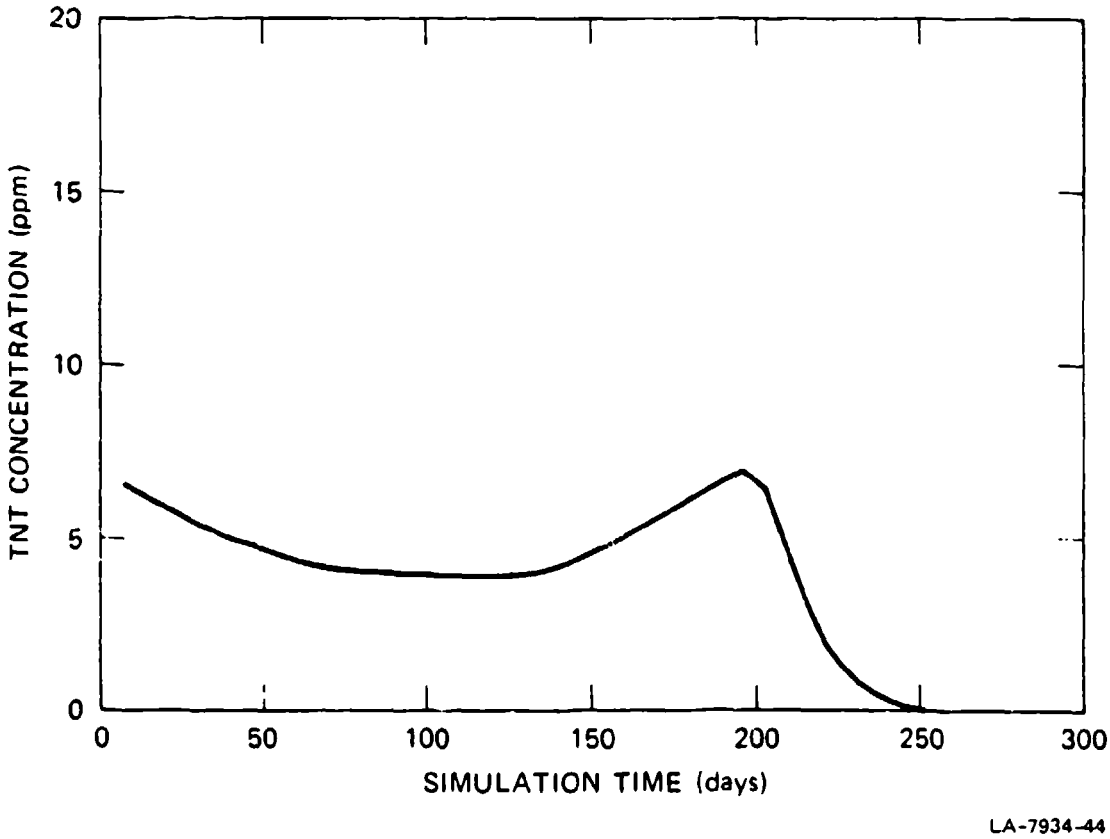

FIGURE 19 SIMULATED TNT CONCENTRATION FROM THE CASE OF SOLE INPUT FROM DISSOLUTION

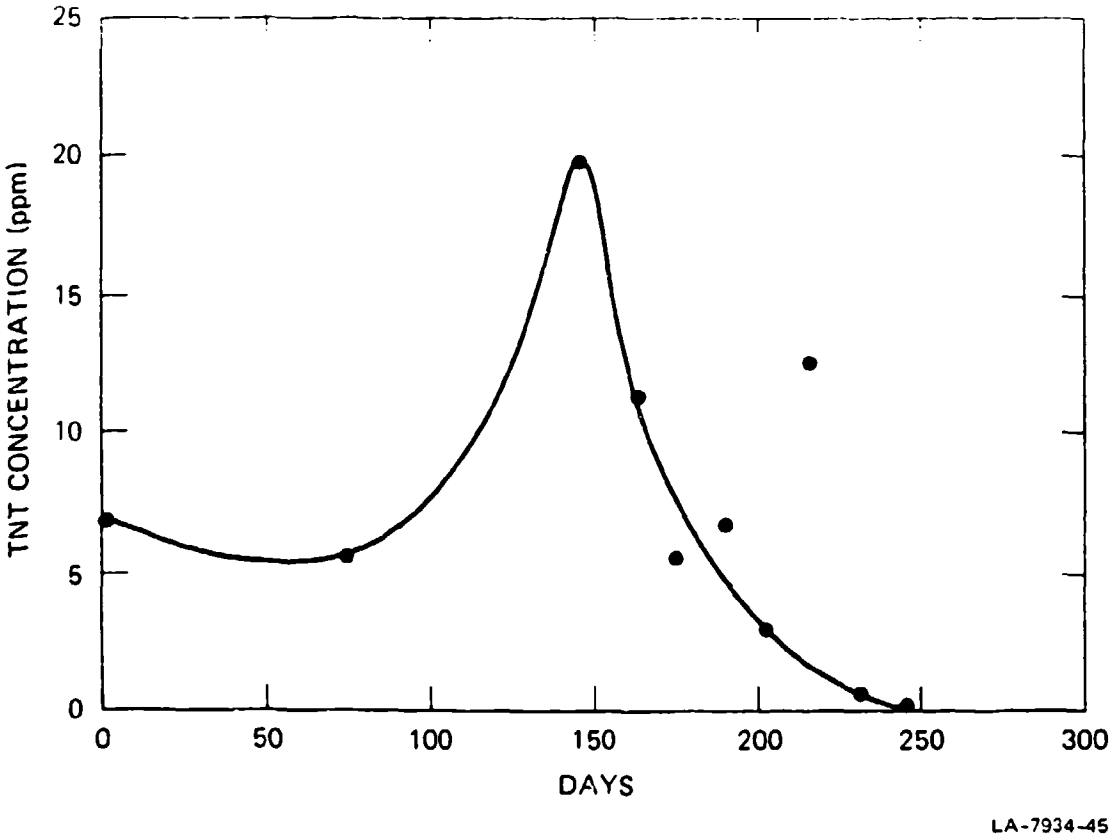

FIGURE 20 CONCENTRATION-TIME-DEPENDENT PROFILE OF TNT MEASURED IN LAGOON NO. 9

b. Case II: Zero Mixing

If the sampling locations become critical, the assumption of complete mixing may not be a valid representation of the distribution of chemicals in the lagoon. Although the data on dissolved oxygen obtained in December indicated that the lagoon was well-mixed in the vertical direction, discrepancies in TNT concentrations at the edge of the lagoon relative to the center were noted. This suggests that the horizontal mixing of lagoon water may not be complete and may intensify as the lagoon becomes shallow.

We performed simulations for the case of zero-mixing for compartments 1 (dump site) and 13 (center). In the case of zero-mixing, the lagoon waters do not interact with neighboring compartments--only with the bottom sediment directly below the water. The simulation results are shown in Figure 21. In compartment 1, the TNT concentration continuously increases until maximum solubility is reached. In compartment 13, the TNT concentration continually decreases due to low TNT levels in the sediment and transformation rates that surpass those of diffusion and dissolution fluxes. In the real environment, partial mixing probably occurs that dissipates the TNT from compartments 1 to other compartments in the lagoon. These results do imply, however, that sampling from the southeast corner and following the water-coverage profile (Figure 16) for further samples may give skewed versions of the TNT concentration profile that are difficult to model. In this respect, the model simulation may be adequately predicting the loss and movement of TNT in the dissolution-input-only case (Figure 19), when compared to the actual data, that may be higher than in a completely mixed reactor (Figure 20). An overlay of the latter profiles appears in Figure 22.

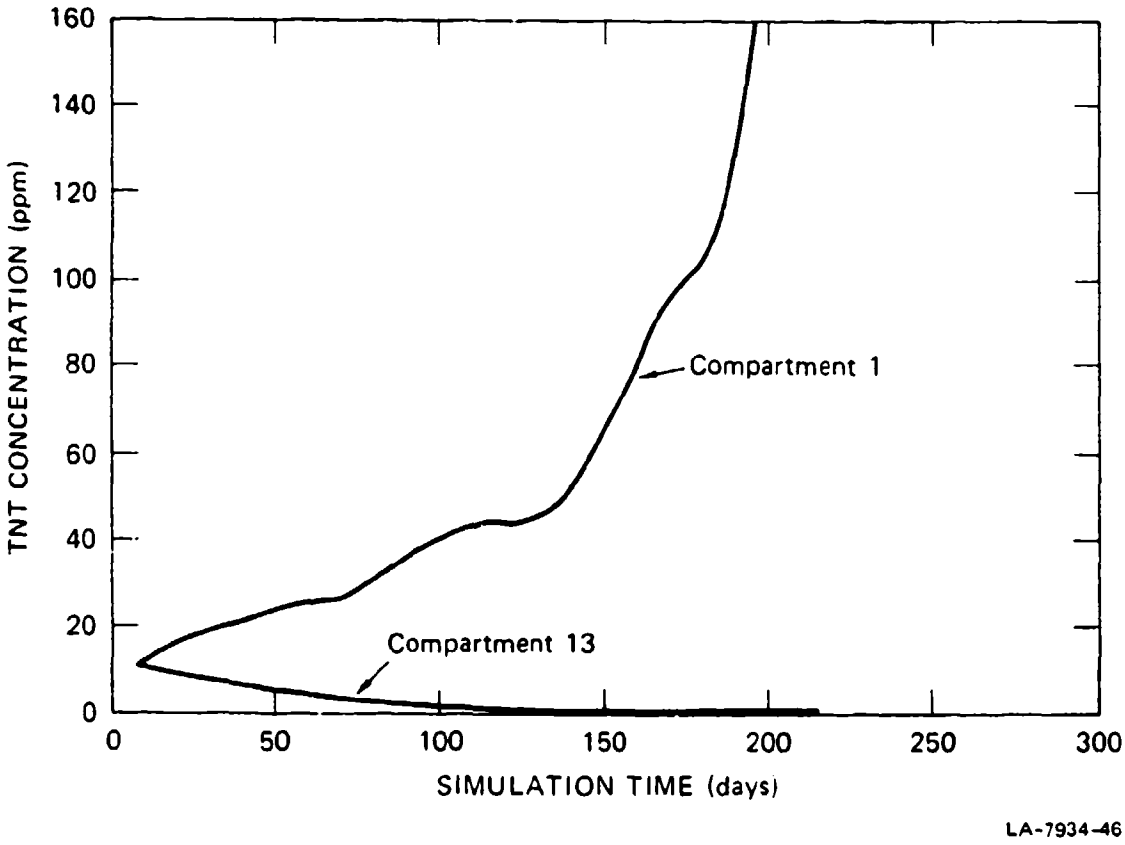

FIGURE 21 SIMULATION RESULTS FOR TNT IN COMPARTMENTS 1 AND 13 FOR THE CASE OF ZERO-MIXING

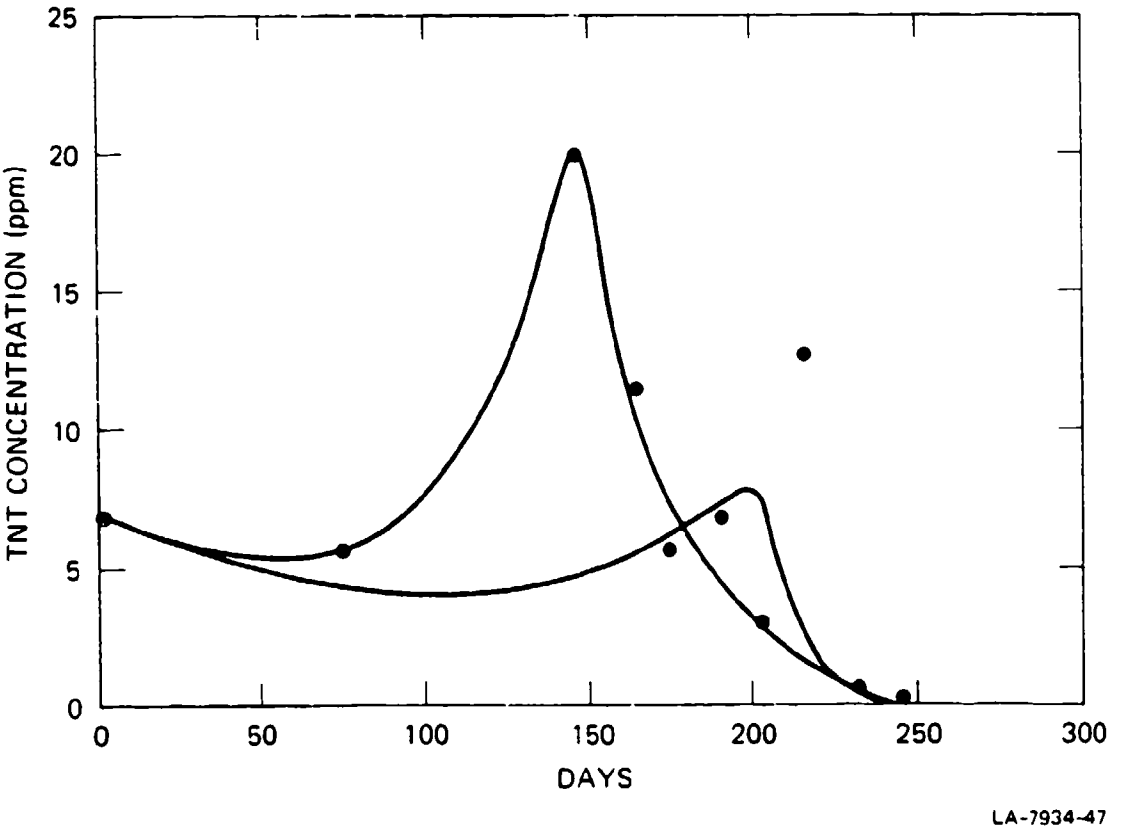

FIGURE 22 COMPARISON OF THE SIMULATION RESULTS FROM THE CASE WITH DISSOLUTION AS THE ONLY INPUT SOURCE OF TNT TO MEASURED DATA FROM THE LAGOON

3. RDX Simulation

The laboratory studies showed that there would be little biotransformation of RDX in the lagoon and that photolysis, although slow, probably would be the dominant transformation process. Knowing the range of the depth-independent photochemical rate constant for the winter through summer seasons, we derived a linear expression relating the rate constant, k_p, to the day of the year, D:

$$K_p = (3.0 \times 10^{-4} \text{ cm day}^{-2}) (D) + 1.6 \times 10^{-2} \text{ cm day}^{-1} \quad . \tag{45}$$

Thus, at Day 0 (January 1) the winter rate constant, 0.016 cm day^{-1}, is applied to the model and linearly increases to Day 200 (July 19), where the summer rate constant is applied. At each simulation interval, the rate constant is adjusted according to the depth of the lagoon for that time period.

Three scenarios were simulated representing the observed rate constants and rate constants representing 75% and 50% of the observed rate constants. The latter rate constants provide a sensitivity analysis of the impact of the photochemical rate constant on RDX loss in the lagoon. The simulation results are plotted in Figure 23. In each case, the simulated results indicate that the removal of RDX is balanced by the diffusion and dissolution input over the first 150 days. As the water gets warmer, the concentration increases up to Day 225; then the effect of photolysis is noted only when the lagoon is very shallow. Also, halving the photolysis rate constant (Curve C) does not have a large effect on the RDX-loss profile.

Superimposed on these curves are the actual measured values for RDX in the lagoon. Considering the problem of partial mixing, the simulation results and the actual values are comparable except for one data point where a very high level (42.1 ppm) of RDX was observed.

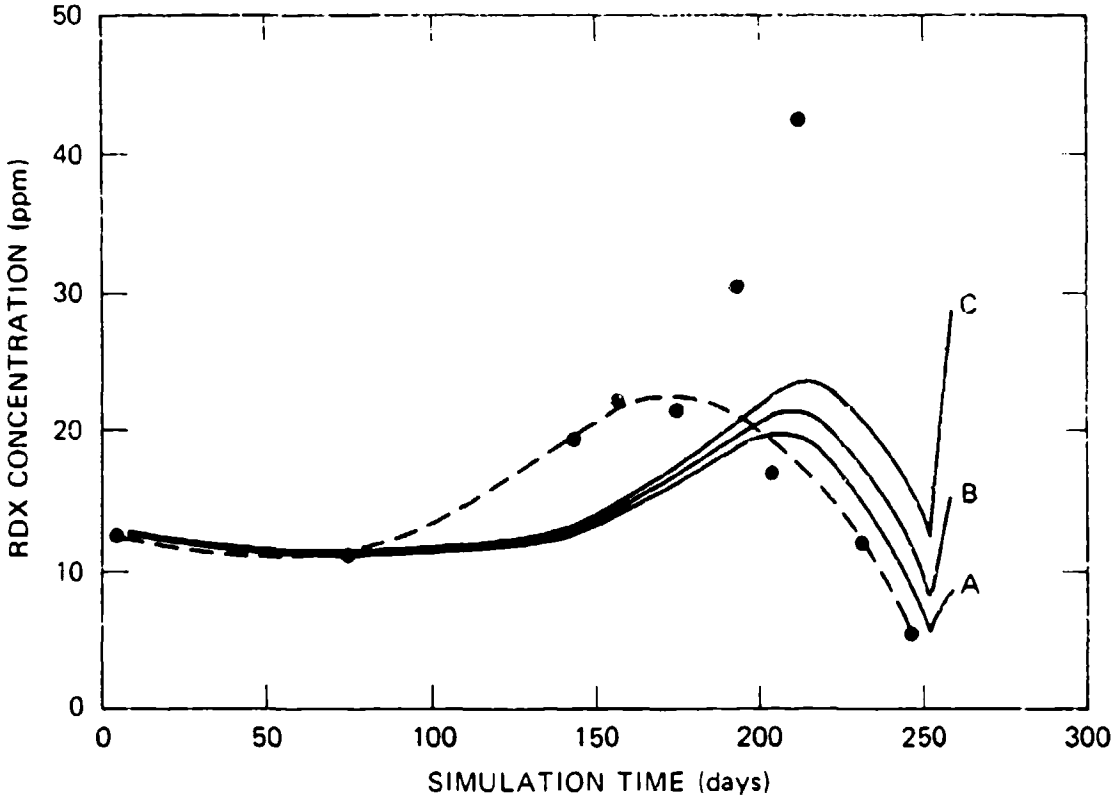

FIGURE 23 SIMULATION RESULTS FOR RDX CONCENTRATION IN LAAP LAGOON WATER

Curve A: $k'_p = k_p$; Curve B: $k'_p = 0.75\ k_p$; Curve C = $k'_p = 0.50\ k_p$

● = Found Value

The remaining data are, however, inconsistent with this point. A curve for the profile of RDX can be approximated (dotted line) that shows a peak in RDX concentration in late July and a decrease in late August. These results suggest that the diffusion/dissolution processes become faster than predicted by the model in May and June (Days 145 to 175) and that the loss rate is faster than predicted in late August (Day 245). This is probably a result of (a) warmer waters near the edge of the lagoon where the samples were taken, which could give high concentrations in May-June, and (b) the low water level and the recession of the water's edge from the munitions-enriched sediment area, which could give low concentrations in late August. If complete mixing were to occur, the simulation results might be fairly accurate.

VII. DISCUSSION

The results of this study show that the lagoons at LAAP are highly complex environments in which the fate of TNT is controlled by photolysis and biotransformation and the fate of RDX probably is controlled by photolysis. If there were no chemical inputs to the lagoon, we would estimate a TNT half-life ranging from 8 days in the winter months to <4 days in the summer and an RDX half-life ranging from 173 days in the summer to >1000 days in the winter in a lagoon 50 cm deep. However, there are chemical inputs to the lagoon from solid and sorbed munitions in the bottom sediment and on the bottom surface. Thus, both diffusion and dissolution kinetics play important roles in the input of chemicals to the lagoon. These processes are complicated by 1) a heterogeneous distribution of munitions in and on the sediment and 2) a temperature-dependence that increases chemical inputs as the lagoon warms. Thus, chemical input is not a constant process, but one that can change dramatically, depending on the time of year and the portion of the lagoon that is covered by water.

Furthermore, each transformation process has additional complications. In the case of biotransformation, the enzymatic reduction of the nitro group should be temperature-dependent, and therefore the biotransformation rate constant could vary by a factor of 8 or more (assuming a doubling of the rate constant for every 10° rise in temperature) between the winter and summer months. Also, we cannot be sure that the population of organisms at 10°C is the same as that at 40°C. The temperature effect could have an impact on the number and type of microorganisms that are available to transform TNT. To average this effect, we used a rate constant determined at 25°C as an average value in one example and doubled the rate constant for every 10°C rise in temperature in another example. The results of these

examples indicated that changes in the biotransformation rate constant did not have a major impact on the loss profile of TNT because the photochemical transformation process overwhelmed any such changes.

There is also a high degree of uncertainty in the photochemical rate constant as a function of the time of year. Photochemical rate constants measured in lagoon water collected in December showed an inverse relationship with depth, which allows the prediction of a rate constant at any depth, provided that the absorptivity of the water is the same. However, as the lagoon waters evaporate, much of the UV-absorbing materials become concentrated, reducing the ability of light to penetrate into the water. The effect of the more concentrated waters will be to lower the photochemical rate constant, but simultaneously the shallower depth will tend to increase it. Because the photochemical transformation of TNT occurs by indirect mechanisms and is governed by unknown sensitizers (both humic materials and TNT transformation products) in the waters, it is difficult to correlate the photochemical rate constant dependences on the absorptivity and depth of the lagoon water from the experiments that were performed during this study.

Sampling was a problem because of poor access to a center location for the bulk water and because the sites from which the samples were collected changed as the lagoon dried. Finally, the lagoon dried up in late August.

In spite of these difficulties, we were able to develop a simulation model that describes the loss profile of TNT and RDX as a function of time of year. Of primary importance in this model is the dissolution rate of pure chemicals from the bottom sediment. This process is temperature-dependent and therefore we expect the concentrations of TNT and RDX to rise as the lagoon warms in the spring and summer months. In the absence of transformation, dissolution will continue until the solubility limit for each chemical is reached.

A concentration buildup in the lagoon is counteracted by the photochemical and biological transformation of TNT and the photochemical transformation of RDX. The rate of photochemical transformation of TNT and RDX follows pseudo-first-order kinetics and first-order kinetics, respectively. Thus, for a given depth, TNT will photolyze approximately 50 times faster than RDX. The rate constant is dependent on the solar radiance; therefore, rates will be two to three times faster in the summer than in the winter months for TNT and up to five times faster for RDX.

The photochemical rate constant is inversely proportional to depth; hence, rates of transformation will increase as water is lost to evaporation and seepage. Usually, the lagoon is shallower in summer than in winter; therefore, rates of photochemical transformation are predicted to be greater in the summer. The biotransformation rate constant for TNT is an order of magnitude smaller than the photochemical rate constant; so a comparison of the dissolution flux and photochemical rate constant will indicate whether the TNT or RDX concentration will increase or decrease over any particular time period. Furthermore, if the input source is eliminated (as was observed when portions of the lagoon dried out), the TNT and RDX will transform at rates defined by the depth and mitigated by the absorptivity of the water. Thus, an overall profile of munitions in the lagoon will show a buildup of munitions when the lagoon is full, periods of equilibrium when the dissolution and transformation fluxes are equal, and periods when transformation flux exceeds that of dissolution--usually in the summer months.

The above theme has a number of variations that can be postulated and for which modeling can serve as a tool to predict chemical behavior. For example, if TNT and RDX were uniformly distributed in the bottom sediment, as was observed at the dump ramp, they would reach their solubility limits in the lagoon water. Similarly, if the sediment had a uniform distribution, as was found at the center of the lagoon, the transformation of TNT and RDX could be predicted from the transformation rate constants developed in this study.

In conclusion, the persistence of TNT and RDX in LAAP lagoons is controlled by dissolution and photochemical processes, with dissolution being complicated by a heterogeneous distribution of solid munitions on the bottom surface and photolysis being complicated by changes in absorptivity of the water that affects the photochemical rate constant as a function of time of year. This effect could not be investigated in detail because of project time and money contraints. A simulation model was developed to describe a first approximation of the loss and movement of TNT and RDX in the lagoon water, but vigorous validation could not be achieved due to sampling and mixing constraints within the lagoon.

Appendix A

ANALYSIS OF LAAP LAGOON NO. 9 SEDIMENT

Sediment Preparation

Twenty-four sediment samples scraped from the bottom surface of Lagoon No. 9 were sieved through a large mesh screen to remove twigs, leaves, and large pebbles. Each sample was homogenized with a mortar and pestle until an even consistency was obtained.

Moisture Determination

A known weight (~20 g) of sediment was placed in a tared beaker and allowed to dry at 75°C for 48 hr. The percent moisture in the sample was calculated as the dry weight minus the wet weight, divided by the wet weight times 100.

Extraction of Sediment

A sample of wet sediment (10-20 g) was placed in a 50-ml screw-cap centrifuge tube and 20 ml of neutral ethyl acetate was added. The tube was vigorously shaken for 2-3 min and then centrifuged at 2000 rpm for 10 min. The ethyl acetate was removed by pipet. This process was repeated twice. The sediment was then acidified by adding 5 ml of 2N HCl and re-extracted with ethyl acetate (3 × 20 ml). The combined extracts were dried over anhydrous sodium sulfate, filtered, and rotary-evaporated to dryness. The residue was dissolved in methanol, and an internal standard was added for HPLC analysis.

HPLC Analysis

The HPLC analyses of the sediment extracts were performed under the following conditions:

Instrument:	Spectra-Physics Model 3500B Liquid Chromatograph
Column:	250 mm × 4.6 mm Altex RP600-C_{18} @ 50°C
Solvent:	A - water, B - 50% methanol: 50% acetonitrile
Program:	30% B in A to 50% B in A in 15 min; linear gradient
Flow rate:	2.0 ml min^{-1}
Detection:	UV @ 254 nm
Retention times:	5.68 min, HMX
	6.65 min, RDX
	10.55 min, 3,5-dinitroaniline
	12.40 min, TNT
	13.77 min, aminodinitrotoluenes
	15.65 min, 3,5-dinitrotoluene (internal standard)

A typical chromatographic profile of the sediment extract appears in Figure A-1.

Results

The results of duplicate analyses of the 24 sediment extracts are presented in Table A-1 (also see Figure 2 in main text). Table A-2 shows the percent water in the sediment samples.

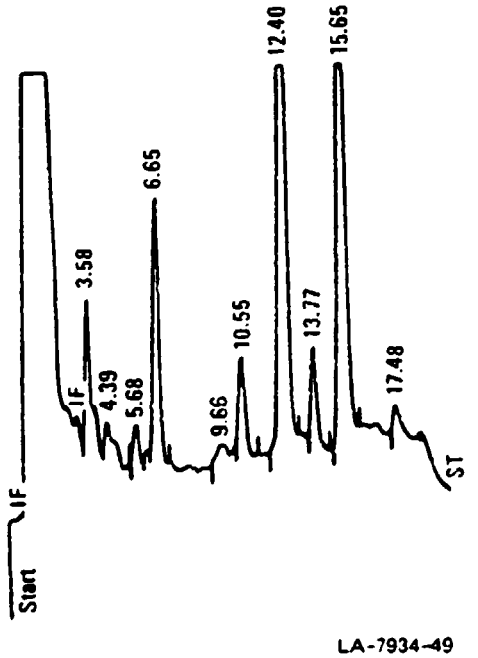

FIGURE A-1 HPLC PROFILE OF LAGOON NO. 9 SEDIMENT EXTRACT

Table A-1

PERCENT COMPOSITION OF MUNITION COMPONENTS
IN LAAP LAGOON NO. 9 SEDIMENT

Sample	TNT	RDX	HMX	ADNTS[a]	3,5-DNA
A-5	27.5	8.7	2.1	6×10^{-3}	---
A-4	29.7	6.6	8.9×10^{-1}	5.9×10^{-2}	---
A-3	1.5	8.9×10^{-1}	$3.\cdot 10^{-1}$	9.7×10^{-2}	---
A-2	4.2×10^{-2}	1.0×10^{-3}	8.7×10^{-2}	8.3×10^{-2}	5.0×10^{-3}
A-1	1.8×10^{-3}	4.7×10^{-3}	1.5×10^{-2}	9.2×10^{-3}	6.0×10^{-3}
B-5	1.4	4.7	8.4×10^{-1}	8.0×10^{-2}	8.0×10^{-3}
B-4	1.4×10^{-1}	1.7	3.5×10^{-1}	3.0×10^{-2}	---
B-3	4.0×10^{-2}	2.9×10^{-1}	1.1×10^{-1}	3.0×10^{-2}	3.3×10^{-2}
B-2	8.3×10^{-4}	7.9×10^{-3}	3.4×10^{-3}	1.3×10^{-2}	9.0×10^{-4}
B-1	1.4×10^{-2}	3.2×10^{-4}	1.5×10^{-2}	2.1×10^{-2}	1.5×10^{-3}
C-5	1.7×10^{-2}	1.0	2.4×10^{-1}	4.2×10^{-2}	4.0×10^{-3}
C-4	2.1×10^{-3}	3.6×10^{-3}	3.0×10^{-2}	5.9×10^{-3}	4.0×10^{-4}
C-3	4.4×10^{-3}	2.2×10^{-4}	1.8×10^{-2}	3.1×10^{-2}	3.1×10^{-3}
C-2	1.5×10^{-3}	2.0×10^{-4}	1.2×10^{-2}	9.1×10^{-3}	2.0×10^{-4}
C-1	5.7×10^{-4}	7.0×10^{-5}	1.5×10^{-2}	2.1×10^{-3}	6.0×10^{-4}
D-5	4.9×10^{-3}	1.7×10^{-2}	6.6×10^{-2}	3.3×10^{-2}	3.4×10^{-3}
D-4	1.2×10^{-2}	1.6×10^{-1}	9.0×10^{-2}	8.2×10^{-3}	1.0×10^{-3}
D-3	7.3×10^{-4}	3.8×10^{-2}	8.0×10^{-3}	1.3×10^{-2}	1.8×10^{-3}
D-2	1.1×10^{-3}	1.0×10^{-4}	1.3×10^{-2}	1.0×10^{-2}	8.5×10^{-4}
D-1	1.2×10^{-3}	9.0×10^{-5}	9.1×10^{-3}	1.4×10^{-2}	1.2×10^{-3}
E-4	1.9×10^{-3}	1.3×10^{-3}	5.0×10^{-3}	8.6×10^{-3}	1.2×10^{-3}
E-3	1.1×10^{-3}	4.9×10^{-4}	1.4×10^{-2}	1.6×10^{-2}	2.6×10^{-3}
E-2	1.1×10^{-3}	7.5×10^{-4}	1.6×10^{-2}	1.5×10^{-2}	9.4×10^{-4}
E-1	2.2×10^{-4}	6.0×10^{-5}	4.0×10^{-4}	3.1×10^{-4}	6.0×10^{-5}

[a]ADNTS = aminodinitrotoluenes.

Table A-2

PERCENT WATER IN LAGOON NO. 9 SEDIMENT SAMPLES

Sample No.	Percent Water
A-5	51.6
A-4	33.6
A-3	34.1
A-2	43.3
A-1	48.5
B-5	41.6
B-4	32.4
B-3	31.0
B-2	33.9
B-1	42.1
C-5	33.3
C-4	38.6
C-3	30.2
C-2	32.9
C-1	58.2
D-5	35.3
D-4	48.1
D-3	38.0
D-2	39.2
D-1	43.3
E-4	32.2
E-3	29.5
E-2	30.1
E-1	45.7

Appendix B

MASS TRANSFER PROBLEMS--ASSUMPTIONS AND SOLUTIONS

Description of Mass Transfer Problems

A body of water containing some concentration of one or more contaminants is in contact with a porous sediment (Figure B-1). Water residing in the pores of the sediment (interstitial water) also contains some concentration of one or more contaminants. The sediment solids may contain the same contaminants, presumed to be at equilibrium with the interstitial water concentration of contaminants. Contaminants will diffuse through the water both in the free-water phase and the sediment/water phase. In addition, chemical reactions (photolysis, biodegradation, hydrolysis) may occur, and contaminants may be transported by bulk convection (seepage of water into the sediment).

Far from the water/sediment interface, one expects the concentrations of contaminants to reach a constant (known) value. Also, on the free-water side of the interface, a region should exist where the macroscale mixing processes of the pond are negligible. With these ideas in mind, one can pose a set of simultaneous differential equations for the concentration profile of a contaminant in the water and sediment/water phases.

The change in concentration of chemical with time $\left(\frac{\partial C_{sw}}{\partial t}\right)$ is equal to the sum of the diffusion and seepage rates $\left(D_1 \frac{\partial^2 C_{sw}}{\partial z^2} \text{ and } v \frac{\partial C_{sw}}{\partial z}, \text{ respectively}\right)$ minus the biotransformation rate (k_o) and the amount of chemical that is sorbed to the sediment:

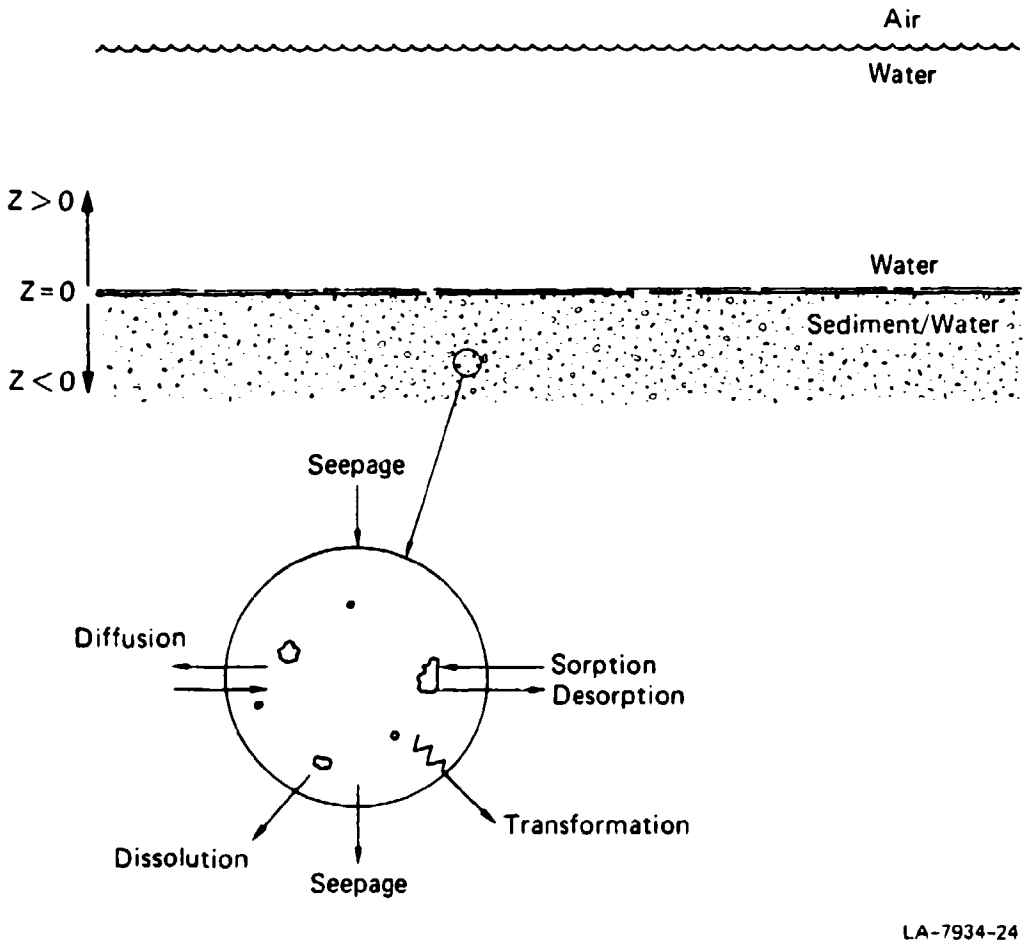

FIGURE B-1 LAGOON WATER RESTS ON SEDIMENT

Pond and sediment are considered to be semi-infinite.

$$\frac{\partial C_{sw}}{\partial t} = D_1 \frac{\partial^2 C_{sw}}{\partial z^2} + v \frac{\partial C_{sw}}{\partial z} - k_o - KnC_{sw}^{n-1} \frac{\partial C_{sw}}{\partial t} \quad . \tag{1}$$

Rearrangement of Equation 1 yields

$$1 + KnC_{sw}^{n-1} \frac{\partial C_{sw}}{\partial t} = D_1 \frac{\partial^2 C_{sw}}{\partial z^2} + v \frac{\partial C_{sw}}{\partial z} - k_o \quad ,$$

where C_{sw} = chemical concentration in the se i w
K = sediment partition coefficient ($C_s = KC_{sw}^n$)
t = time
D_1 = diffusion coefficient in the sediment/water phase
v = seepage velocity
z = distance from the sediment
k_o = zero-order rate constant for biotransformation in sediment.

Similarly, for the free-water phase, the change in concentration of a chemical with time can be described by

$$\frac{\partial C_w}{\partial t} = D_2 \frac{\partial^2 C_w}{\partial z^2} + v \frac{\partial C_w}{\partial z} - \Sigma k_1 C_w \quad , \tag{3}$$

where C_w = concentration of chemical in the free-water phase
t = time
D_2 = diffusion coefficient in the free-water phase
v = seepage velocity
$\Sigma k_1 C_w$ = first-order rate expression for transformation process.

The boundary conditions for these equations are that

$$\phi D_1 \frac{\partial C_{sw}}{\partial z} = D_2 \frac{\partial C_w}{\partial z} \quad \text{at } z=0 \quad , \tag{4}$$

where ϕ is the sediment porosity (void volume fraction) and

$$C_{sw}(0) = C_w(0) \quad , \tag{5}$$

$$C_{sw}(-\infty) = C_{sw,\infty} = \text{known} \quad , \tag{6}$$

$$C_w(\infty) = C_{w,\infty} = \text{known} \quad , \tag{7}$$

$$C_{sw}(z) = \text{known at time zero} = C_{sw,o} \quad , \tag{8}$$

$$C_w(z) = \text{known at time zero} = C_{w,o} \quad . \tag{9}$$

Because of Equations 5 and 6, Equations 2 and 3 must be solved simultaneously and are not amenable to a closed-form analytical solution. The equation could be solved on a digital computer, but the additional complexity would greatly increase the expense of running the overall SRI pond simulation model. Therefore, we have made several simplifying assumptions, described below.

Comparison of Diffusion, Convection, Reaction Rates

Because there is a strong incentive to reach a closed-form, analytical solution, the first assumption is that the concentration of chemical is constant everywhere in the free-water phase. This assumption allows Equation 3 to be eliminated.

Further simplifications could be made if either the convective term $\left(v\frac{\partial C_w}{\partial z}\right)$ or the reaction term (k_o) could be neglected. By non-dimensionalizing the equations, one can evaluate the relative importance of diffusion, reaction, and convection. Unfortunately, even the single differential equation cannot be solved analytically if there is no boundary on the sediment phase. Therefore, to compare the importance of diffusion, reaction, and convection, we pose a problem where the sediment phase has a boundary layer of finite thickness, ℓ, near the water/sediment interface (Figure B-2). Furthermore, we assume steady-state conditions. This assumption leaves a simple differential equation describing the concentration in the sediment-water phase. In dimensionless form, this equation is

$$\frac{d^2C^*_{sw}}{dz^{*2}} + \xi_o \frac{dC^*_{sw}}{dz^*} - \gamma_o = 0 \quad , \tag{10}$$

where ξ_o = ratio of convective transport rate to diffusive transport rate

γ_o = ratio of chemical reaction rate to diffusive transport rate

with boundary conditions

$$C^*_{sw}(0) = \frac{C_w}{C_{sw,\infty}} \quad C^*_w = \text{known} \tag{11}$$

and

$$C^*_{sw}(-1) = 1 \quad . \tag{12}$$

The dimensionless parameters are

$$C^*_{sw} = \frac{C_{sw}}{C_{sw,\infty}} \tag{13}$$

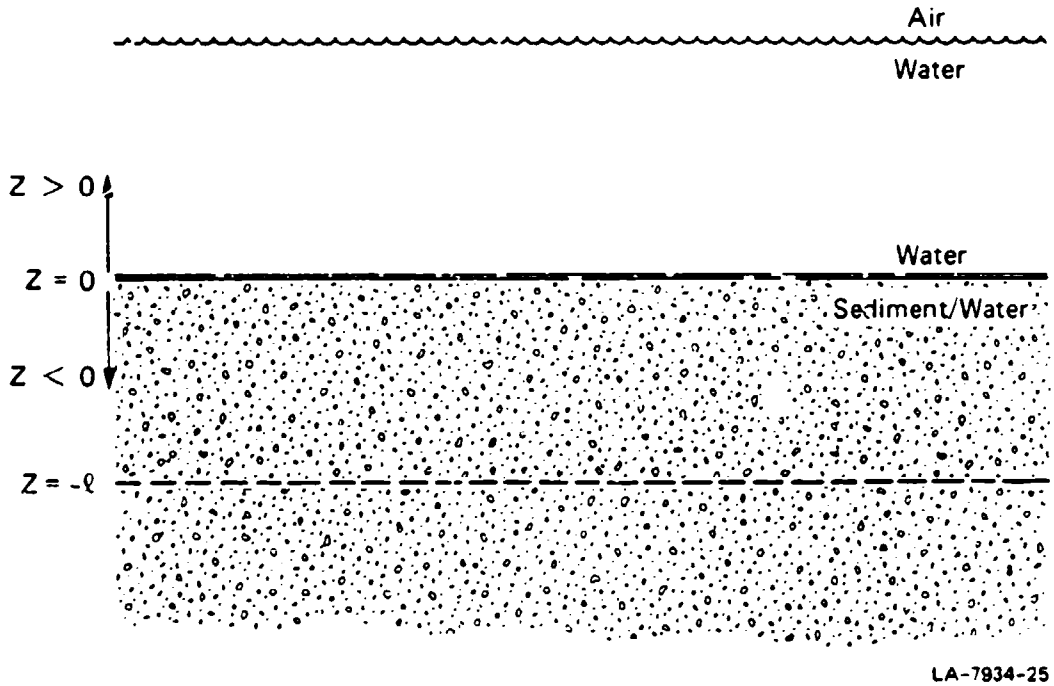

FIGURE B-2 BOUNDARY LAYER APPROXIMATION IN SEDIMENT/WATER PHASE

Beyond a depth of ℓ, the sediment is undisturbed by the mass transfer. Hence, flux can be computed as if sediment/water phase extended only to $z = -\ell$.

$$z^* = \frac{z}{\ell} \quad , \tag{14}$$

$$\xi_o = \frac{\ell v}{D_l} \quad , \tag{15}$$

and

$$\gamma_o = \frac{k_o \ell^2}{C_{sw,\infty} D_l} \quad . \tag{16}$$

The parameter ξ_o is a measure of the ratio of convective flux to diffusive flux, and γ_o is a measure of the ratio of the rate of reaction to the rate of diffusion. The flux, N, in dimensional form is

$$N = - \phi D_l \left(\frac{\partial C}{\partial z}\right)_{z=0} - \phi v C_{sw}(0) \quad . \tag{17}$$

Defining a dimensionless flux,

$$N_1^* = \frac{N\ell}{\phi D_l C_{sw,\infty}} \quad , \tag{18}$$

we find, by solving Equation 10 for C_{sw}^* and substituting into Equation 17, that

$$N_1^* = \frac{\xi_o C_w^* + \frac{\gamma_o}{\xi_o} e^{\xi_o} - \xi_o - \frac{\gamma_o}{\xi_o} - \gamma_o}{1 - e^{\xi_o}} \quad . \tag{19}$$

To evaluate the relative importance of the various phenomena, Equation 8 was solved with $\gamma_o = 0$ (no chemical reaction, N_2^*), with $\xi_o = 0$ (no convection, N_3^*), and with $\gamma_o = \xi_o = 0$ (no chemical reaction and no convection). The dimensionless fluxes for each of these cases, N_2^*, N_3^*, N_4^*, are given as follows:

$$N_2^* = \frac{\xi_o(1 - C_w^* e^{\xi_o})}{e^{\xi_o} - 1} \tag{20}$$

$$N_3^* = (1 - C_w^*) - \gamma_o/2 \tag{21}$$

$$N_4^* = (1 - C_w^*) \quad . \tag{22}$$

To compare N_1^* to N_2^*, N_3^*, and N_4^*, we need to pose some reasonable values of the parameters C_w^*, ξ_o, and γ_o. SRI has taken data from field samples of the waste disposal pond and found the following numbers:

v	$= 2.2 \times 10^{-6}$ cm s^{-1}		(23a)
k_o	$= 1.2 \times 10^{-5}$ μg cm^{-3} s^{-1}	(for TNT)	(23b)
D_l	$= 3.05 \times 10^{-6}$ cm^2 s^{-1}	(for TNT)	(23c)
$C_{sw,\infty}$	$= 50$ μg cm^{-3}	(for TNT)	(23d)
C_w^*	$= 0.1$	(for TNT)	(23e)

Because the boundary thickness, ℓ, exists only in our model (not in the real pond), reasonable estimates for ℓ must be made. Therefore, in Table B-1, the results are presented for various boundary thicknesses. The table shows the dimensionless flux (N_1^*) and flux values neglecting chemical reaction (N_2^*), convection (N_3^*), and reaction and convection (N_4^*), along with the ratios N_2^*/N_1^*, N_3^*/N_1^*, and N_4^*/N_1^*. These ratios show how much difference it makes if the convection, the reaction, or both are neglected. It can be seen that N_2^* is not much different from N_1^* and that N_3^* is not much different from N_4^*. Hence, the chemical reaction term can be neglected. In contrast, N_3^* can be much larger than N_1^* and N_4^* can be much larger than N_2^*. These results imply that the convective term cannot be neglected. Hence, the reaction can be neglected but convection must be considered. This conclusion was expected from the magnitude of the dimensionless numbers [$\xi_o \sim 1$ and $\gamma_o < 1$ (Table B-1)].

Table B-1

CALCULATED FLUX VALUES CONSIDERING ALL PARAMETERS (N_1^*),
NO CHEMICAL REACTION (N_2^*), NO CONVECTION (N_3^*),
NO REACTION OR CONVECTION (N_4^*), AND THEIR RATIOS TO (N_1^*)

Boundary Layer Thickness, ℓ (cm)	ξ_o	γ	N_1^*	N_2^*	N_3^*	N_4^*	N_2^*/N_1^*	N_3^*/N_1^*	N_4^*/N_1^*
0.5	0.355	0.019	0.705	0.714	0.890	0.900	1.013	1.263	1.276
1.0	0.710	0.076	0.514	0.547	0.863	0.901	1.065	1.679	1.753
1.5	1.066	0.171	0.327	0.397	0.815	0.900	1.215	2.491	2.752
2.0	1.42	0.304	0.148	0.265	0.748	0.900	1.793	5.056	6.081

Unsteady Solution with Convection, Without Reaction

By neglecting the chemical reaction term, we can develop a closed-form solution for flux without appeal to some arbitrary boundary layer thickness, ℓ. In this regard, the solution developed below is the most realistic situation for which a closed-form solution can be developed. The solution will apply to TNT and RDX because the RDX was found not to react in the sediment/water phase (i.e., $k_o = 0$ for RDX).

Physically, we envision a situation like that in Figure B-1. We retain the assumption that the concentration in the water phase is constant and known. For this situation, the following equations apply in the sediment/water phase:

$$1 + Kn\, C_{sw}^{n-1} \frac{\partial C_{sw}}{\partial t} = D_1 \frac{\partial^2 C_{sw}}{\partial z^2} + v \frac{\partial C_{sw}}{\partial z} \quad , \qquad (24)$$

with the following boundary conditions:

$$C_{sw}(-\infty, t) = C_{sw,\infty} = \text{known} \quad , \qquad (25a)$$

$$C_{sw}(0, t) = C_w = \text{known} \quad , \qquad (25b)$$

$$C_{sw}(z, 0) = C_{sw,\infty} = \text{known} \quad . \qquad (25c)$$

With $n = 1$ (linear isotherm assumption) and in dimensionless form, these equations become

$$\frac{\partial C_{sw}^*}{\partial t^*} = \frac{\partial^2 C_{sw}^*}{\partial z^{*2}} + \beta_o \frac{\partial C_{sw}^*}{\partial z^*} \quad , \qquad (26)$$

where β_o = dimensionless ratio of convective transport rate to diffusive transport rate,

and

$$C^*_{sw}(-\infty, t^*) = 0 \tag{27a}$$

$$C^*_{sw}(0, t^*) = C^*_w - 1 \tag{27b}$$

$$C^*_{sw}(z^*, 0) = 0 \quad , \tag{27c}$$

where the dimensionless variables have been defined as follows:

$$C^*_{sw} = \frac{C_{sw} - C_{sw,\infty}}{C_{sw,\infty}} \tag{28a}$$

$$t^* = \frac{D_1 t}{z_o^2 (1+K)} \tag{28b}$$

$$z^* = z/z_o \tag{28c}$$

$$\beta_o = \frac{z_o v}{D_1} \quad . \tag{28d}$$

The quantity z_o is an arbitrary length scale that, if reasonably chosen, can give some idea of the relative importance of diffusion and convection. (The final answer will not, of course, depend on z_o.)

Equation 26, subject to the boundary conditions of Equations 27a-27c, can be solved by using LaPlace transformations. One finds

$$C^*_{sw}(z^*, t^*) = \frac{(C^*_w - 1)}{2} \left\{ \operatorname{erfc}(\eta_1) + \exp\left(-\beta_o z^*\right) \operatorname{erfc}(\eta_2) \right\} \quad , \tag{29a}$$

where

$$\eta_1 = \frac{-z^*}{2t^{*1/2}} - \frac{\beta_o t^{*1/2}}{2} \qquad (29b)$$

and

$$\eta_2 = \frac{-z^*}{2t^{*1/2}} + \frac{\beta_o t^{*1/2}}{2} \quad . \qquad (29c)$$

The flux, N, is given by

$$N = -\phi D_1 \left(\frac{\partial C_{sw}}{\partial z}\right)_{z=0} - \phi v\, C_{sw}(o) \quad . \qquad (30)$$

In dimensionless form,

$$N^* = \frac{z_o N}{\phi D_1 C_{sw,\infty}} = -\left(\frac{\partial C^*_{sw}}{\partial z^*}\right)_{z^*=0} - \beta_o C^*_w \quad . \qquad (31)$$

Differentiating Equation 28 and substituting into Equation 31, one finds

$$N^* = \frac{(1 - C^*_w)}{(\pi t^*)^{1/2}} \exp\left(\frac{-\beta_o^2 t^*}{4}\right) - \frac{\beta_o}{2}(1 - C^*_w)\,\mathrm{erfc}\left(\frac{\beta_o t^{*1/2}}{2}\right) - \beta_o C^*_w \quad . \qquad (32)$$

Equation 32 can be cast in a form that explicitly removes z_o from the equation for the flux. If we define a new dimensionless flux,

$$\tilde{N} = \frac{N}{\phi v C_{sw,\infty}} \quad , \qquad (33)$$

and a new dimensionless time,

$$\tilde{t} = \frac{v^2 t}{D_1(1+K)} \quad , \tag{34}$$

then Equation 32 becomes

$$\tilde{N} = \frac{(1 - C_w^*)}{(\pi\tilde{t})^{1/2}} \exp(-\tilde{t}/4) - \left(\frac{1-C_w^*}{2}\right) \operatorname{erfc}\left(\frac{\tilde{t}^{1/2}}{2}\right) - C_w^* \quad . \tag{35}$$

Relationship To SRI Lagoon Model

Equation 32 is the basis for computing how much material transfers into or out of the sediment during a given time interval.* If M is the total mass of material per unit area transported across the water/sediment interface in a time interval, τ,

then

$$\tilde{M} = \int_0^{\tau^*} \tilde{N} d\tilde{t} \quad , \tag{36}$$

with

$$\tilde{M} = \frac{vM}{\phi D_1 (1+K) C_{sw,\infty}} \tag{37}$$

*Note that the z direction was chosen positive in Figure B-1. Therefore N > 0 implies that material moves from the sediment into the water.

and

$$\tau^* = \frac{v^2 \tau}{D_1 (1+K)} \quad . \tag{38}$$

Substituting Equation 35 into Equation 36, one finds

$$\tilde{M} = \left(1-C_w^*\right) \left\{ \text{erf} \left(\frac{\tau^{*1/2}}{2}\right) - \frac{\tau^*}{2} \text{erfc} \left(\frac{\tau^{*1/2}}{2}\right) + \frac{\tau^{*1/2}}{\sqrt{\pi}} \exp(-\tau^*/4) \right\} - C_w^* \tau^* \quad . \tag{39}$$

The functions erf and erfc are well-known, tabulated integrals.* These functions are available on any computer that has the standard IMSL math library software.†

In the SRI lagoon model, one knows C_w^* and $C_{sw,\infty}$ at the beginning of a time step (and, by implication, at time zero). During a time step, one allows mass to transfer between the water and the sediment/water phases. The total amount of mass transferred is given by Equation 39. At the end of the time step, the new values of C_w^* and $C_{sw',\infty}$ are computed based on the addition or depletion of contaminant mass in the water or sediment/water phases. Computations are repeated as desired with these new values of C_w^* and $C_{sw',\infty}$.

---

*Carslaw, H.S. and J.C. Jaeger (1959) Conduction of Heat in Solids. Oxford-at-the-Clarendon, London.

†Abramowitz, M. and I.A. Stegun (1964) Handbook of Mathematical Functions, National Bureau of Standards, Applied Mathematics Series 55, June, 1964.

Sample Calculation

The flux, N, and the total amount transformed, M, will be computed for the particular parameters relevant to the TNT and RDX disposal lagoon. The values of the parameters are given by Equations 23a, 23b, 23c, and 23d. In addition, we must specify a value for K and ϕ. For TNT, $K \tilde{=} 10$; no data are available for RDX. Consequently, the calculations below apply only to TNT. The porosity, ϕ, which has been measured by SRI, is 0.2.

With those values of the parameters, Tables B-2 and B-3 can be generated from Equations 33 and 39. It is worthwhile to record the values of the groups of parameters appearing in Equations 33, 34, and 37. Each group is a "characteristic" value, and we define the following parameters:

$$N_o = \phi v C_{sw,\infty} = 1.872 \ \mu g \ cm^{-2} \ day^{-1} \qquad (40)$$

$$M_o = \frac{\phi D_l \ (1+K) \ C_{sw,\infty}}{v} = 154.8 \ \mu g \ cm^{-2} \qquad (41)$$

Table B-2

FLUX CALCULATIONS FOR SAMPLE LAGOON PROBLEM

Time		Flux	
$\tilde{t}$	t (hr)	$\tilde{N}$	N ($\mu g\ cm^{-2}\ day^{-1}$)
0.01	19.8	4.57	8.55
0.04	79.3	2.01	3.77
0.09	178	1.18	2.21
0.16	317	0.769	1.44
0.25	496	0.528	0.989
0.36	714	0.371	0.695
0.49	971	0.263	0.491
0.64	1269	0.184	0.344
1.00	1982	0.080	0.149

Table B-3

TOTAL MASS PER UNIT AREA TRANSFERRED DURING A TIME INTERVAL FOR SAMPLE LAGOON PROBLEM

Time Interval		Mass Transferred	
τ^*	τ (hr)	$\tilde{M}$	M ($\mu g\ cm^{-2}$)
0.01	19.8	0.0961	14.88
0.04	79.3	0.182	28.14
0.09	178	0.257	39.86
0.16	317	0.324	50.10
0.25	496	0.381	58.95
0.36	714	0.429	66.48
0.49	971	0.470	72.78
0.64	1269	0.503	77.89
1.00	1982	0.548	84.86

$$t_o = \frac{D_l(1+K)}{v^2} = 1982 \text{ hr} \qquad (42)$$

Equation 42 shows that a steady-state solution for the flux would be inadequate unless time scales of interest were much longer than 1982 hr (~ 83 days). Time steps taken in the SRI lagoon model are variable; however, time steps shorter than 83 days necessitate the use of an unsteady solution as developed herein. Equation 40 states that a characteristic value of the flux is approximately 2 $\mu g\ cm^{-2}\ day^{-1}$.

Part of the significance of N_o, M_o, and t_o is that any situation with the same values of N_o, t_o, and C_w^* will be the same. M_o is <u>not</u> an independent characteristic value because

$$M_o = N_o t_o \quad . \qquad (43)$$

<u>Addition of Dissolution to the Mass Transfer Problem</u>

The above solutions and assumptions were derived for the case where the dissolution rate constant (k_r) equals zero. We must also account for the case where $k_r \neq 0$, which occurs when the lagoon is full or when the lagoon waters cover the area near the dump ramp. As previously developed, the dissolution rate of solid TNT or RDX, $\frac{dw}{dt}$, can be written as

$$\frac{dw}{dt} = k_r(C_{sat} - C_i) \quad , \qquad (44)$$

where k_r is an experimentally determined dissolution rate constant, C_{sat} is the saturation concentration of the dissolving species in the liquid phase, and C_i is the concentration of the dissolved species at the solid/liquid interface. If diffusion from the interface to the surrounding liquid is fast compared to dissolution, then Equation 44

can be represented as shown in Equation 45:

$$\frac{dw}{dt} = k_r(C_{sat} - C_{sw}) \quad , \tag{45}$$

where C_{sw} is the concentration of TNT or RDX in the sediment/water phase at any depth in the sediment. Therefore, Equation 45 can be incorporated into the transport equation developed in the previous section, as shown in Equation 46:

$$(1 + K)\frac{\partial C_{sw}}{\partial t} = D_l\frac{\partial^2 C_{sw}}{\partial z^2} + k_{dis}[C_{sat} - C_{sw}] + v\frac{\partial C_{sw}}{\partial z} \quad , \tag{46}$$

where

$$K = (\frac{1-\phi}{\phi})K_{eq}F_{oc} \quad , \tag{47}$$

and

$$k_{dis} = \frac{Fk_r S_{bet}\rho_{bs}(1-\phi)}{\phi} \quad , \tag{48}$$

and where F_{oc} is the organic fraction of the sediment solids, S_{bet} is the surface area of solid per unit mass of solid (typically determined by the BET absorption method), ρ_{bs} is the mass density of the sediment solids, ϕ is the void fraction and F is the fraction of the solid surface area that is covered by the dissolving species.

A linear isotherm has been assumed in deriving Equation 46, with

$$C_s = K_{eq}C_{sw} \quad , \tag{49}$$

where C_s is the concentration of TNT or RDX dissolved in the organic

fraction of the sediment solids and K_{eq} is experimentally determined.

The boundary conditions for Equation 46 are:

$$C_{sw}(-\infty,t) = \text{known} = C_{sw,\infty} \quad t > 0 \tag{50a}$$

$$C_{sw}(0,t) = C_w \quad t > 0 \tag{50b}$$

$$C_{sw}(z,0) = C_{sat} \quad , \tag{50c}$$

where C_w is the concentration of TNT or RDX in the bulk-water phase.

The flux, N, is given by

$$N = -\phi D_l \left(\frac{\partial C_{sw}}{\partial z}\right)_{z=0} + (1-\phi)k_r F\left(C_{sat} - C_w\right) - \phi v C_w \quad . \tag{51}$$

If Equation 46 can be solved subject to Equations 50a-50c, then the flux can be computed from Equation 51. Equation 46 will describe the flux in the laboratory experiment and in the lagoon. With laboratory data, we can find the value of k_r and use it to predict the flux in the lagoon.

Solution to Flux Equations for Laboratory Experiment

In the previous sections, Equation 46 was solved with $k_r = 0$ (i.e., no dissolution). In the laboratory experiment, however, $v = 0$ and $k_r \neq 0$ (i.e., there is no seepage but there is dissolution of solid TNT and RDX). Also in the laboratory, $C_{sw,\infty} = C_{sat}$. Consequently, the mass transfer equations become

$$(1 + K) \frac{\partial C_{sw}}{\partial t} = D_l \frac{\partial^2 C_{sw}}{\partial z^2} + k_{dis}[C_{sat} - C_{sw}] \quad , \tag{52}$$

$$\text{with } C_{sw}(-\infty, t) = C_{sat} \quad , \tag{53a}$$

$$C_{sw}(0,t) = C_w \quad , \tag{53b}$$

$$\text{and} \quad C_{sw}(z,0) = C_{sat} \quad . \tag{54}$$

The flux is given by

$$N = -\phi D_l \left(\frac{\partial C_{sw}}{\partial z}\right)_{z=0} + (1-\phi)\, Fk_r (C_{sat} - C_w) \quad . \tag{55}$$

At steady state, we can solve Equation 52 subject to the boundary conditions 53a and 53b. We find

$$\frac{C_{sat} - C_{sw}}{C_{sat} - C_w} = \exp\left(\left(\frac{k_{dis}}{D_l}\right)^{1/2} z\right) \quad . \tag{56}$$

The flux, N, is then given by

$$\frac{N}{N_o} = (1 + \beta_D)\,(1 - C_w^*) \quad , \tag{57}$$

$$\text{with } N_o = C_{sat}\,(\phi D_l k_r F S_{bet} \rho_{bs} (1-\phi))^{1/2} \quad , \tag{58}$$

$$\beta_D = \left(\frac{F k_r (1-\phi)}{S_{bet} \rho_{bs} \phi D_l} \right)^{1/2} , \qquad (59)$$

$$\text{and } C_w^* = \frac{C_w}{C_{sat}} . \qquad (60)$$

In Equations 58, 59, and 60, ϕ, D, and C_{sat} are known. The surface fraction, F, approximately equals the (known) mass fraction. The product $S_{bet}\rho_{bs}$ can be estimated by assuming a reasonable particle size for the sediment solids. If the particle diameter is d_p, then

$$S_{bet}\rho_{bs} = \frac{6}{d_p} . \qquad (61)$$

Sediment that can be described as fine soil or clay has particle sizes in the range of 10 to 100 μm. (The square root dependence of the flux on $S_{bet}\rho_{bs}$ de-emphasizes the importance of a proper choice for d_p.)

Because all parameters in Equations 58, 59, and 60 except k_r are known or can be reasonably estimated, the laboratory flux data can be used to find a best value of k_r. To make this procedure a bit more transparent, we rearrange Equations 57 through 62, substitute Equation 61 for $S_{bet}\rho_{bs}$, and obtain

$$N = (C_{sat} - C_w) \left\{ \left| \phi(1-\phi) \left(\frac{6D_l}{d_p} \right) k_r F \right|^{1/2} + k_r F (1-\phi) \right\} . \qquad (62)$$

In the flux experiments, N and C_w are measured and a plot of N versus $C_{sat}-C_w$ will have a slope equal to the bracketed expression in Equation 17.

A least-squares fit of the data to the form y = mx yields the following values for the bracketed expression in Equation 62:

TNT

$$\left[\phi(1-\phi)\left(\frac{6D_l}{d_p}\right)k_rF\right]^{1/2} + k_rF(1-\phi) = 1.0776 \times 10^{-4} \text{ cm sec}^{-1} \quad (63)$$

RDX

$$\left[\phi(1-\phi)\left(\frac{6D_l}{d_p}\right)k_rF\right]^{1/2} + k_rF(1-\phi) = 7.752 \times 10^{-5} \text{ cm sec}^{-1} \quad . \quad (64)$$

The values of the known parameters in Equations 63 and 64 are listed in Table B-4 for TNT and RDX. The diffusion coefficient is the average result from Equations 8-34 and 8-36 of Reid and Sherwood.* The void volume fraction, ϕ, was calculated from the dry weight of sediment solids, measured prior to the flux experiments. The saturation concentrations are known from solubility data reported in Section V.A., Physical Transport. The surface fraction, F, is assumed equal to the mass fraction of TNT or RDX in the sediment solids, a quantity measured prior to the flux experiments. The value of d_p is an estimate.

From Equations 63 and 64 and the values of the parameters in Table B-4, we find that the k_r is 1.172×10^{-5} cm sec for TNT and 1.164×10^{-5} cm sec^{-1} for RDX.

*Reid, R.D. and T.K. Sherwood (1958) The Properties of Gases and Liquids. McGraw-Hill, New York.

The flux derived from Equation 62 with these values of k_r has been placed on Figure B-3 with the data points to show the goodness of fit. One can see that Equation 62 is within a factor of 2 in predicting the flux over the range studied experimentally. This degree of accuracy can be disturbing unless one allows for the inherent difficulty of performing the flux measurements and of describing analytically the mass transfer in a multicomponent, heterogeneous system. One must also refrain from the temptation to fit the data in Figure B-3 to a straight line of the form $y = mx + b$. The result of this seemingly intuitive approach is a model that predicts negative flux values, a physically impossible situation in the laboratory experiment.

Table B-4

PARAMETERS FOR ANALYZING FLUX DATA

Parameter	TNT	RDX
ϕ	0.579	0.579
D_l (25°C)	2.13×10^{-5} cm^2 sec^{-1}	2.24×10^{-5} cm^2 sec^{-1}
C_{sat} (25°C)	131 μg cm^{-3}	50.6 μg cm^{-3}
F	0.156	0.078
d_p	50 μm	50 μm

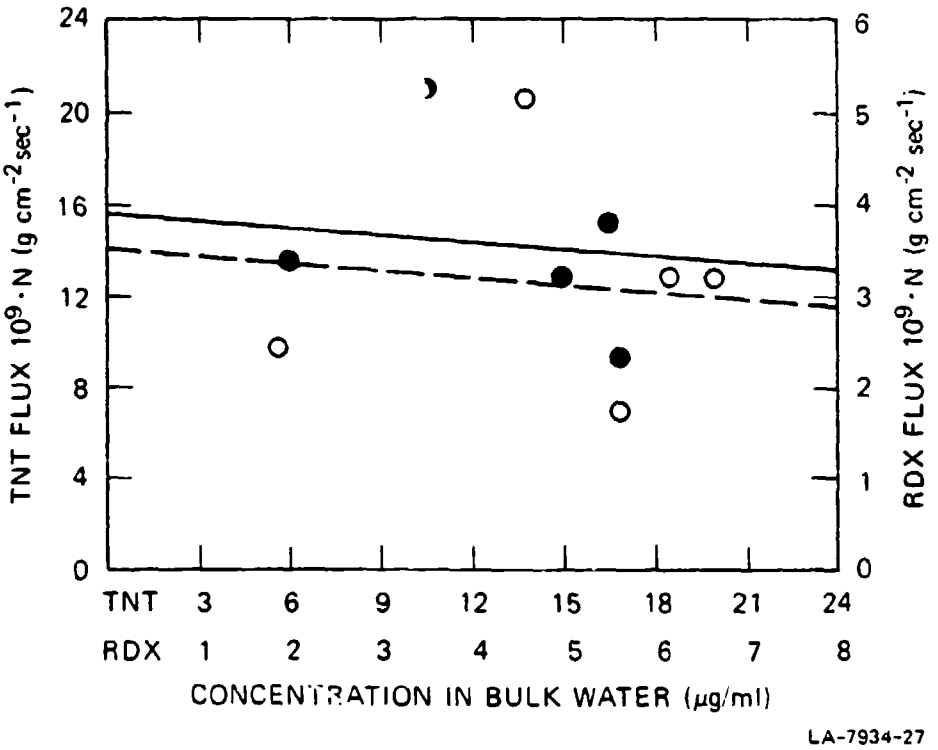

FIGURE B-3 TNT (●) AND RDX (○) FLUX DATA COMPARED WITH CURVE FIT (EQUATION 62)

Appendix C

SRI COMPUTER PROGRAM FOR MODELING THE FATE OF TNT AND RDX IN LAGOONS CONTAINING MUNITIONS WASTES

This appendix presents the computer program developed to simulate TNT and RDX in a waste-lagoon environment. It encompasses a number of subroutines to determine changes in volume, surface area, and depth of the lagoon and the transport of munitions (flux) from the bottom sediment to the free-water phase. The subroutine COMPS performs the calculation of munition concentration in the bulk-water phase and in the suspended sediment. The data output can be conveniently displayed graphically by the subroutine GRAPH 4.

```
00100  0001          PROGRAM POND
00200  0002    C     THIS IS A PROGRAM TO SIMULATE TNT IN A NATURE
00300  0003    C     POND. IT IS SPECIFICALLY TO EMPHASIZE THE
00400  0004    C     DIFFUSION OF TNT FROM THE BOTTOM SEDIMENT
00500  0005    C     BACKING TO THE FREE WATER. THE PROGRAM STARTS
00600  0006    C     TO ASSUME A GIVEN CONDITION IN THE SEDIMENT
00700  0007    C     AND ESTIMATE THE FLUX OF TNT TRANSPORTING
00800  0008    C     THROUGH THE interface IN EACH TIME INTERVAL.
00900  0009    C
01000  0010    C     FLUX IS ESTIMATED BASED UPON THE ASSUMPTION
01100  0011    C     OF REACTION TERMS ARE SMALLER THAN EITHER
01200  0012    C     CONVECTIVE AND DIFFUSION TERM.
01300  0013    C
01400  0014    C     TERMINOLOGY AND UNIT
01500  0015    C     T  SIMULATION TIME
01600  0016    C     DT  TIME INTERVAL
01700  0017    C     VOL  FREE WATER VOLUME, LITERS
01800  0018    C     Cw  CONCENTRATION IN FREE WATER, MICROGRAM/LITER
01900  0019    C     CSW CONCENTRATION IN SEDIMENT WATER, MICROGRAM/LITER
02000  0020    C     CSS CONCENTRATION IN SUSPENDED SOLID,MICROGRAM/LITER
02100  0021    C     PC  PARTITION
02200  0022    C     SD  DENSITY OF SEDIMENT
02300  0023    C     WKO  OXIDATION RATE CONSTANT
02400  0024    C     WKP  PHOTOLYSIS RATE CONSTANT
02500  0025    C     WKH  HYDROLYSIS RATE CONSTANT
02600  0026    C     WKV  VOLATILIZATION RATE CONSTANT
02700  0027    C     WKB  BIODEGRATION RATE CONSTANT
02800  0028    C     PR  PRECIPITATION RATE, CM/DAY
02900  0029    C     EV  EVAPORATION RATE, CM/DAY
03000  0030    C     SP  SEEPAGE RATE, CM/DAY
03100  0031    C     DIF  DIFFUSIVITY
03200  0032    C     PDEPTH  DEPHTH AT THE LOCATION CORRESPONDENTING TO SEDIMENT
03300  0033    C             COMPARTMENT
03400  0034    C     TMASS  TOTAL TRANSPORTATION RATE OF TNT ACROSSING THE
03500  0035    C            INTERPHASE
03600  0036    C     NS  NUMBERS OF SEDIMENT COMPARTMENTS
03700  0037    C     Nw  NUMBERS OF SEDIMENT COMPARTMENTS COVERED WITH FREE WATER
03800  0038    C     PHI  VOID FRACTION
03802  0039    C     KK  is equal to 2, only dissolution process is considered,
03804  0040    C     rk  is the dissolution rate constant
03806  0041    C     ts and sm are the parameters for calculating the solubility
03808  0042    C     ts is the solubility
03810  0043          DIMENSION Y(100),X(100),IT(3),IA(7)
03850  0044          COMMON/PARA/NS,Nw,DT,TIME,PRT,T,WT
03855  0045          COMMON/CONST/A,B
03860  0046          COMMON/RATE/WKO,WKP,WKH,WKV,WKB
03870  0047          COMMON/PHYS1/NJ,ALPHA,TMASS,PC,DIF,PHI,SD,SCOOR,SETL
03872  0048          COMMON/GRAPH4/SCA,ANG,UX,UY,VX,VY,XMI,YMI,XMA,YMA
03880  0049          COMMON/PHYS2/PR,EV,SP,VOL,PDEPTH(50),area,depth(50)
03881  0050          COMMON/CONCN/C,TSS,SSP,CSW(50),CMT(50)
03883  0051          CHARACTER*80 IT,ISTR
03884  0052          DATA IT(1)/'SIMULATION TIME'/
03885  0053          DATA IT(2)/'DAYS'/,IT(3)/'rdx concentration, ppm'/
03886  0054          DATA IA/0,0,0,0,1,0,1/
03887  0055          LOGICAL TPRINT
03888  0056          OPEN(UNIT=5,NAME='RDX.DAT',STATUS='OLD')
03890  0057          OPEN(UNIT=6,NAME='SSL.DAT',STATUS='NEW')
```

```
29700   0001            subroutine flux1
29800   0002    c       mass transfer rate coefficient is 0.235 for tnt is 15%
29900   0003    c       it is assumed that mass transfer coefficient is proportional to
30000   0004    c       the tnt deposition percentage.
30100   0005            common/concn/c,tss,ssp,cs#(50),cmt(50)
30110   0006            COMMON/PARA/NS,NN,DT,TIME,PH1,I,M1
30200   0007            COMMON/PHYS2/PK,EV,SP,VOL,PDEPTH(50),AREA,DEPTH(50)
30300   0008            COMMON/PHYS3/DM(50),DMASS,TMAS(50)
30310   0009            COMMON/RATEP/R(50)
30320   0010            COMMON/PHYS1/NJ,ALPHA,TMASS,PC,DIF,PH1,SD,SCOUR,SETL
30322   0011            common/solu/ta
30324   0012            common/solu1/rk,sm,ts
30400   0013            DMASS=0.
30402   0014            if(t .le. 70.) go to 300
30404   0015            if(t .gt. 70. .and. t .le. 130.) go to 350
30406   0016            if(t .gt. 130. .and. t .le. 210) go to 400
30408   0017            if(t .gt. 210.) go to 450
30500   0018      300   temp=263.
30501   0019            go to 500
30502   0020      350   temp=293.
30503   0021            go to 500
30504   0022      400   temp=303.
30505   0023            go to 500
30506   0024      450   temp=308.
30507   0025      500   ta=sm*10.**(8.)*exp(-ts/temp)
30508   0026            do 100 j=1,nj
30510   0027            J=N((NS+1)-1)
30600   0028            dm(j)=rk*cmt(j)*area/1000.*(ta*1000.*c)
30610   0029    c       dm(j) is in ug per day
30700   0030      100   DMASS=DMASS+DM(J)
30710   0031            WRITE(6,200)DMASS
30720   0032      200   FORMAT(7H DMASS=,E12.4)
30800   0033            RETURN
30900   0034            END
```

```
27500  0001
27600  0002              SUBROUTINE FLUX
27700  0003      C       THIS SUBROUTINE IS TO CALCULATE THE TOTAL TRANSPORT OF
27800  0004      C       CHEMICAL THROUGH SEDIMENT INTERFACE
27810  0005              common/para/ns,nw,dt,time,prt,t,wt
27900  0006              COMMON/PHYS1/NJ,ALPHA,TMASS,PC,DIF,PHI,SD,SCOUR,SETL
28000  0007              COMMON/CONCN/C,TSS,SSP,CSW(50),CHT(50)
28010  0008              COMMON/PHYS3/DM(50),UMASS,TMAS(50)
28050  0009              COMMON/PHYS2/PR,EV,SP,VOL,PDEPTH(50),area,depth(50)
28055  0010              common/water/n(50)
28057  0011              common/solu/ta
28070  0012              write(6,1000)nj
28080  0013       1000   format(5h flux,15)
28100  0014              TMASS=0.
28200  0015              DO 100 I=1,NJ
28300  0016              j=N((NS+1)-1)
28310  0017      C
28320  0018      C***      temperature adjustment on solubility
28330  0019      C
28340  0020              tp=ta/csw(j)*1000.
28450  0021              if(csw(j) .lt. ta*1000.) tp=1.
28400  0022              cond1=c/(csw(j)*tp)
28500  0023              TD=SP**2.*DT/(DIF*(1.+ALPHA))
28700  0024              aa=1.-COND1
28800  0025              bb=exp(-td/4.0)
28900  0026              d=1.-erf(td**(0.5)/2.)
29000  0027              tmas(j)=188*bb/(3.1416*td)**(0.5)-aa/2.0*d-cond1)
29010  0028      C
29020  0029      C***      beta in microgram per square centimeter per day
29030  0030      C
29100  0031              beta=phi*sp*csw(j)*tp*10.**(-3)
29105  0032              tmas(j)=beta*tmas(j)
29300  0033              TMASS=TMASS+TMAS(J)*AREA
29400  0034       100    CONTINUE
29500  0035              RETURN
29600  0036              END
```

```
26810   0058          $+tmass/vol-cu*(ropr-roev-rosp)/vol)/(1.-tss*pc*10.**(-3.))
26820   0059             if(c .gt. 0.) go to 500
26900   0060             c=c0+dt*(-sumk*c
26910   0061          $+tmass/vol-c*(ropr-roev-rosp)/vol)/(1.-tss*pc*10.**(-3.))
26912   0062      500    if(c .GT. 0.) GO TO 700
26913   0063             if(d1 .EQ. 1.) GO TO 700
26914   0064             DT=DT/7.
26916   0065             PRT=PRT/7.
26918   0066             GO TO 600
26920   0067      700    CONTINUE
26930   0068             if(c .gt. ta*1000.) c=ta*1000.
26950   0069             if(c .le. 0.) c=0.
27000   0070             SSP=C/1000.*PC
27100   0071     C         SSP IN UG/G
27110   0072             tm=c*vol
27200   0073             RETURN
27400   0074             END
```

PROGRAM SECTIONS

	Name	Bytes	Attributes
0	$CODE	688	PIC CON REL LCL SHR EXE RD NOWRT LONG
1	$PDATA	158	PIC CON REL LCL SHR NOEXE RD NOWRT LONG
2	$LOCAL	52	PIC CON REL LCL NOSHR NOEXE RD WRT LONG
3	PARA	28	PIC OVR REL GBL SHR NOEXE RD WRT LONG
4	RATE	20	PIC OVR REL GBL SHR NOEXE RD WRT LONG
5	PHYS1	36	PIC OVR REL GBL SHR NOEXE RD WRT LONG
6	PHYS2	420	PIC OVR REL GBL SHR NOEXE RD WRT LONG
7	PHYS3	404	PIC OVR REL GBL SHR NOEXE RD WRT LONG
8	CONCN	412	PIC OVR REL GBL SHR NOEXE RD WRT LONG
9	MASS	4	PIC OVR REL GBL SHR NOEXE RD WRT LONG
10	RATE1	8	PIC OVR REL GBL SHR NOEXE RD WRT LONG
11	CONST	8	PIC OVR REL GBL SHR NOEXE RD WRT LONG
12	WATER	200	PIC OVR REL GBL SHR NOEXE RD WRT LONG
13	HEATH	12	PIC OVR REL GBL SHR NOEXE RD WRT LONG
14	SOLU	4	PIC OVR REL GBL SHR NOEXE RD WRT LONG
15	CON1RL	12	PIC OVR REL GBL SHR NOEXE RD WRT LONG
	Total Space Allocated	2466	

ENTRY POINTS

Address	Type	Name
0-00000000		COMPS

```
25200   0001
25300   0002
25400   0003            SUBROUTINE COMPS
25500   0004    C       THIS SUBROUTINE IS TO CALCULATE THE CONCENTRATION IN FREE WATER
25600   0005    C       AND ON SUSPENDED SOLID
25700   0006            COMMON/PARA/NS,Nm,DI,TIME,PR1,I,m1
25800   0007            COMMON/RATE/WKU,WKF,WKH,WKV,WKB
25900   0008            COMMON/PHYS1/NJ,ALPHA,TMASS,PC,DIF,PM1,SD,SCOUR,SETL
26000   0009            COMMON/PHYS2/PR,EV,SP,VOL,PDEPTH(50),area,depth(50)
26010   0010            COMMON/PHYS3/DM(50),DMASS,TMAS(50)
26100   0011            COMMON/CONCN/C,TSS,SSP,CSW(50),CM1(50)
26105   0012            common/mass/tm
26110   0013            COMMON/RATE1/AWKP,AWKB
26120   0014            COMMON/CONST1/A,B
26130   0015            COMMON/WATER/N(50)
26132   0016            common/weath/topr,roev,rosp
26134   0017            common/solu/ta
26136   0018            common/contrl/kk,kl,kn
26140   0019            avh=vol*10**(3.)/(area*nj)
26160   0020            write(6,400) avh,awkp
26170   0021      400   format(15h average depth=,e10.4,2hh adjusted photolysis rate=,
26180   0022         se10.4)
26182   0023            if(amod(t,5e.) .ne. 0.) go to 900
26184   0024            if(t .gt. 224.) a=-1
26186   0025            n=b+a
26188   0026            awkb=wkb*2.**(b)
26189   0027            if(kl .eq. 1) awkb=wkb
26190   0028       900  write(6,800) awkb
26192   0029       800  format(6h awkb=,e12.4)
26200   0030            SUMK=WKD+awkp+WKH+WKV+AWKB
26400   0031            c0=c
26410   0032    C
26420   0033    C***    call for flux1
26430   0034    C
26440   0035            call flux1
26445   0036    C
26450   0037    C***    call for flux
26455   0038    C
26457   0039            call flux
26460   0040            do 300 i=1,nj
26462   0041            J=N((NS+1)-1)
26465   0042            TT=TMAS(J)*AREA+DM(J)
26467   0043            if(kk .eq. 2) tt=am(j)
26468   0044            IF(AMOD(T,7.) .NE. 0.) GO TO 300
26470   0045            WRITE(6,200) J,TT
26475   0046       200  FORMAT(20H DIFFUSION RATE FROM,I5,4H IS ,E12.4)
26480   0047       300  CONTINUE
26485   0048            TMASS=TMASS+DMASS
26487   0049            if(kk .eq. 2) tmass=amass
26490   0050            WRITE(6,350)TMASS
26492   0051
26495   0052       350  FORMAT(40H TOTAL DIFFUSION RATE THROUGH BOTTOM SEDIMENT=,E12.4)
26500   0053    C
26600   0054    C***        SS IN G/LITER,C IN UG/LITER
26700   0055    C
26710   0056       600  continue
26800   0057            c=c0+(dt/2)*(-sumk*c0
```

```
24736   0058            if(kk .ne. 2) go to 500
24737   0059            if(t .gt. 16h.) wkpt=2.*wkpt
24738   0060     500    continue
24740   0061            if(wkpt .gt. wkp*6.) wkpt=wkp*6.
24745   0062            awkp=awkp+wkpt
24760   0063            if(AMOD(I,7.) .NE. 0.) GO TO 200
24800   0064            write(6,150) n((ns+1)-L),poepth(i),delta
24810   0065      200 continue
24812   0066            if(nj .eq. 0) go to 350
24820   0067            AwKP=AWKP/NJ
24900   0068      150   format(15,2e12.4)
24902   0069      350   continue
24910   0070            write(6,1000)nj
24920   0071     1000   format(8h surface,15)
25000   0072            RETURN
25100   0073            END
```

PROGRAM SECTIONS

	Name	Bytes	Attributes
0	$CODE	645	PIC CON REL LCL SHR EXE RD NOWRT LONG
1	$DATA	31	PIC CON REL LCL SHR NOEXE RD NOWRT LONG
2	$LOCAL	56	PIC CON REL LCL NOSHR NOEXE RD WRT LONG
3	PARA	28	PIC OVR REL GBL SHR NOEXE RD WRT LONG
4	PHYS1	36	PIC OVR REL GBL SHR NOEXE RD WRT LONG
5	PHYS2	420	PIC OVR REL GBL SHR NOEXE RD WRT LONG
6	WATER	200	PIC OVR REL GBL SHR NOEXE RD WRT LONG
7	RATE1	8	PIC OVR REL GBL SHR NOEXE RD WRT LONG
8	CONTRL	12	PIC OVR REL GBL SHR NOEXE RD WRT LONG
9	RATE	20	PIC OVR REL GBL SHR NOEXE RD WRT LONG

Total Space Allocated 1456

ENTRY POINTS

Address	Type	Name
0-00000000		SURFACE

VARIABLES

Address	Type	Name	Address	Type	Name
4-00000004	R*4	ALPHA	5-000000D8	R*4	AREA
2-00000014	R*4	DELTA	2-00000018	R*4	DELTD
5-00000004	R*4	EV	2-00000008	I*4	I
8-00000000	I*4	KK	8-00000004	I*4	KL
2-0000001C	I*4	M	4-00000000	I*4	NJ
4-0000000C	R*4	PC	4-00000014	R*4	PHI
4-0000001C	R*4	SCOUR	4-00000018	R*4	SD
2-00000000	R*4	SUM	2-00000010	R*4	SUM1

Address	Type	Name	Address	Type	Name
7-00000004	R*4	AWKB	7-00000000	R*4	AWKP
4-00000010	R*4	DIF	3-00000008	R*4	D1
2-00000004	I*4	J	2-0000000C	I*4	K
8-00000008	I*4	KN	2-00000024	I*4	L
3-00000000	I*4	NS	3-00000004	I*4	NW
5-00000000	R*4	PP	3-00000010	R*4	PRT
4-00000020	R*4	SETL	5-00000008	R*4	SP
3-00000014	R*4	T	3-0000000C	R*4	TIME

```
21800   0001
21900   0002
22000   0003            subroutine surface
22100   0004    C       THIS SUBROUTINE IS TO CHECK THE SURFACE WHICH IS COVERED
22200   0005    C       WITH FREE WATER
22300   0006            COMMON/PARA/NS,NW,DT,TIME,PR1,I,NT
22400   0007            COMMON/PHYS1/NJ,ALPHA,TMASS,PC,DIF,PHI,SD,SCOUR,SETL
22500   0008            COMMON/PHYS2/PF,EV,SP,VOL,PDEPTH(50),area,depth(50)
22505   0009            common/water/n(50)
22507   0010            COMMON/RATE1/AWKP,AWKB
22508   0011            common/contr1/kk,k1,kn
22509   0012            COMMON/RATE/WKD,WKP,WKM,WKV,WKB
22510   0013    C
22515   0014    C***      WHEN POND IS DRIED
22520   0015    C
22525   0016            IF(VOL .GT. 0.) GO TO 300
22530   0017            NJ=0
22531   0018            WRITE(6,400) NJ,VOL
22532   0019      400   FORMAT(15,E12.4)
22535   0020            GO TO 200
22540   0021      300   CONTINUE
22600   0022            SUM=0.
22700   0023            DO 100 J=1,(NS-1)
22800   0024            I=N((NS+1)-J)
22900   0025            K=N(NS-J)
23000   0026            SUM=SUM+(DEPTH(I)-DEPTH(K))*AREA*J*10.**(-3.)
23010   0027            IF(J .EQ. 1) SUM1=SUM
23100   0028            IF(VOL .GT. SUM) GO TO 110
23300   0029            DELTA=VOL-SUM1
23310   0030            IF(DELTA .LT. 0.) DELTA=VOL
23400   0031            DELTD=DELTA/(AREA*(j+1)*10.**(-3.))
23410   0032            NJ=J
23500   0033            GO TO 120
23600   0034      110   SUM1=SUM
23800   0035      100   CONTINUE
23901   0036            NJ=J
23902   0037    c
23904   0038    c***      when pond is full
23906   0039    c
23810   0040            if(vol .le. sum) go to 120
23820   0041            delta=vol-sum1
23830   0042            delta=delta/(area*(j+1)*10.**(-3.))
23840   0043
23900   0044      120   CONTINUE
24000   0045    C
24100   0046    C***      DETERMINE WATER DEPTH ABOVE EACH SEDIMENT COMPARTMENT
24110   0047    c
24120   0048            m=n((ns+1)-nj)
24130   0049            AWKP=0.
24140   0050            WKP1=WKP
24200   0051            DO 200 L=1,nj
24400   0052            I=N((NS+1)-L)
24700   0053            PDEPTH(I)=+(DEPTH(I)-DEPTH(M))+DELTD
24710   0054    C
24720   0055    C       ADJUSTING PHOTOLYSIS RATE
24730   0056    C
24735   0057            wkpt=wkp*2.8/Pdepth(I)
```

```
19400   0001
19500   0002            SUBROUTINE VOLUME
19600   0003      C     THIS SUBROUTINE IS TO ESTIMATE THE FREE WATER VOLUME.
19700   0004            COMMON/PHYS2/PR,EV,SP,VOL,PUEPTH(50),area,depth(50)
19702   0005            common/water/n(50)
19704   0006            COMMON/PHYS1/NJ,ALPHA,TMASS,PC,DIF,PHI,SD,SCOUR,SETL
19706   0007            common/para/ns,nw,dt,time,prt,t,wt
19708   0008            common/weath/ropr,roev,rosp
19800   0009      C
19900   0010      C***   CALCULATE THE TOTAL SEEPAGE DURING THE TIME INTERVAL
20000   0011      C
20100   0012            TAREA=AREA*NJ
20200   0013            rosp=TAREA*SP*10.**(-3.)
20300   0014      C
20400   0015      C***    CALCULATE THE TOTAL EVAPORATION DURING THE TIME INTERVAL
20500   0016      C
20600   0017            ROEV=EV*TAREA*10.**(-3.)
20700   0018      C
20800   0019      C***    CALCULATE THE TOTAL PRECIPITATION DURING THE TIME INTERVAL
20900   0020      C
21000   0021            ROPR=PR*TAREA*10.**(-3.)
21100   0022      C
21200   0023      C***    INTEGRATE THE VOLUME BALANCE EWQUATION
21300   0024      C
21310   0025            VOL1=VOL
21400   0026        300 VOL=VOL1+DT*(ROPR-ROEV-ROSP)
21402   0027            IF(abs((Vol-Vol1)/Vol1) .lt. 0.5) GO TO 200
21404   0028            IF(DT.EQ. 1.) GO TO 200
21406   0029            DT=DT/7.
21408   0030            GO TO 300
21409   0031        200 CONTINUE
21410   0032      c
21420   0033      c***    check surface area
21430   0034      c
21440   0035            call surface
21500   0036            IF(VOL .LE. 0.) VOL=0.
21600   0037            RETURN
21700   0038            END
```

```
17000   0001
17100   0002
17200   0003            SUBROUTINE INITL
17300   0004    C       THIS SUBROUTINE IS TO INITIALIZE THE SIMULATION SYSTEM
17400   0005            COMMON/CONCN/C,TSS,SSP,CSW(50),CMT(50)
17410   0006            COMMON/PHYS2/PR,EV,SP,VOL,PDEPTH(50),area,depth(50)
17420   0007            common/para/ns,nw,DT,Time,prt,I,Wl
17430   0008            common/mass/tm
17500   0009    C
17600   0010    C***      READ IN INITIAL CONCENTRATIONS
17700   0011    C
17800   0012            READ(5,100) C,TSS,SSP
17900   0013      100   FORMAT(10E8.2)
17910   0014    c
17920   0015    c***      read in initial concentrations in sediment
17930   0016    c
17935   0017            do 200 i=1,ns
17940   0018            READ(5,150) CSW(1),CMT(1)
17942   0019            WRITE(6,150) CSW(1),CMT(1)
17945   0020      200   continue
17950   0021      150   format(8e10.4)
18000   0022    C
18100   0023    C***      READ IN INITIAL VOLUME
18200   0024    C
18210   0025    C       VOL IN LITER, AREA IN (CM)**2
18300   0026            READ(5,100) VOL,AREA
18310   0027            tm=c*vol
18400   0028            WRITE(6,110)
18500   0029      110   FORMAT(1h1,20h INITIAL CONDITIONS )
18600   0030            WRITE(6,120) VOL
18700   0031      120 FORMAT(6H  VOL=,E12.4)
18800   0032            WRITE(6,130)
18900   0033      130   FORMAT(8H  COMP ,10h Cw (UG/L),10H SS (UG/L),10H Cs (UG/L))
19000   0034            WRITE(6,140) C,TSS,SSP
19100   0035      140   FORMAT(10X,3E10.2)
19200   0036            RETURN
19300   0037            END
```

```
13500  0056      C
13600  0059      C          COMPARED TO THE ONE BEFORE THE PREVIOUS ONE
13700  0060      C
13800  0061            IF(DEPTH(N(M)) .GT. DEPTH(N(M-1))) GO TO 130
13900  0062            L=N(M-1)
14000  0063            N(M-1)=N(M)
14100  0064            N(M)=L
14200  0065            M=M-1
14300  0066            GO TO 140
14400  0067       120 N(K+1)=1
14500  0068       130 CONTINUE
14700  0069            K=K+1
14800  0070       410 CONTINUE
14900  0071      C
15000  0072      C***       DEFINE ALPHA AND DELTI
15100  0073      C
15200  0074            ALPHA=1.8*10.**(-3.)*PC*(1.-PHI)/PHI
15400  0075            WRITE(6,300)
15500  0076       300  FORMAT(1H1,29HINPUTS OF KINETIC INFORMATION // 9H COMPART-
15600  0077          $,4X,5HPART.,9X,4H X1,8X,7HPMUTUL=,6X,7HHYDROL=,5X,8HVOLATL=
15700  0078          $,6X,6HMICRO. / 3X,4HMENT,6X,6HCOEFF.,7X,6HDATION,2(6X,4HXSIS,
15800  0079          $1X),6X,7HIZATION,8X,6HBIODEG)
15900  0080            WRITE(6,125)NS,PC,WKO,WKP,WKH,WKV,WKB
16000  0081       125  FORMAT(/ 15,3X,9(3X,E10.3))
16100  0082      C
16200  0083      C***       WRITE DEPTH
16300  0084      C
16310  0085            write(6,500)
16320  0086       500  format(1h1,7x,4hcomp,2x,5hdeptn/2x,5horder,4x,1h#,3x,2hcm)
16400  0087            DO 170 K=1,NS
16500  0088            WRITE(6,160)K,N(K),DEPTH(n(k))
16600  0089       160  format(2I5,e10.2)
16700  0090       170 CONTINUE
16800  0091            RETURN
16900  0092            END
```

```
08500   0001
08600   0002            SUBROUTINE INPUT
08700   0003      C     THIS SUBROUTINE IS TO DEFINE SIMULATION PARAMETERS
08800   0004            COMMON/PARA/NS,Nm,DT,TIME,PHI,I,m1
08900   0005            COMMON/RATE/mKO,mKP,mKH,mKV,mKB
09000   0006            COMMON/PHYS1/AJ,ALPHA,TMASS,PC,Dif,PHI,SD,SCOUR,SETL
09100   0007            COMMON/PHYS2/PH,EV,SP,VOL,PDEPHIM(50),area,depth(50)
09110   0008            common/water/n(50)
09120   0009            COMMON/RATE1/AmKP,AmKb
09130   0010            common/solut/rk,sm,ts
09140   0011            common/contr1/kk,k1,kn
09300   0012      C
09400   0013      C***      READ TITLE INFORMATION
09500   0014      C
09600   0015            READ(5,90) TITLE
09610   0016            write(6,90) title
09700   0017        90  FORMAT(8A10)
09800   0018      C
09900   0019      C***      READ RUN CONTROL DATA
10000   0020      C
10100   0021            READ(5,100) NS,TIME,DT,PRT,mt,KK,K1,KN
10200   0022       100  format(i5,4f5.1,3i5)
10210   0023            write(6,100) ns,time,dt,prt,mt
10300   0024      C
10400   0025      C***      READ IN SETTLING AND SCOURING RATE
10500   0026      C
10600   0027            READ(5,150) SETL,SCOUR
10700   0028       150 FORMAT(2E10.3)
10800   0029      C
10900   0030      C***      READ IN SYSTEM PARAMETERS
11000   0031      C
11100   0032            READ(5,200)PC,phi,dif,SD,mKO,mKP,mKH,mKV,mKB
11110   0033            read(5,200)rk,sm,ts
11200   0034        200 FORMAT(9F8.4)
11210   0035            AmKB=mKB
11300   0036      C
11400   0037      C***      READ IN DEPTH DATA
11500   0038      C
11600   0039            DO 490 J=1,NS
11700   0040        490 READ(5,400) DEPTH(J)
11800   0041        400 FORMAT(8E12.4)
11900   0042      C
12000   0043      C***      ARRANGE COMPARTMENTS IN ACCORDANCE WITH DEPTH
12100   0044      C
12200   0045            K=1
12300   0046            N(K)=1
12400   0047            N(K+1)=2
12500   0048            DO 410 I=2,NS
12600   0049      C
12700   0050      C         COMPARED TO THE PREVIOUS DEPTH
12800   0051      C
12900   0052        450 IF(DEPTH(I) .GT. DEPTH(N(K))) GO TO 120
13000   0053            L=N(K)
13100   0054            N(K)=I
13200   0055            N(K+1)=L
13300   0056            M=K
13400   0057        140 IF(M .EQ. 1) GO TO 130
```

```
08005   0115            IF(AMOD(T,7.) .NE. 0.) GO TO 180
08010   0116    C
08020   0117    C       STORE THE DATA
08030   0118    C
08040   0119            X(11)=T
08050   0120            Y(11)=C/1000.
08060   0121            11=11+1
08070   0122      180   CONTINUE
08100   0123      170   FORMAT(2X,2HT=,F8.2,1X,7HVOLUME,E12.4,1X,5HAREA=,E12.4,
08110   0124         $5X,2HC=,E12.4)
08200   0125            GO TO 100
08201   0126      110   continue
08211   0127    C
08221   0128    C       DRAW THE CURVE
08231   0129    C
08233   0130            FROG=0.
08235   0131            DO 10 I=1,100
08237   0132       10   FROG=AMAX1(FROG,Y(I))
08239   0133            IF(FROG .GT. 20.) FROG=20.
08240   0134            II=II-1
08241   0135            CALL GIN11K(0)
08251   0136            CALL GRAPH4(X(1),Y(1),II,1,300.,0.,80.,0.,1T(_),IA(1))
08261   0137    C
08271   0138    C       TERMINATION OF GRAPH
08281   0139    C
08291   0140            CALL GRAPH4(X(1),Y(1),-1,1,0.,0.,0.,0.,II(1),IA(1))
08293   0141            CALL GPLOT(0.,0.,999)
08300   0142            stop
08400   0143            END
```

```
04000   0058            T=0.
04100   0059    C
04200   0060    C***      CALL FOR INPUT
04300   0061    C
04400   0062            CALL INPUT
04500   0063            DTH12=DT/2.
04600   0064    C
04700   0065    C***      CALL FOR INITIAL CONCENTRATIONS
04800   0066    C
04900   0067            call init1
04910   0068            e=1.
04920   0069            p=0.
04930   0070            II=1
05000   0071      100   T=T+DT
05100   0072            IF(T .GT. TIME) GO TO 110
05200   0073            T2=T+.00000001
05300   0074            TPRINT=.FALSE.
05400   0075            IF(AMOD(T2,PRT) .LT. .000001) TPRINT=.TRUE.
05700   0076    C
05800   0077    C***      READ IN RATES OF EVAPORATION, SEEPAGE, AND PRECIPITATION
05900   0078    C
05910   0079            IF(T .NE. 1. .AND. AMOD(T2,=T) .GT. .000001) GO TO 160
06000   0080            READ(5,150) EV,SP,PR
06100   0081      150   FORMAT(3E10.4)
06110   0082    c
06120   0083    c       determination of scouring and settling
06130   0084    c
06500   0085            RATIO=PR*AREA*NS/VOL*10.**(-3.)
06600   0086            IF(RATIO .LT. 0.1) GO TO 160
06700   0087            SCR=(1.+RATIO-0.1)*SCOUR
06800   0088            SEL=(1+RATIO-0.1)*SETL
06900   0089      160   CONTINUE
07000   0090    C
07100   0091    C***      CALL FOR VOLUME
07200   0092            CALL VOLUME
07202   0093    c
07204   0094    c       check to see the pond is dried out or not?
07206   0095    c
07210   0096            IF(VOL .GT. 0.) GO TO 300
07220   0097            WRITE(6,350)T
07230   0098      350   FORMAT(20H THE POND IS DRIED OUT AT ,F5.1,5H DAYS)
07240   0099            GO TO 110
07250   0100      300   CONTINUE
07300   0101    C
07400   0102    C***      CALL FOR COMPS
07500   0103    C
07600   0104            CALL COMPS
07700   0105    C
07800   0106    C***      PRINT OUT THE SIMULATION RESULTS
07900   0107    C
07910   0108            if(vol .gt. 0.) go to 210
07920   0109            write(6,200)
07930   0110      200   format(22h the pond is dried out)
07940   0111            go to 110
07950   0112      210   continue
07955   0113            if(prt .eq. 1.) tprint=.true.
08000   0114            IF(TPRINT) WRITE(6,170) T,VOL,AREA,C
```

LITERATURE CITED

Campbell, P. N. (1930). Apparatus for the determination of solubility. J. Chem. Soc. (London), Part I, 179-180.

Dulin, D. and T. Mill (1982). Development and evaluation of sunlight actinometers. Environ. Sci. Technol. 16, 815-820.

Kaplan, L. A., N. E. Burlinson, and M. E. Sitzmann (1975). Photochemistry of TNT: Investigation of the "Pink Water" Problem--Part II. Naval Surface Weapons Center. Report No. NSWC/WOL/TR 75-152.

Mabey, W. R., J. H. Smith, R. T. Podoll, H. L. Johnson, T. Mill, T-W. Chou, J. Gates, I. W. Partridge, and D. Vandenberg (1982). Aquatic Fate Process Data for Organic Priority Pollutants. Prepared by SRI International, Menlo Park, California, for the U.S. Environmental Protection Agency under Contracts 68-1-3867 and 68-03-2981.

May, W. E., S. P. Wasik, and D. H. Freeman (1978). Determination of the aqueous solubility of polynuclear aromatic hydrocarbons by a coupled column liquid chromatographic technique. Anal. Chem. 50, 175-179.

Mill, T., W. R. Mabey, D. C. Bomberger, T-W Chou, D. G. Hendry, and J. H. Smith (1982). Laboratory Protocols for Evaluating the Fate of Organic Chemicals in Air and Water. Prepared by SRI International, Menlo Park, California, for the U.S. Environmental Protection Agency under Contract 68-03-2227.

Spanggord, R. J., W. R. Mabey, T. Mill, T-W. Chou, J. H. Smith, and S. Lee (1981). Environmental Fate Studies on Certain Munition Wastewater Constituents. Phase III, Part I--Model Validation. Final Report, September 1981. Prepared by SRI International, Menlo Park, California, for the U.S. Army Medical Research and Development Command under Contract DAMD17-78-C-8081.

Thayer, J. R. (1979). Rapid simultaneous determination of nitrite and nitrate. Altex Chromatogram 3(1), 2.

Wentzel, R. S., S. Sommerer, and J. F. Kitchens (1981). Engineering and Development Support of General Decon Technology for the DARCOM Installation Restoration Program. Task 2, Laboratory Evaluation--Phase II. Final Report, November-July 1981. Prepared by Atlantic Research Corporation for the U.S. Army Medical Research and Development Command under Contract DAAK11-80-C-0027.

Wurster, R.D. and D.D. Kildsig (1965). Effect on complex formation of dissolution kinetic of m-aminobenzoic acid. J. Pharm. Sci. 54, 1491-1494.

Zepp, R. G. and D. M. Cline (1977). Rates of direct photolysis in aquatic environments. Environ. Sci. Technol. 11, 359-366.

DISTRIBUTION LIST

25 copies	Commander US Army Medical Bioengineering Research and Development Laboratory ATTN: SGRD-UBG Fort Detrick, Frederick, MD 21701
4 copies	Commander US Army Medical Research and Development Command ATTN: SGRD-RMS Fort Detrick, Frederick MD 21701
12 copies	Defense Technical Information Center (DTIC) ATTN: DTIC-DDA Cameron Station Alexandria, VA 22314
1 copy	Dean School of Medicine Uniformed Services University of the Health Sciences 4301 Jones Bridge Road Bethesda, MD 20014
1 copy	Commandant Academy of Health Sciences, US Army ATTN: AHS-CDM Fort Sam Houston, TX 78234
1 copy	Commander US Army Medical Bioengineering Research and Development Laboratory ATTN: SGRD-UBD-A/Librarian Fort Detrick, Frederick, MD 21701